Phylogeny and Revised Generic Classification of African Ricinulei (Ricinoididae), Descriptions of Five New Genera, Three New Species, and Comparative Morphology of the Male Copulatory Apparatus

Ricardo Botero-Trujillo and Lorenzo Prendini

Bulletin of the American Museum of Natural History

PHYLOGENY AND REVISED GENERIC CLASSIFICATION OF AFRICAN RICINULEI (RICINOIDIDAE), DESCRIPTIONS OF FIVE NEW GENERA, THREE NEW SPECIES, AND COMPARATIVE MORPHOLOGY OF THE MALE COPULATORY APPARATUS

RICARDO BOTERO-TRUJILLO
AND LORENZO PRENDINI

Arachnology Lab, Division of Invertebrate Zoology, American Museum of Natural History

BULLETIN OF THE AMERICAN MUSEUM OF NATURAL HISTORY
Number 480, 92 pp., 35 figures, 2 tables
Issued February 26, 2026

 ISSN 0003-0090

CONTENTS

ABSTRACT

Ricinulei Thorell, 1876, or "hooded tick-spiders," are an ancient, relictual, and cryptic order of arachnids comprising 104 extant species traditionally accommodated in three genera. Although six phylogenetic hypotheses have been proposed to date (Platnick, 1980; Selden, 1992; Murienne et al., 2013; Fernández and Giribet, 2015; Benavides et al., 2021; Sato et al., 2024), the relationships among the three currently recognized genera of Ricinulei remain unresolved and the monophyly of both New World genera has been questioned. The first quantitative intraordinal phylogeny of Ricinulei based on morphology is presented, focusing on the African taxa, currently assigned to the genus *Ricinoides* Ewing, 1929, and selected exemplar species of the New World genera, *Cryptocellus* Westwood, 1874, and *Pseudocellus* Platnick, 1980, as outgroups. The character matrix, comprising 80 discrete characters scored for 27 species, was analyzed with parsimony and Maximum Likelihood. A preferred topology, corresponding to the consensus of three optimal trees, the stability of which was insensitive to a range of weighting regimes, is presented. This topology recovered the African Ricinulei as monophyletic, in turn forming a monophyletic group with *Cryptocellus*, to the exclusion of *Pseudocellus*. Although this hypothesis of ricinuleid intraordinal relationships differs from the hypotheses obtained by molecular phylogenetic analyses, it is consistent with the sequence of vicariance events resulting from the breakup of Pangaea (ca. 200–180 Ma), which separated *Pseudocellus* from all other ricinuleids, and Gondwana (ca. 140–120 Ma), which separated *Cryptocellus* from the African Ricinulei. Due to the high levels of morphological divergence among the clades recovered by the analysis, *Ricinoides* is redefined and restricted to nine species from Côte d'Ivoire, Ghana, Guinea, Guinea-Bissau, Nigeria, Sierra Leone, and Togo, but also present in the Gambia and Senegal, and five new genera are defined: *Alantakun*, gen. nov., comprising a single species from Cameroon, Congo, Equatorial Guinea, and Gabon; *Bambara*, gen. nov., comprising three species from Côte d'Ivoire, Guinea, and Sierra Leone, but also present in Liberia; *Gizoo*, gen. nov., comprising a single species from Cameroon and Equatorial Guinea (Bioko Island); *Tautau*, gen. nov., comprising two species from Guinea and Sierra Leone, but also present in Côte d'Ivoire; and *Ududo*, gen. nov., comprising two species from Cameroon and Nigeria. Six new combinations are presented: *Alantakun karschii* (Hansen and Sørensen, 1904), comb. nov.; *Bambara hanseni* (Legg, 1976), comb. nov.; *Bambara megahanseni* (Legg, 1982), comb. nov.; *Gizoo crassipalpe* (Hansen and Sørensen, 1904), comb. nov.; *Tautau leonensis* (Legg, 1978), comb. nov.; and *Ududo sjostedtii* (Hansen and Sørensen, 1904), comb. nov. Three new species are described and illustrated: *Bambara jocquei*, sp. nov., and *Tautau ziama*, sp. nov., both from Guinea, and *Ududo tuxeni*, sp. nov., from Nigeria. A new synonym is presented: *Ricinoides olounoua* Legg, 1978 = *Alantakun karschii* (Hansen and Sørensen, 1904), syn. nov. Revised diagnoses are provided for all other African species. In all, six genera and 18 species of Ricinulei are presently recorded from 14 African countries. A key to the identification of the African genera and species is presented, as well as maps plotting their known distributions. The male copulatory apparatus of the African species is studied and six "types" are recognized. Morphological characters useful for the classification and identification of African Ricinulei, are illustrated.

INTRODUCTION

Ricinulei Thorell, 1876, or "hooded tick-spiders," are an ancient, relictual, and cryptic order of arachnids, currently comprising 104 extant and 23 extinct species (Selden, 1992; Benavides et al., 2021; Whalen and Selden, 2021; Botero-Trujillo et al., 2022; Wunderlich, 2022; Botero-Trujillo and Prendini, 2025; Prendini, 2025). Extant ricinuleids are traditionally classified into three genera. *Cryptocellus* Westwood, 1874, with 47 valid species, is distributed from Honduras to Brazil and occurs on the Caribbean island of Tobago (Republic of Trinidad and Tobago). *Pseudocellus* Platnick, 1980, with 41 valid species, is distributed from southern Texas, in the United States, to Panama, and occurs on the Caribbean island of Cuba. *Ricinoides* Ewing, 1929, with 16 species, is restricted

to western and central Africa (Benavides et al., 2021; Botero-Trujillo et al., 2021a, 2021b; Valdez-Mondragón and Cortez-Roldán, 2021; Valdez-Mondragón and Juárez-Sánchez, 2021; Botero-Trujillo and Prendini, 2025).

Platnick (1980) proposed the first hypothesis of ricinuleid intraordinal relationships, based on morphology, according to which *Cryptocellus* and *Ricinoides* formed a monophyletic group to the exclusion of *Pseudocellus*. Selden (1992), proposed a different hypothesis, also based on morphology, in which the positions of *Pseudocellus* and *Ricinoides* were reversed such that the New World genera formed a monophyletic group. Neither of the morphological hypotheses presented by Platnick (1980) and Selden (1992) were based on quantitative phylogenetic analysis, however. Two decades later, Murienne et al. (2013) presented the first quantitative phylogenetic analysis of Ricinulei, based on four nuclear and mitochondrial markers, which recovered the monophyly of all three genera and a third hypothesis of intergeneric relationships, according to which *Pseudocellus* and *Ricinoides* formed a monophyletic group to the exclusion of *Cryptocellus*. Soon after, in an analysis of transcriptomes, Fernández and Giribet (2015) obtained the hypothesis of intergeneric relationships proposed earlier by Selden (1992), i.e., *Cryptocellus* and *Pseudocellus* formed a monophyletic group to the exclusion of *Ricinoides*; however, the monophyly of *Cryptocellus* was questioned for the first time based on an analysis of Cytochrome *c* Oxidase subunit I (COI) sequences presented in the same contribution. Subsequently, Benavides et al. (2021), also using transcriptomics, attained similar results to Fernández and Giribet (2015) for the relationships among the three genera. The most taxonomically inclusive molecular study of ricinuleid phylogeny to date, using ultraconserved elements (UCEs) was presented by Sato et al. (2024). Although the intergeneric hypothesis of Selden (1992), Fernández and Giribet (2015) and Benavides et al. (2021) was again recovered, both *Cryptocellus* and *Pseudocellus* were paraphyletic. Considering the six studies published to date (Platnick, 1980; Selden, 1992; Murienne et al., 2013; Fernández and Giribet, 2015; Benavides et al., 2021; Sato et al., 2024), the relationships among the three currently recognized genera of Ricinulei are unresolved and the monophyly of both New World genera is in doubt (Prendini, 2025).

The first quantitative intraordinal phylogenetic analysis of Ricinulei based on morphology is presented here, focusing on the African taxa, currently assigned to *Ricinoides*, with selected exemplar species of the New World genera, *Cryptocellus* and *Pseudocellus*, as outgroups. Collectively, 188 specimen lots from Africa containing 181 adults (79 males, 102 females) and over 430 juveniles were examined, in addition to material from the New World and a fossil species. The character matrix, comprising 80 discrete characters scored for 27 species, was analyzed with parsimony and Maximum Likelihood (ML). A preferred topology, corresponding to the consensus of three optimal trees, the stability of which was insensitive to a range of weighting regimes, is presented. This topology recovered the African Ricinulei as monophyletic, in turn forming a monophyletic group with *Cryptocellus*, to the exclusion of *Pseudocellus*. Although this hypothesis of ricinuleid intraordinal relationships, first proposed by Platnick (1980), differs from the hypotheses obtained by molecular phylogenetic analyses, it is consistent with the sequence of vicariance events resulting from the break-up of Pangaea (ca. 200–180 Ma), which separated *Pseudocellus* from all other ricinuleids, and Gondwana (ca. 140–120 Ma), which separated *Cryptocellus* from the African Ricinulei.

Due to the high levels of morphological divergence among the clades recovered by the analysis, *Ricinoides* is redefined and restricted to the nine "giant" species revised by Botero-Trujillo et al. (2021a) from Côte d'Ivoire, Ghana, Guinea, Guinea-Bissau, Nigeria, Sierra Leone, and Togo, but also present in the Gambia and Senegal. Five new genera are defined: *Alantakun*, gen. nov., comprising a single species from Cameroon, Congo, Equatorial Guinea, and Gabon; *Bambara*, gen. nov., comprising three species from Côte

d'Ivoire, Guinea, and Sierra Leone, but also present in Liberia; *Gizoo*, gen. nov., comprising a single species from Cameroon and Equatorial Guinea (Bioko Island); *Tautau*, gen. nov., comprising two species from Guinea and Sierra Leone, but also present in Côte d'Ivoire; and *Ududo*, gen. nov., comprising two species from Cameroon and Nigeria. Six new combinations are presented: *Alantakun karschii* (Hansen and Sørensen, 1904), comb. nov.; *Bambara hanseni* (Legg, 1976), comb. nov.; *Bambara megahanseni* (Legg, 1982), comb. nov.; *Gizoo crassipalpe* (Hansen and Sørensen, 1904), comb. nov.; *Tautau leonensis* (Legg, 1978), comb. nov.; and *Ududo sjostedtii* (Hansen and Sørensen, 1904), comb. nov. Three new species are described and illustrated: *Bambara jocquei*, sp. nov., and *Tautau ziama*, sp. nov., both from Guinea, and *Ududo tuxeni*, sp. nov., from Nigeria. A new synonym is presented: *Ricinoides olounoua* Legg, 1978 = *Alantakun karschii* (Hansen and Sørensen, 1904), syn. nov. Revised diagnoses are provided for all other African species. In all, six genera and 18 species of Ricinulei are presently recorded from 14 African countries. A key to the identification of the African genera and species is presented, as well as maps plotting their known distributions. The male copulatory apparatus of the African species is studied and six "types" are recognized. Although it was impossible to prepare illustrations of all characters used in the phylogenetic analysis and taxonomic revision, the illustrations provided offer a comprehensive selection of informative structures observed in African ricinuleids, which facilitate the classification and identification of genera and species.

MATERIAL AND METHODS

Material Examined: Material is deposited in the following collections: the American Museum of Natural History (AMNH), including the Ambrose Monell Cryocollection for Molecular and Microbial Research (AMCC), New York; the Natural History Museum (BMNH), London; the California Academy of Sciences (CAS), San Francisco; the Coleção de História Natural, Universidade Federal do Piauí (CHNUFPI), Floriano, Brazil; the Colección Nacional de Arácnidos (CNAN), Universidad Nacional Autónoma de México, Mexico City; the Coleção Zoológica Prof. Paulo Bührnheim, Universidade Federal do Amazonas (CZPB/UFAM), Manaus, Brazil; the Field Museum of Natural History (FMNH), Chicago; the Instituto de Investigación de Recursos Biológicos "Alexander von Humboldt" (IAvH), Villa de Leyva, Colombia; the Arachnological Collection, Instituto de Ciencias Naturales (ICN), Universidad Nacional de Colombia, Bogotá; the Museo Argentino de Ciencias Naturales "Bernardino Rivadavia" (MACN), Buenos Aires; the Museu de Ciências Naturais (MCN), Fundação Zoobotânica do Rio Grande do Sul, Porto Alegre, Brazil; the Museum of Comparative Zoology (MCZ), Harvard University, Cambridge, MA; the Muséum d'Histoire Naturelle, Geneva (MHNG); the Museo Javeriano de Historia Natural "Lorenzo Uribe, S.J.," Pontificia Universidad Javeriana (MPUJ), Bogotá; the Musée Royal de l'Afrique Centrale (MRAC), Tervuren, Belgium; the Museo Civico di Storia Naturale "Giacomo Doria" (MSNG), Genoa, Italy; the Naturhistoriska Riksmuseet, Stockholm (NHRS); the Oxford University Museum of Natural History (OUMNH), Oxford; the Senckenberg Forschungsinstitut und Naturmuseum, Frankfurt (SMF); the U.S. National Museum of Natural History (USNM), Smithsonian Institution, Washington, DC; the Museum für Naturkunde der Humboldt-Universität, Berlin (ZMB); and the Natural History Museum of Denmark, University of Copenhagen (ZMUC).

Taxon Sampling: Twenty-seven species were scored as terminal taxa. The ingroup comprises all 18 known species of African ricinuleids, including three new species (table 1). The outgroup comprises nine species, including four species of both New World genera, *Cryptocellus* and *Pseudocellus*, and one fossil species from Cretaceous Burmese amber, as the root (appendix 1). Exemplar species of the New World genera were selected to minimize the number of missing entries in the charac-

TABLE 1

Genera and Described Species of African Ricinulei Thorell, 1876, and Known Countries of Occurrence

	Cameroon	Congo	Côte d'Ivoire	Equatorial Guinea (Bioko Island)	Gabon	Ghana	Guinea	Guinea-Bissau	Nigeria	Sierra Leone	Togo
Alantakun, gen. nov.											
*Alantakun karschi*i (Hansen and Sørensen, 1904), comb. nov.	x	x		x	x						
Bambara, gen. nov.											
Bambara hanseni (Legg, 1976), comb. nov.										x	
Bambara jocquei, sp. nov.							x				
Bambara megahanseni (Legg, 1982), comb. nov.			x								
Gizoo, gen. nov.											
Gizoo crassipalpe (Hansen and Sørensen, 1904), comb. nov.	x			x							
*Ricinoide*s Ewing, 1929											
Ricinoides afzelii (Thorell, 1892)										x	
Ricinoides atewa Naskrecki, 2008						x					
Ricinoides eburneus Botero-Trujillo et al., 2021			x								
Ricinoides feae (Hansen, 1921)								x			
Ricinoides iita Botero-Trujillo et al., 2021									x		
Ricinoides kakum Botero-Trujillo et al., 2021						x					
Ricinoides nzerekorensis Botero-Trujillo et al., 2021							x				
Ricinoides taii Botero-Trujillo et al., 2021			x								
Ricinoides westermannii (Guérin-Méneville, 1838)											x
Tautau, gen. nov.											
Tautau leonensis (Legg, 1978), comb. nov.										x	
Tautau ziama, sp. nov.							x				
Ududo, gen. nov.											
Ududo sjostedtii (Hansen and Sørensen, 1904), comb. nov.	x										
Ududo tuxeni, sp. nov.									x		

ter matrix and maximize morphological diversity and geographical coverage (Prendini, 2001). Species were scored from direct examination of adult male and female specimens when possible. The male is unknown for *B. megahanseni* and ?†*Poliochera cretacea* Wunderlich, 2012, whereas the female is unknown for *Ricinoides eburneus* Botero-Trujillo et al., 2021, *Ricinoides iita* Botero-Trujillo et al., 2021, *Ricinoides westermannii* (Guérin-Méneville, 1838), *T. leonensis*, *T. ziama*, and *U. sjostedtii*.

The tree was rooted on the fossil, ?†*P. cretacea*, one of seven ricinuleid species known from the Cretaceous period (Botero-Trujillo et al., 2022; Wunderlich, 2022), excluding two species that were described as ricinuleids but subsequently determined to be opilionids (Dunlop et al., 2020; Selden and Ren, 2017). This species belongs to the extinct suborder Palaeoricinulei Selden, 1992, the most recent extinct lineage (ca. 99 Ma), other members being Carboniferous in age (ca. 319–305 Ma). Only one other extinct suborder of Ricinulei, i.e., Primoricinulei Wunderlich, 2015, is currently recognized. However, Palaeoricinulei has closer affinities with Neoricinulei Selden, 1992, to which all extant ricinuleids belong, e.g., the presence of chelate pedipalps (Wunderlich, 2012, 2015, 2017). ?†*Poliochera cretacea* was scored from a female specimen (AMNH) presumed to be adult, based on its large size, marked development of the cuticular structures (e.g., granulation and paired anterosubmedian carinae on the carapace), and what appears to be a genital aperture on the ventral surface, resembling the genital aperture in adult females of extant ricinuleid taxa. However, the specimen may be a tritonymph based on the separation of its opisthosomal sternites (X–XIII) by transverse membranes, a character observed in immatures of extant species. Irrespective of the uncertainty, most of the characters scored in this species are expected to share the same state in the tritonymph and the adult female, based on observations on extant ricinuleids. Only character 9, the posteromedian moundlike excrescence on the carapace of the female, may manifest differently in the tritonymph. However, this is unlikely to be true for ?†*P. cretacea*, as the character state exhibited by this specimen (excrescence absent) has the broadest taxonomic distribution and represents the plesiomorphic condition.

Character Matrix: The matrix comprises 80 discrete morphological characters, 57 binary and 23 multistate (appendices 2, 3), from the following body parts: tegument (4 characters/5%), carapace (6/7.5%), cucullus (7/8.75%), coxosternal region (2/2.5%), chelicerae (4/5%), pedipalps (4/5%), legs (28/35%), male copulatory apparatus (15/18.75%), opisthosoma (8/10%), and female genital structures (2/2.5%). Forty-two (52.5%) male characters and three (3.75%) female characters were determined to be sexually dimorphic in the adult stage or otherwise applicable to only one sex (e.g., spermathecal characters). Thirty-five (43.75%) characters are applicable to adults of both sexes. Although immatures were not examined in all species, the expression of monomorphic characters in immature stages (especially tritonymphs) and adults appears to be similar among ricinuleid species. All characters were treated as unordered (i.e., nonadditive).

Phylogenetic Analysis: Parsimony analyses and nodal support measures were conducted using TNT 1.5-beta (Goloboff et al., 2008; Goloboff and Catalano, 2016; http://www.lillo.org.ar/phylogeny/tnt). An exact search by implicit enumeration was accomplished without tree overflow or delay in the analysis (memory allocation set to hold up to 150,000 trees). In addition to analyzing the matrix with equal weighting, nine implied-weighting analyses were conducted with different values of the concavity constant, k, ranging from strong to mild (k = 4, 8, 12, 16, 22, 29, 37, 48, 60) to evaluate the sensitivity of specific clades to different character weighting regimes (Prendini, 2000), resulting in ten different weighting regimes with which to evaluate nodal stability. Nodal support was assessed with bootstrap (standard) and jackknife (removal probability p = 0.36) resampling, each with 1,000 pseudoreplicates, as well as with absolute Bremer support, by

using a script to run successive searches of suboptimal trees, starting with an exact search and gradually increasing the suboptimality score and memory allocation (command series ‹‹ *hold 900000; ienum; subopt 1* [*+2 in each search that followed, up to subopt 35*]*; hold 10000* [*+10000 in each search that followed, up to hold 180000*]*; bb=tbr fillonly; bsupport;* ››). Synapomorphies common to all optimal tree topologies were mapped on the strict consensus using TNT.

A ML analysis was conducted using IQ-TREE multicore version 1.6.12 (Nguyen et al., 2015) with the MK+F model (Lewis, 2001) and a uniform model of rate heterogeneity; 1000 replications were used for ultrafast bootstrap (UFBoot) calculation (Hoang et al., 2017).

Diagnoses, Descriptions, and Terminology: Taxon diagnoses and descriptions follow Botero-Trujillo et al. (2021a). Characters refer to male and female unless specified otherwise. Terminology of somatic and genitalic morphology mostly follows Botero-Trujillo et al. (2021a). However, many new terms are introduced and/or illustrated for the first time, including: tegumentary saucer-shaped granules; carapacial posterolateral pleurite and lateral hyaline line; pedipalp tibia apical longitudinal carinae; and leg III metatarsus dorsobasal excavation and distal planar excrescence.

In recent years, the terms "carapacial translucent areas" and (carapacial) "dorsolateral translucent areas" were used interchangeably to refer to the visual structures (or areas) of Ricinulei (e.g., Botero-Trujillo et al., 2021a, 2021b; Botero-Trujillo and Prendini, 2025). These terms became more prevalent after Botero-Trujillo and Valdez-Mondragón (2016) proposed the former to encompass an assortment of different, related terms (e.g., eyes, ocelli, eye fields, ocular spots, pale areas, ocellar areas) mentioned in the literature. As discussed by Botero-Trujillo and Valdez-Mondragón (2016), diversity in the shape, size, and other characteristics of these structures is evident across the order but, to date, no study determined whether the external differences reflect differences in internal structure and/or function (e.g., image forming, light detection) and no evidence has been presented to confirm or refute whether morphologically different structures are homologous. In the present study, the differences were considered sufficient to merit a more precise terminology, as implemented in the character descriptions. Although the character matrix includes only a limited sample of New World taxa, the exemplar species represent the most significant diversity in these structures, as follows.

Species of *Pseudocellus* (except blind taxa) exhibit pale areas or spots dorsolaterally, referred to here as "pseudocellar spots," which form part of the setose (dorsal) portion of the carapace. Pseudocellar spots are visible in dorsal aspect near the lateral margins of the carapace, as a pair of diffuse, yellowish areas without well-defined borders, and are at least partially covered with setae. The size and shape of the "pseudocellar spots" provides important variation among species. In the African Ricinulei and most *Cryptocellus*, the lateral hyaline line that runs along the ventrolateral margin of the carapace is expanded dorsal to the junction of the coxae of legs I and II; these lateral expansions are referred to here as "semiocelli," as are structures that are approximately semicircular in shape. Depending on the degree of development, moderate to large semiocelli are visible dorsolaterally (if moderate) or both dorsolaterally and dorsally (if large) whereas vestigial semiocelli are visible laterally as a slight expansion of the hyaline line. The term "semiocelli" replaces the term "dorsolateral translucent areas" used in recent works on African Ricinulei, including Botero-Trujillo et al. (2021a).

Measurements, Microscopy, Imaging, and Illustration: Measurements, recorded following Botero-Trujillo et al. (2021a), were obtained from a male and female, when available. Digital photomicrographs were taken with a Nikon DS-Ri2 camera adapted to a Nikon SMZ 18 stereomicroscope with a SHR Plan Apo 1× Objective, using NIS-Elements Imaging Software, ver. 4.6, at the AMNH Microscopy and Imaging Facility. Dehydrated sections for scanning electron microscopy

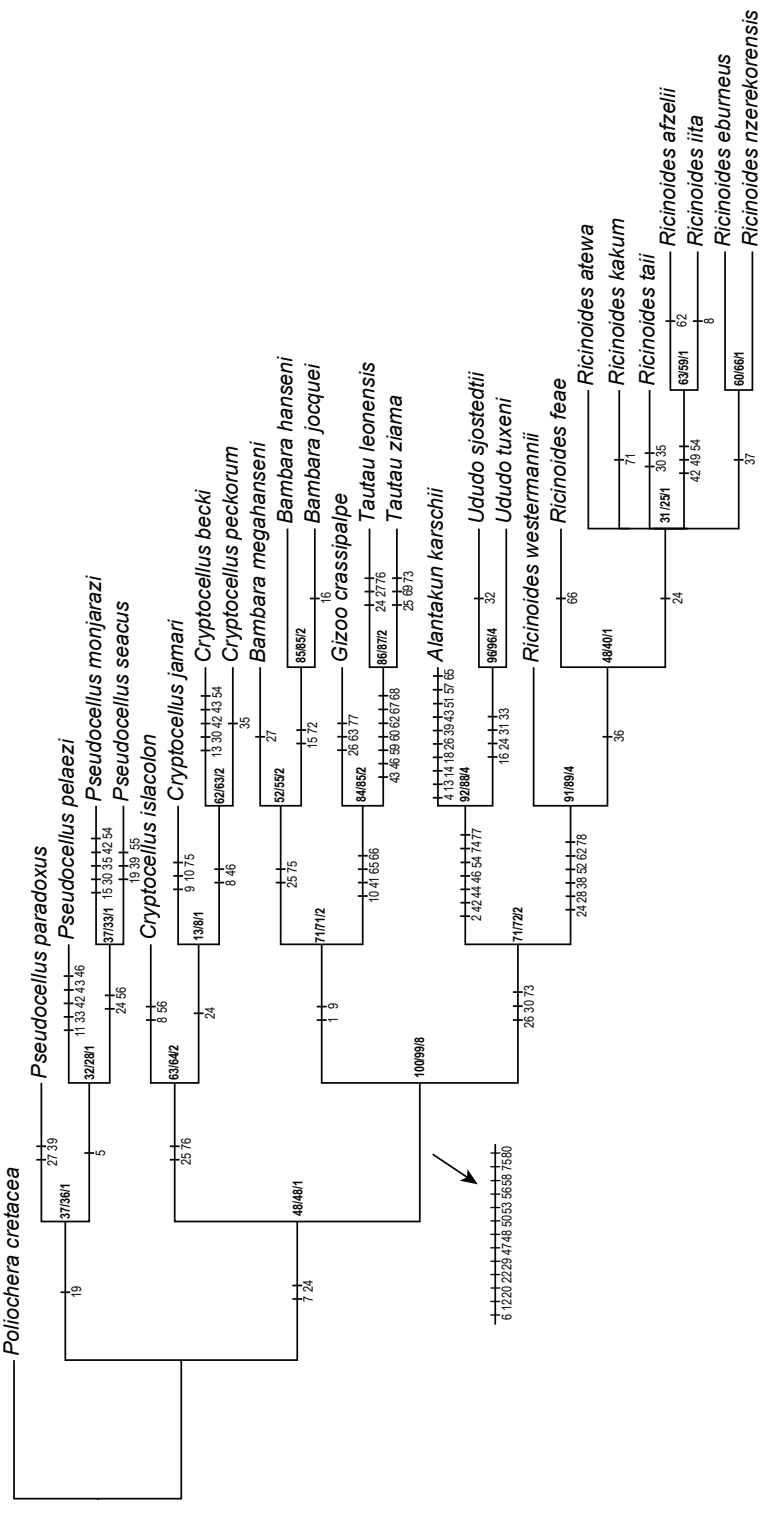

FIGURE 1. Strict consensus of three most parsimonious trees (L = 150) obtained by analysis of 80 morphological characters for 27 species of Ricinulei Thorell, 1876, with implicit enumeration and equal weighting. Same three trees obtained under nine implied weighting regimes with strong to mild values of the concavity index (k = 4–60). Unambiguous synapomorphies common to these trees indicated along branches. Nodal support values obtained with equal weights indicated at nodes in following order: jackknife support values (36% removal probability)/bootstrap percentages/absolute Bremer support values. Refer to appendix 2 for character list.

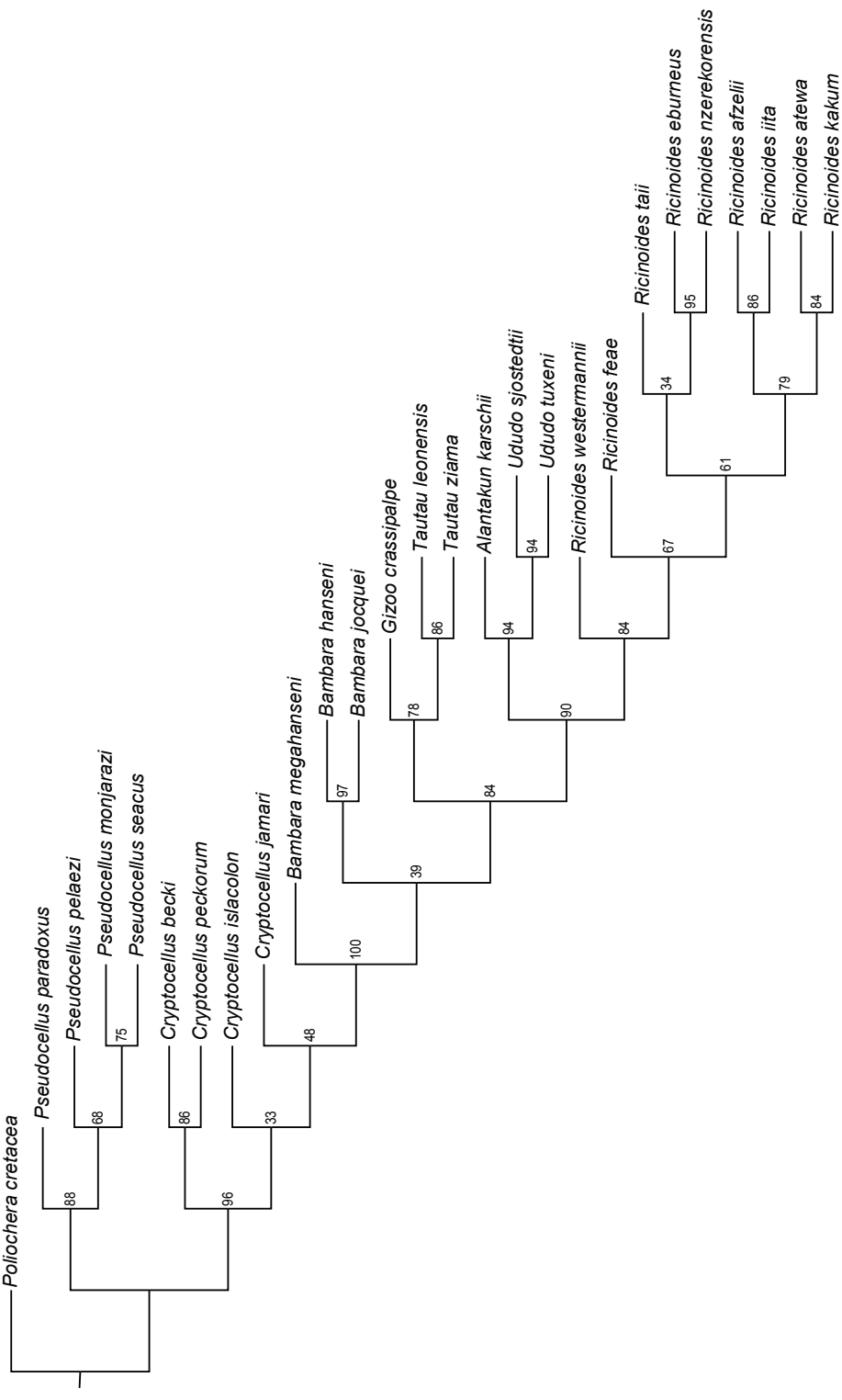

FIGURE 2. Consensus tree (log-likelihood -673.560389) obtained by analysis of 80 morphological characters for 27 species of Ricinulei Thorell, 1876, with Maximum Likelihood (MK+F model, uniform model of rate heterogeneity). Nodal support values (bootstrap percentages) indicated at nodes.

were gold-palladium coated in a VG Scientific SC 7620 mini sputter-coater. Scanning electron micrographs were taken under high vacuum with a Philips FEI XL30 TMP at the MACN. Line drawings were prepared using a camera lucida mounted on a Nikon SMZ 1500 stereomicroscope. Prior to illustration, female genitalia were dissected and, where necessary, cleared with lactophenol solution with glacial acetic acid (BioQuip, Rancho Dominguez, CA).

Georeferencing and Mapping: Locality records from the material examined were retroactively georeferenced, as necessary, mostly using Google Earth. Distribution maps were produced by plotting the georeferences onto a relief layer with graticules from SimpleMappr (Shorthouse, 2010).

PHYLOGENY OF AFRICAN RICINULEI THORELL, 1876

Parsimony: All 10 phylogenetic analyses, conducted with different weighting regimes (equal weighting and implied weighting with *k* values = 4–60), recovered three most parsimonious trees (L = 150), implying that the stability of the nodes was insensitive to the weighting regime as well as to the strength of weighting against homoplasy (*k* value). The three topologies differed only in the relationships within *Ricinoides* (as redefined below). In all three, *R. westermannii* was placed basal in the clade, followed by *Ricinoides feae* (Hansen, 1921). Two groups, respectively comprising *Ricinoides afzelii* (Thorell, 1892) and *R. iita*, and *R. eburneus* and *Ricinoides nzerekorensis* Botero-Trujillo et al., 2021, were invariably recovered as monophyletic, whereas the relationships between these two clades and the remaining species, *Ricinoides atewa* Naskrecki, 2008, *Ricinoides kakum* Botero-Trujillo et al., 2021, and *R. taii* differed among the three hypotheses. Nodal support measures, i.e., bootstraps (bs), jackknifes (jk), and Bremer supports, calculated with equal weighting, are presented on the preferred topology, which corresponds to the strict consensus of the three most parsimonious trees (fig. 1).

Both New World genera, *Cryptocellus* and *Pseudocellus*, each represented by four exemplar species, were recovered as monophyletic. A more comprehensive taxon sample is needed to rigorously test the monophyly of these genera, however.

All analyses confirmed the monophyly of the African Ricinulei with high support (bs = 100%; jk = 99%; fig. 1), in turn forming a monophyletic group with *Cryptocellus*, to the exclusion of *Pseudocellus*, consistent with the relationships proposed by Platnick (1980). Although differing from other published hypotheses (Selden, 1992; Murienne et al., 2013; Fernández and Giribet, 2015; Benavides et al. 2021; Sato et al., 2024), this hypothesis is consistent with the sequence of vicariance events resulting from the breakup of Pangaea (ca. 200–180 Ma), which separated *Pseudocellus* from all other ricinuleids, and Gondwana (ca. 140–120 Ma), which separated *Cryptocellus* from the African Ricinulei.

Two major clades of African Ricinulei were recovered, each comprising subclades with high support values. One major clade (bs = 71%; jk = 71%) comprised the new genera *Bambara*, *Gizoo*, and *Tautau*, with three, one, and two species respectively. The other major clade (bs = 72%; jk = 71%) was divided into two subclades, one comprising the new genera *Alantakun* and *Ududo* (bs = 88%; jk = 92%), with one and two species respectively, and *Ricinoides*, redefined to comprise only the nine species of "giant" Ricinulei, the taxonomy of which was studied in detail by Botero-Trujillo et al. (2021a). Each of the six African genera was monophyletic with high support (fig. 1).

The African Ricinulei share the following synapomorphies (fig. 1): carapace ventrolateral margin, posterolateral pleurite absent or indistinct, corresponding area not sclerotized; cucullus anterior surface, sublateral longitudinal sulci distinct; cheliceral manus, dorsal toothlike process present; cheliceral movable finger, mucron prolateral excavation present; leg tarsi, ventrodistal papillae absent; leg III metatarsus, prodorsal proximal sulcus (♂) present; leg III metatarsus, prodorsal margin distal region, planar excrescence on ipsilateral surface (♂) present; leg III metatarsus and tarsus dorsal

surfaces, reciprocal fit when tarsus retracted (♂) precise, copulatory apparatus completely enclosed; legs III and IV terminal tarsomere apex, dorsal and lateral margins projected, sublinear (ungues predominantly covered in dorsal and lateral aspects); copulatory apparatus, fixed process, apex (♂) with distinct raised lobular region situated on prolateral surface (relative to dorsal longitudinal sulcus), comprising two primary lobes and, usually, with ventral secondary lobes in more proximal position; copulatory apparatus, fixed process, prolateral laminar (*PL*) lobe (♂) present; opisthosoma, dorsal and ventral pleural membranes, surfaces finely and densely granular; *bursa copulatrix*, anterior wall, supernumerary sacculiform formations (♀) present.

The clade comprising *Bambara*, *Gizoo*, and *Tautau* is supported by the following synapomorphies: tegument, polygonal (calyxlike to navicular) setae present; carapace, posteromedian moundlike excrescence (♀) present. The clade comprising *Gizoo* and *Tautau* is supported by the following synapomorphies: carapace, posteromedian moundlike excrescence (♂) present; leg II, fifth (terminal) tarsomere fixed, fused to preceding tarsomere; copulatory apparatus, fixed process, distal lobular region, prolateral distal (*pd*) lobe (♂) absent or indistinct; copulatory apparatus, fixed process, distal lobular region, retrolateral distal (*rd*) lobe (♂) absent or indistinct. The clade comprising *Alantakun*, *Ricinoides*, and *Ududo* is supported by the following synapomorphies: pedipalp tibia distal region, dorsal and lateral surfaces, raised tubercles present, oval; leg I femur (♂) slightly swollen, moderately robust; tergal membranes, surface granular. The clade comprising *Alantakun* and *Ududo* is supported by the following synapomorphies: tegument, saucer-shaped granules present; leg III femur (♂) slightly swollen, moderately robust; leg III metatarsus, dorsal surface, basal region (♂) excavated; leg III metatarsus, dorsal concavity (♂) very deep, forming well-defined chamber in distal half of segment; leg IV femur (♂) slightly swollen, moderately robust; opisthosoma, segment XIII, posterior granulation posteroventral margin and, to lesser extent, posterodorsal margin, armed with large and posteriorly directed subspiniform granules; opisthosoma, pygidium basal segment, posterior margin entirely broad, more markedly so ventrally. Diagnostic characters of the six African genera are presented below.

Maximum Likelihood: The log-likelihood of the consensus tree constructed from 1000 bootstrap trees was -673.560389 (fig. 2). *Pseudocellus* was monophyletic (bs = 88%) whereas *Cryptocellus* was paraphyletic. The topology for the African Ricinulei obtained by the ML analysis was congruent with that obtained by parsimony, but differed in the placements of *Bambara* and the group comprising *Gizoo* and *Tautau* relative to other genera, as well as in the paraphyly of *Bambara*. All African genera formed a monophyletic group with high bootstrap support (bs = 100%). *Ricinoides* (bs = 84%), *Tautau* (bs = 86%), and *Ududo* (bs = 94%) were monophyletic with strong support. *Alantakun* and *Ududo* grouped together (bs = 94%), both grouping with *Ricinoides* (bs = 90%), all three genera in turn forming a well-supported group with *Gizoo* and *Tautau* (bs = 84%).

COMPARATIVE MORPHOLOGY OF THE MALE COPULATORY APPARATUS

The morphology of the male copulatory apparatus is similar in the African species of Ricinulei. Many of the distinctive structures of the apparatus occur on the fixed process, which possesses most of the taxonomically and phylogenetically informative features of the secondary genitalia. These include three nonhomoplastic character states: fixed process, prolateral surface with raised lobular region distally (relative to dorsal longitudinal sulcus); fixed process with large prolateral laminar (*PL*) lobe; movable process originating dorsally from fixed process, its origin visible in prolateral aspect.

The fixed process is modified to varying degrees in different taxa and is highly complex in some species. The morphology of this process is best understood by dividing it into regions and individual components (fig. 15). The trunk, or main body, is the largest component of the fixed process and is mostly unmodified. On its dorsal surface, the dorsal longitudinal sulcus accommodates the movable

process in the resting position. The trunk consists of proximal and distal regions, each defined relative to the position of the submedian emargination (sm), which separates the *PL* lobe from the distal region of the trunk. The retrolateral subdistal (*rsd*) lobe originates subdistally from the trunk and is situated retrolateral to the dorsal longitudinal sulcus. Opposite the *rsd* lobe and separated from it by the subdistal emargination, the distal lobular region is an elaborate surface with a series of lobes situated prolateral to the dorsal longitudinal sulcus. The distal lobular region comprises two primary and two secondary lobes. The primary lobes, alpha (α) and beta (β), present in all African species, are the largest and most distinct. The secondary lobes, termed prolateral distal (*pd*) and retrolateral distal (*rd*) lobes due to their relative positions (rather than to the dorsal longitudinal sulcus), are not present in all species and, if present, are usually less developed than the primary lobes and therefore more difficult to identify.

No studies have yet evaluated the mechanisms under which ricinuleid genitalia evolved nor how the interaction between male and female genitalia differs among taxa with different genitalic morphologies (e.g., African vs. New World taxa). Considering that sperm transfer in Ricinulei requires direct interaction between the male copulatory apparatus and the female genitalia during mating (Cooke, 1971; Talarico et al., 2008a), sexual selection is presumed to have played a crucial role in driving male genitalic diversification. In the case of the African species, the observation that morphological diversity in the copulatory apparatus is concentrated in the fixed process suggests that this process might have been more affected by sexual selection than other parts of the apparatus.

Recently, the copulatory apparatus of *Ricinoides* was studied from a taxonomic perspective (Botero-Trujillo et al., 2021a). To enhance understanding of the diversification of Ricinulei genitalia, six distinct types of copulatory apparatus observed among the African species, are defined below, based on characteristics of the fixed process. Types are named after the species that typifies the morphology.

atewa Type

The *atewa* type of copulatory apparatus is restricted to the known species of *Ricinoides* (fig. 15).

Trunk: Trunk distal region short.

Prolateral Laminar Lobe: *PL* lobe moderately to greatly expanded, except in *R. feae*, in which it is relatively narrow; dorsoventrally compressed; apex aligned with *rsd* lobe.

Alpha Lobe: Primary α lobe very long and narrow, otherwise moderately elongate (*R. feae*, *R. nzerekorensis*, *R. taii*), in all cases larger than other lobes of distal lobular region; dorsoventrally compressed in most species, except *R. iita*, in which subcircular in cross section, and *R. feae*, in which laterally compressed; margins smooth to slightly irregular with distinct subdistal serrations on retrolateral margin in *R. atewa* and *R. kakum*. The α lobe is broken and the missing part lost in the neotype and only known male specimen of *R. westermannii*.

Beta Lobe: Primary β lobe medium-sized, distinctly bicuspid (β_1, β_2) in most species, except *R. afzelii*, in which entire; β_1 and β_2 widely separated in *R. feae*, β_1 noticeably larger than β_2 in *R. westermannii*, β_2 larger in *R. iita*.

Prolateral and Retrolateral Distal Lobes: Secondary *pd* and *rd* lobes well developed and usually pointed, except in *R. taii*, in which both lobes vestigial and represented by slightly raised ridges; *pd* dorsoventrally expanded and laterally compressed in *R. afzelii*, *pd* forming moderately broad, raised surface and *rd* comprising cluster of small spines in *R. feae*; both lobes small but evident in *R. nzerekorensis*.

Retrolateral Subdistal Lobe: *rsd* lobe medium-sized, pronounced, associated with distinct subdistal emargination.

crassipalpe Type

The *crassipalpe* type of copulatory apparatus is restricted to *Gizoo crassipalpe* (fig. 16).

Trunk: Trunk distal region short.

Prolateral Laminar Lobe: *PL* lobe narrow and predominantly linear, spiniform, slightly

compressed dorsoventrally; apex acute, aligned with *rsd* lobe.

Alpha Lobe: Primary α lobe moderately large and elongate, basally expanded; margins smooth, without serrations; forming "Y" configuration with β lobe and main axis of trunk.

Beta Lobe: Primary β lobe large, entire, with small, ventrally directed accessory denticular process subdistally.

Prolateral and Retrolateral Distal Lobes: Secondary *pd* and *rd* lobes absent or indistinct.

Retrolateral Subdistal Lobe: *rsd* lobe large, similar in size to α and β lobes, pronounced and erect, associated with distinct U-shaped subdistal emargination.

hanseni Type

The *hanseni* type of copulatory apparatus is restricted to the species of *Bambara*; the male of *B. megahanseni* is unknown (figs. 17, 18).

Trunk: Trunk distal region short.

Prolateral Laminar Lobe: *PL* lobe moderately narrow, curved (*B. hanseni*) or predominantly linear (*B. jocquei*), dorsoventrally compressed; apex round (*B. hanseni*) or acute (*B. jocquei*), aligned with *rsd* lobe.

Alpha Lobe: Primary α lobe moderately large, partially (*B. jocquei*) or completely (*B. hanseni*) bifid (α_1, α_2); elongate, with α_1 longer than α_2; margins almost smooth, otherwise retrolateral margin (i.e., same side as α_2) slightly irregular.

Beta Lobe: Primary β lobe entire, large, and thumb shaped (*B. hanseni*) or medium sized and tuberculate (*B. jocquei*); retrolateral surface with small but distinct accessory granule basally.

Prolateral and Retrolateral Distal Lobes: Secondary *pd* lobe evident, forming moderately broad, raised region. Secondary *rd* lobe small but evident, forming pointed protrusion.

Retrolateral Subdistal Lobe: *rsd* lobe large, pronounced, pointed (*B. hanseni*) or broad and laminar (*B. jocquei*), associated with distinct U-shaped subdistal emargination (narrower in *B. jocquei*).

karschii Type

The *karschii* type of copulatory apparatus is restricted to *Alantakun karschii* (fig. 19).

Trunk: Trunk distal region short.

Prolateral Laminar Lobe: *PL* lobe moderately expanded, dorsoventrally compressed; apex aligned with *rsd* lobe.

Alpha and Beta Lobes: Distal lobular region membranous and whitish, "fleshy" in appearance; primary α and β lobes close together, forming region with irregular margins and vesicular appearance; β lobe small, resembling retrolateral protuberance.

Prolateral and Retrolateral Distal Lobes: Secondary *pd* lobe divided into two, well separated prolateral distal lobes (pd_1 and pd_2); pd_1 well developed, pointed and fingerlike; pd_2 similar to pd_1, otherwise small and inconspicuous. Secondary *rd* lobe obsolete, at most forming slightly raised ridge.

Retrolateral Subdistal Lobe: *rsd* lobe large, pronounced and erect, associated with distinct U-shaped subdistal emargination.

leonensis Type

The *leonensis* type of copulatory apparatus is restricted to the two known species of *Tautau* (fig. 20).

Trunk: Trunk distal region elongate, truncate distally and without retrolateral subdistal emargination; margin with (*T. ziama*) or without (*T. leonensis*) large lanceolate projection.

Prolateral Laminar Lobe: *PL* lobe very narrow, markedly curved (*T. leonensis*) or predominantly linear (*T. ziama*), subcircular in cross section but with laterally compressed apex; apex distinctly proximal to *rsd* lobe; separated from trunk by broad submedian emargination.

Alpha Lobe: Primary α lobe very large, basally expanded and moderately (*T. leonensis*) or markedly (*T. ziama*) hook-shaped; margins smooth, without serrations.

Beta Lobe: Primary β lobe very large and planar, distinctly trifid; tips acute and apically

directed, all simple (*T. leonensis*) or distalmost tip bicuspid (*T. ziama*).

Prolateral and Retrolateral Distal Lobes: Secondary *pd* and *rd* lobes absent or indistinct.

Retrolateral Subdistal Lobe: *rsd* lobe vestigial.

sjostedtii Type

The *sjostedtii* type of copulatory apparatus is restricted to the two known species of *Ududo* (fig. 21).

Trunk: Trunk distal region short.

Prolateral Laminar Lobe: *PL* lobe narrow and curved, dorsoventrally compressed; apex aligned with *rsd* lobe.

Alpha Lobe: Primary α lobe moderate and elongate, somewhat expanded basally; margins almost smooth to slightly irregular, without serrations; connected to β lobe by slight curvature.

Beta Lobe: Primary β lobe medium sized, entire.

Prolateral and Retrolateral Distal Lobes: Secondary *pd* and *rd* lobes obsolete, at most forming slightly raised ridges.

Retrolateral Subdistal Lobe: *rsd* lobe large, similar to or larger than α lobe, larger than β lobe, pronounced and erect, associated with distinct U-shaped subdistal emargination.

SYSTEMATICS

Family Ricinoididae Ewing, 1929

Key to the Genera and Species of African Ricinulei Thorell, 1876

Characters apply to both sexes unless specified otherwise. Refer to generic diagnoses for complete list of characters. *Male of *Bambara megahanseni* (Legg, 1982), comb. nov., and females of *Ricinoides eburneus* Botero-Trujillo et al., 2021, *Ricinoides iita* Botero-Trujillo et al., 2021, *Ricinoides westermannii* (Guérin-Méneville, 1838), *Tautau leonensis* (Legg, 1978), comb. nov., *Tautau ziama*, gen. et sp. nov., and *Ududo sjostedtii* (Hansen and Sørensen, 1904), comb. nov., unknown.

1. Tegument without polygonal (calyxlike to navicular) setae (figs. 34, 35); carapace (♀) without posteromedian moundlike excrescence* (fig. 35A); pedipalp tibia, distal region with raised oval or elongate tubercles (figs. 10A, B, 11B, D, F, 36C, D); leg I femur (♂) slightly swollen and moderately robust or, if unmodified and slender (in *Ricinoides taii* Botero-Trujillo et al., 2021), leg I metatarsus with proventral proximal depression (fig. 12B) 2
– Tegument with polygonal (calyxlike to navicular) setae (figs. 25, 26, 27B, 30, 31); carapace (♀) with posteromedian moundlike excrescence* (e.g., fig. 26A); pedipalp tibia, distal region without raised tubercles (figs. 11C, E, 27C, D, 31D, E) or, if raised elongate tubercles present (*Gizoo*, gen. nov.), leg II fifth (terminal) tarsomere fused to preceding tarsomere (fig. 32E); leg I femur (♂) slender* 3
2. Tegument surface without saucer-shaped granules; pedipalp tibia unmodified or slightly swollen proximally compared to rest of segment, otherwise tibia robust along entire length (fig. 11D); leg femora with dorsal longitudinal sulcus; leg II metatarsus (♂) with shallow to deep ventral subproximal depression (fig. 12E); legs III and IV femora (♂) slender [slightly swollen and moderately robust in *Ricinoides afzelii* (Thorell, 1892) and *R. iita*]; leg III metatarsus (♂) dorsal surface not excavated basally, dorsal concavity moderately deep distally, gradually becoming shallower proximally (fig. 14D), third tarsomere with acute dorsodistal process (fig. 13B); copulatory apparatus (♂) fixed process with beta (β) lobe bicuspid (entire in *R. afzelii*; fig. 15); opisthosomal segment XIII, posterodorsal and posteroventral margins without series of large granules; pygidium basal segment with posterior margin narrow and posterior opening distinctly

narrow (width two-fifths to one third lateral width of basal segment) . . . . . 5 (*Ricinoides* Ewing, 1929)

– Tegument surface with saucer-shaped granules; pedipalp tibia moderately or markedly swollen proximally compared with rest of segment (figs. 11A, F, 36C); leg femora without dorsal longitudinal sulcus; leg II metatarsus (♂) without ventral subproximal depression (fig. 37E); legs III and IV femora (♂) slightly swollen and moderately robust; leg III metatarsus (♂) dorsal surface moderately to deeply excavated basally, dorsal concavity very deep, forming well-defined chamber in distal half of segment (figs. 14A, F, 38D), third tarsomere without acute dorsodistal process (e.g., fig. 13A); copulatory apparatus (♂) fixed process with β lobe entire (figs. 19, 21); opisthosomal segment XIII, posteroventral margin and, to lesser extent, posterodorsal margin armed with large and posteriorly directed subspiniform granules (figs. 23B, 34C, D, 35C, D, 36B); pygidium basal segment with posterior margin entirely broad, more markedly so ventrally (fig. 23C, D, G, H) and posterior opening broad (width at least half lateral width of basal segment) 4

3. Carapace (♂) without posteromedian moundlike excrescence (fig. 25A); cucullus ventrolateral margins moderately truncate (rounded, at least in ♀, in *B. megahanseni*; figs. 8C, 27A); pedipalp tibia with apical longitudinal carinae (figs. 11C, 27C, D); leg II fifth (terminal) tarsomere movable, not fused to preceding tarsomere (fig. 28E); copulatory apparatus (♂) fixed process, alpha (α) lobe partially (apically) (fig. 18) or completely bifid (fig. 17), β lobe with small accessory granule basally on retrolateral surface, prolateral distal (*pd*) and retrolateral distal (*rd*) lobes present (figs. 17, 18); opisthosomal tergite XIII, median sclerite cup shaped (rectangular to trapezoid in *B. megahanseni*), dorsal and, sometimes, ventral pleural membrane moderately to sparsely granular (figs. 23A, 25C, 26C, 27B) . . . . . 13 (*Bambara*, gen. nov.)

– Carapace (♂) with posteromedian moundlike excrescence (figs. 30A, 31A); cucullus ventrolateral margins rounded (fig. 31B); pedipalp tibia without apical longitudinal carinae (present in *T. ziama*; figs. 11E, 31D, E); leg II fifth (terminal) tarsomere fixed, fused to preceding tarsomere (fig. 32E); copulatory apparatus (♂) fixed process, α lobe entire (simple), β lobe without accessory granule on retrolateral surface, and *pd* and *rd* lobes absent or indistinct (figs. 16, 20); opisthosomal tergite XIII, median sclerite rectangular to trapezoid (figs. 30C, 31C), dorsal and ventral pleural membranes finely and densely granular (fig. 31C) 15

4. Tegument surface with distinct saucer-shaped granules; carapace and opisthosoma dorsal surface with granules arranged in distinct clusters; cucullus (♂) anterior surface with flat, coarsely granular, triangular area ventrally (fig. 8F); tritosternum extremely small, not exposed (only visible when pedipalp coxae pulled) (fig. 22A); pedipalp tibia markedly swollen proximally compared with rest of segment, distal region with raised elongate tubercles (fig. 11B); leg I tibia (♂) without ventral apophyses, metatarsus sublinear in lateral aspect, subcircular in cross section, with proventral proximal depression; leg II femur (♂) moderately to markedly swollen and robust, metatarsus with ventrosubmedian concavity; leg III metatarsus (♂), dorsal surface deeply excavated basally (fig. 14A); copulatory apparatus (♂) fixed process, distal lobular region membranous and whitish, "fleshy" in appearance (unlike rest of apparatus), *pd* lobe divided into two distal lobes (pd_1 and pd_2) (fig. 19) . . . . . *Alantakun karschii* (Hansen and Sørensen, 1904), comb. nov.

– Tegument surface with obsolete saucer-shaped granules; carapace and opisthosoma

dorsal surface with separate granules (figs. 34A, C, 35A, C, 36B); cucullus (♂) anterior surface without particularly coarse granules, shallowly convex ventrally (as rest of cucullus) (fig. 36A); tritosternum vestigial, barely visible (fig. 34B, 35B); pedipalp tibia moderately swollen proximally compared to rest of segment (figs. 11F, 36C, D), distal region with raised oval tubercles (figs. 11F, 36C, D); leg I tibia (♂) with one (proventral) or two (pro- and retroventral) ventral apophyses (figs. 12A, C, 37C, D), metatarsus markedly convex ventrally in lateral aspect, dorsoventrally elongate in cross section, without proventral proximal depression (figs. 12C, 36E); leg II femur (♂) slender (fig. 37A, B), metatarsus without ventrosubmedian concavity (fig. 37E); leg III metatarsus (♂), dorsal surface moderately excavated basally (figs. 14F, 38D); copulatory apparatus (♂) fixed process, distal lobular region sclerotized and pigmented, similar to rest of apparatus (fig. 38), *pd* lobe simple (undivided) (fig. 21) ..... 17 (*Ududo*, gen. nov.)

5. Cucullus (♂) ventral part modified anteromedially, i.e., with knoblike tubercle, elevation, or group of slightly raised granules (fig. 8B, E, G) 6
– Cucullus (♂) ventral part unmodified 7
6. Cucullus (♂) ventral part with pronounced anteromedian knoblike tubercle (fig. 8B), without elevation or group of slightly raised granules; pedipalp tibia (♂) distal retroventral tubercles greatly enlarged; leg femora (♂) width (at midline) increasing in order: leg III < IV < I << II; leg I metatarsus (♂) with prominent ventral excrescence; copulatory apparatus (♂) fixed process with β lobe entire, *pd* lobe dorsoventrally expanded and laterally compressed ..... *R. afzelii*
– Cucullus (♂) ventral part with anteromedian elevation or group of slightly raised granules (fig. 8E, G), without knoblike tubercle; pedipalp tibia (♂) distal ventral tubercles moderately enlarged; leg femora (♂) width (at midline) increasing in order: leg IV = III < I << II (*Ricinoides atewa* Naskrecki, 2008), leg III < I < IV << II (*R. iita*), or leg IV < III < I << II (*Ricinoides kakum* Botero-Trujillo et al., 2021); leg I metatarsus (♂) without prominent ventral excrescence; copulatory apparatus (♂) fixed process with β lobe distinctly bicuspid, *pd* lobe pointed 8
7. Leg II tibia (♂) without ventromedian apophysis; copulatory apparatus (♂) fixed process with β_1 component of β lobe noticeably larger than β_2 ..... *R. westermannii*
– Leg II tibia (♂) with ventromedian apophysis (fig. 12D); copulatory apparatus (♂) fixed process with β_1 and β_2 components of β lobe similar 9
8. Cucullus (♂) ventral part with anteromedian elevation, without slightly raised granules (fig. 8G); pedipalp tibia (♂) ventral surface with tubercles not noticeably enlarged or arranged into distinct rows; leg III metatarsus (♂) proventral surface with apical brushlike row of yellowish setae; leg femora (♂) width (at midline) increasing in order: leg III < I < IV << II; copulatory apparatus (♂) fixed process with α lobe subcircular in cross section, curving toward retrolateral surface, retroventral margin smooth, β_2 component of β lobe fingerlike and larger than β_1 ..... *R. iita*
– Cucullus (♂) ventral part with group of slightly raised granules, without anteromedian elevation (fig. 8E); pedipalp tibia (♂) ventral surface with enlarged tubercles arranged into one (retroventral) or two (proventral and retroventral) rows; leg III metatarsus (♂) proventral surface without apical brushlike row of yellowish setae; leg femora (♂) width (at midline) increasing in order: leg IV ≤ III < I << II; copulatory apparatus (♂) fixed process with α lobe dorsoventrally compressed, curving toward ventral surface, retroventral margin with distinct subdistal serrations, β_1 and β_2 components of β lobe pointed, similar (fig. 15) 10

9. Tergite XIII median sclerite noticeably longer than wide; opening on basal segment of pygidium approximately two-fifths lateral width of segment at base; copulatory apparatus (♂) fixed process with laterally compressed α lobe; β_1 and β_2 components of β lobe widely separated; *pd* lobe forming moderately broad, raised surface; *rd* lobe comprising cluster of small spines . . . . . *Ricinoides feae* (Hansen, 1921)
– Tergite XIII median sclerite about as long as wide; opening on basal segment of pygidium approximately one-third lateral width of segment at base; copulatory apparatus (♂) fixed process with dorsoventrally compressed α lobe; β_1 and β_2 components of β lobe adjacent; *pd* lobe pointed (weakly developed in *Ricinoides nzerekorensis* Botero-Trujillo et al., 2021, and *R. taii*); *rd* lobe simple 11
10. Pedipalp tibia (♂) ventral surface with enlarged tubercles arranged into two (proventral and retroventral) rows; tergite X lateral sclerites well developed, tergal membranes narrow . . . . . *R. atewa*
– Pedipalp tibia (♂) ventral surface with enlarged tubercles arranged into single (retroventral) row; tergite X lateral sclerites obsolete, tergal membranes broad. . . . . *R. kakum*
11. Leg II tibia (♂) ventromedian apophysis smooth dorsally and prolaterally, covered with tuberose granules on other surfaces; copulatory apparatus (♂) fixed process, α lobe very long, narrow, prolateral margin sublinear, smooth . . . . . *R. eburneus*
– Leg II tibia (♂) ventromedian apophysis entirely covered with tuberose granules; copulatory apparatus (♂) fixed process, α lobe moderately long, thumb shaped, prolateral margin basally expanded, sinuous 12
12. Leg II tibia (♂) ventromedian apophysis moderate to very large (fig. 12D); leg II tibia and metatarsus (♂) with pad of bristlelike setae on ventral surface; leg II femur (♂) markedly incrassate. . . . . *R. nzerekorensis*
– Leg II tibia (♂) ventromedian apophysis small; leg II tibia and metatarsus (♂) without pad of bristlelike setae ventrally; leg II femur (♂) moderately incrassate . . . . . *R. taii*
13. Cucullus ventrolateral margins rounded; tergite XIII median sclerite rectangular . . . . . *B. megahanseni*
– Cucullus ventrolateral margins truncate (figs. 8C, 27A); tergite XIII median sclerite cup shaped (figs. 23A, 25C, 26C, 27B) 14
14. Cucullus ventral margin bilobate in anterior aspect in male and, to lesser extent, female (figs. 8C, 27A); copulatory apparatus (♂) fixed process, *PL* lobe predominantly linear with acute apex, α lobe partially bifid, β lobe medium sized and tuberculate, *rsd* lobe broad and laminar (figs. 18, 29). . . . . *Bambara jocquei*, gen. et sp. nov.
– Cucullus ventral margin sublinear in anterior aspect; copulatory apparatus (♂) fixed process, *PL* lobe curved with rounded apex, α lobe completely bifid, β lobe large and thumb shaped, *rsd* lobe pointed (fig. 17) . . . *Bambara hanseni* (Legg, 1976), comb. nov.
15. Leg III metatarsus (♂) not swollen, dorsal surface with moderate distal concavity; pygidium basal segment, posterior margin broad ventrally (fig. 23E, F); copulatory apparatus (♂) fixed process, apex of *PL* lobe dorsoventrally compressed, β lobe simple (not trifid) (fig. 16). . . . . *Gizoo crassipalpe* (Hansen and Sørensen, 1904), comb. nov.
– Leg III metatarsus (♂) slightly swollen, dorsal surface with deep concavity (figs. 14E, 33); pygidium basal segment, posterior margin narrow (fig. 31C); copulatory apparatus (♂) fixed process, apex of *PL* lobe laterally compressed, β lobe trifid (fig. 20). . . . . 16 (*Tautau*, gen. nov.)
16. Pedipalp tibia robust along entire length, entirely, densely granular, and acarinate apically; copulatory apparatus (♂) fixed process without lanceolate projection, β lobe with distalmost tip simple . . . . . *T. leonensis*
– Pedipalp tibia swollen proximally, predominantly smooth, and bearing apical longitudinal carinae (figs. 11E, 31D, E); copulatory apparatus (♂) fixed process with large lan-

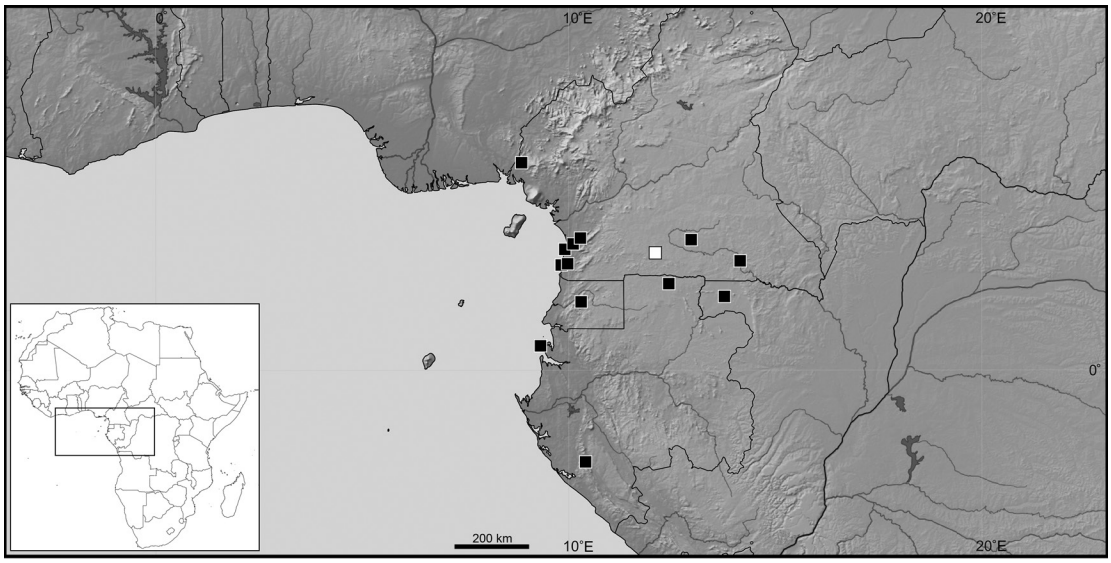

FIGURE 3. Map of West Africa, plotting known locality records of *Alantakun karschii* (Hansen and Sørensen, 1904), comb. nov. (squares), based on material examined and verified identifications (precise locality of lectotype uncertain). Type locality of *Ricinoides olounoua* Legg, 1978, syn. nov., indicated with white square.

ceolate projection, β lobe with distalmost tip bicuspid (fig. 20) ..... *T. ziama*

17. Leg I tibia (♂) with retroventral apophysis (fig. 12A); semiocelli medium sized, clearly visible; opisthosomal tergite XIII median sclerite longer than wide ..... *U. sjostedtii*

– Leg I tibia (♂) without retroventral apophysis (fig. 37D); semiocelli medium sized, barely visible in dorsal aspect (figs. 34A, 35A); opisthosomal tergite XIII median sclerite wider than long (figs. 34C, 35C) ..... *Ududo tuxeni*, gen. et sp. nov.

***Alantakun*, gen. nov.**

Figures 1–3, 8F, 11A, B, 13A, 14A, 19, 22A, 23C, D, 24A, table 1

Type Species: *Cryptostemma karschii* Hansen and Sørensen, 1904 [= *Alantakun karschii* (Hansen and Sørensen, 1904), comb. nov.], here designated.

Diagnosis: *Alantakun* may be separated from other African genera of Ricinulei as follows. The tegument of *Alantakun* lacks polygonal (calyxlike to navicular) setae, which are present in *Bambara* (figs. 25, 26, 27B), *Gizoo*, and *Tautau* (figs. 30, 31), and bears distinct saucer-shaped granules, which are absent in *Bambara*, *Gizoo*, *Ricinoides*, and *Tautau*, and obsolete in *Ududo*. The granules on the carapace and dorsal surface of the opisthosoma are distinctly clustered in *Alantakun*, but separated in the other genera (figs. 26A, C, 30A, C). The carapace lacks a posteromedian moundlike excrescence in the male and female of *Alantakun* that is present in the males of *Gizoo* and *Tautau* (figs. 30A, 31A) and the females of *Bambara* (fig. 26A) and *Gizoo*. The ventral part of the anterior surface of the cucullus (♂) is triangular, approximately flat, and coarsely granular, in *Alantakun* (fig. 8F), whereas it is shallowly convex and not particularly coarsely granular, in the other genera (fig. 8A–E, G). The ventrolateral margins of the cucullus are rounded in *Alantakun*, but moderately truncate in *Bambara* (except in *B. megahanseni*, known only from the female) (figs. 8C, 27A). The ventral margin of the cucullus is linear or sublinear in *Alantakun*,

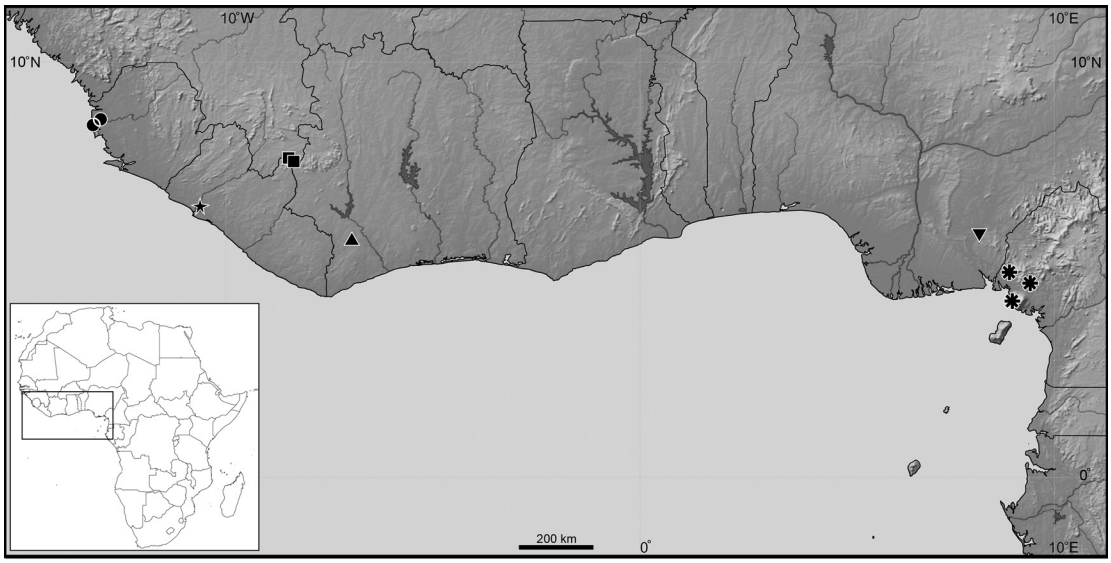

FIGURE 4. Map of West Africa, plotting known locality records of species of *Bambara*, gen. nov., and *Ududo* gen. nov., based on material examined and verified identifications: *Bambara hanseni* (Legg, 1976), comb. nov. (circles); *Bambara jocquei*, sp. nov. (squares); *Bambara megahanseni* (Legg, 1982), comb. nov. (triangle); *Bambara* sp. (star); *Ududo sjostedtii* (Hansen and Sørensen, 1904), comb. nov. (asterisks); *Ududo tuxeni*, sp. nov. (inverted triangle).

but bilobate in the male and female of *Ududo* (at least in *U. tuxeni*, as the female of *U. sjostedtii* is unknown), and bilobate in the male and, to a lesser extent, the female of *B. jocquei* (fig. 27A). The tritosternum is extremely small, not exposed and only visible when the pedipalp coxae are pulled, in *Alantakun* (fig. 22A), but vestigial, yet visible, in the other genera (figs. 22B, 25B, 26B, 30B, 34B, 35B). The pedipalp tibia is markedly swollen proximally compared to the rest of segment, in *Alantakun* (fig. 11A, B), but moderately swollen proximally in *Ududo* (figs. 11F, 36C), and robust along its entire length in most *Ricinoides* (except *R. feae* and *R. westermannii*, in which it is not noticeably robust) (fig. 11D) and *T. leonensis*. The pedipalp tibia lacks apical longitudinal carinae in *Alantakun* (fig. 11A, B), which are present in *Bambara* (figs. 11C, 27D) and *T. ziama* (figs. 11E, 31D, E). The distal region of the pedipalp tibia bears raised tubercles, which are elongate in *Alantakun* (fig. 11B), oval in *Ricinoides* (fig. 11D) and *Ududo* (fig. 11F), and absent in *Bambara* (figs. 11C, 27D) and *Tautau* (figs. 11E, 31D, E). A dorsal longitudinal sulcus is absent on the leg femora in *Alantakun*, but present in *Ricinoides*. The leg I tibia (♂) lacks ventral apophyses in *Alantakun*, which are present in *Ududo* (figs. 12A, C, 37C, D). The leg I metatarsus (♂) is sublinear in lateral aspect and subcircular in cross section, in *Alantakun*, but convex ventrally in lateral aspect and dorsoventrally elongate in cross section, in *Ududo* (figs. 12C, 36E). The leg I metatarsus (♂) exhibits a proventral proximal depression in *Alantakun*, which is absent in *Bambara*, *Gizoo*, *Tautau*, and *Ududo* (fig. 12C). The leg II femur (♂) is moderately to markedly swollen and robust in *Alantakun*, but slender in *Bambara* (fig. 28A, B), *Gizoo*, *Tautau* (fig. 32A, B), and *Ududo* (fig. 37A, B). The leg II tibia (♂) lacks a ventromedian apophysis in *Alantakun*, which is present in *Ricinoides* (except *R. westermannii*) (fig. 12D). The leg II metatarsus (♂) of *Alantakun* lacks a ventral subproximal depres-

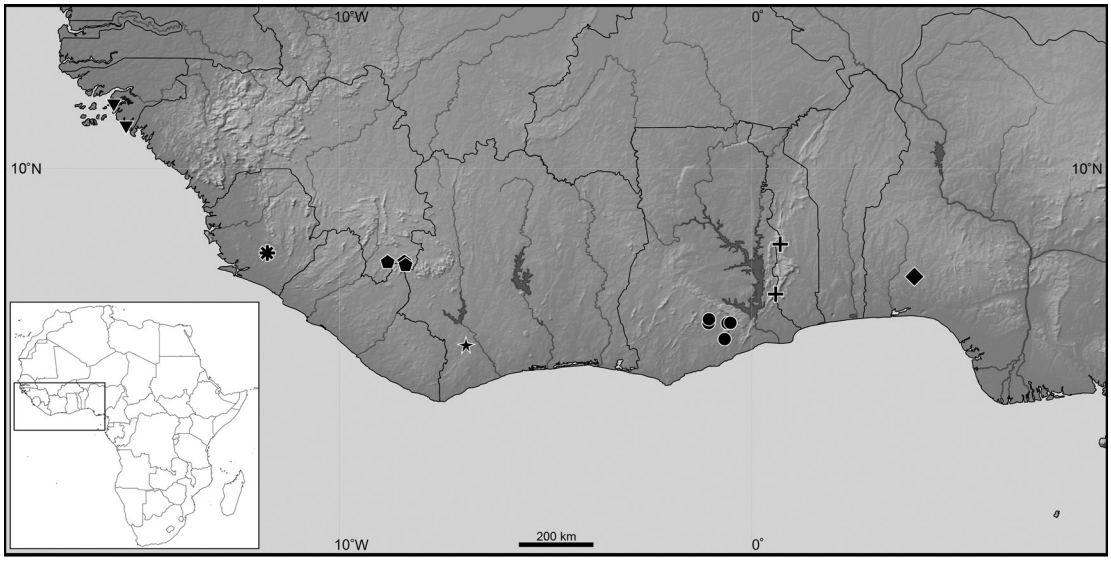

FIGURE 5. Map of West Africa, plotting known locality records of species of *Ricinoides* Ewing, 1929, based on material examined and verified identifications: *Ricinoides afzelii* (Thorell, 1892) (asterisk); *Ricinoides atewa* Naskrecki, 2008 (circles); *Ricinoides feae* (Hansen, 1921) (inverted triangles); *Ricinoides iita* Botero-Trujillo et al., 2021 (diamond); *Ricinoides nzerekorensis* Botero-Trujillo et al., 2021 (pentagons); *Ricinoides taii* Botero-Trujillo et al., 2021 (star); *Ricinoides westermannii* (Guérin-Méneville, 1838) (crosses).

sion, which is present in *Ricinoides* (fig. 12E), and exhibits a ventrosubmedian concavity, which is absent in the other genera. The terminal (fifth) tarsomere of leg II is movable, not fused to the preceding tarsomere, in *Alantakun*, but fixed, fused to the preceding (fourth) tarsomere, in *Gizoo* and *Tautau* (fig. 32E). The leg III femur (♂) is slightly swollen in *Alantakun*, but slender in *Bambara*, *Gizoo*, *Ricinoides* (except *R. afzelii* and *R. iita*), and *Tautau*. The leg III metatarsus (♂) is slightly swollen in *Alantakun* (fig. 14A), but relatively slender in *Bambara* (figs. 14B, C, 29), *Gizoo*, *Ricinoides* (fig. 14D), and *Ududo* (figs. 14F, 38). The dorsal surface of the leg III metatarsus (♂) is deeply excavated basally in *Alantakun* (fig. 14A), moderately excavated in *Ududo* (figs. 14F, 38D), and not excavated in the other genera (figs. 14B–E, 29D, 33D). The dorsal concavity on the leg III metatarsus (♂) is very deep, forming a well-defined chamber in the distal half of the segment, in *Alantakun* (fig. 14A), which extends to the attachment point of the metatarsal process, in *Tautau* (fig. 14E), but is moderately deep, gradually becoming shallower proximally, in *Bambara* (fig. 14B, C), *Gizoo*, and *Ricinoides* (fig. 14D). The prodorsal margin of the second tarsomere of leg III (♂) is moderately angular proximally (in prolateral aspect) in *Alantakun* (fig. 13A), but sublinear to slightly curved in the other genera (figs. 13B, 29B, 33B, 38B). The third tarsomere of leg III (♂) lacks an acute dorsodistal process in *Alantakun*, which is present in *Ricinoides* (fig. 13B). The male copulatory apparatus fixed process is of the *karschii* Type in *Alantakun* (fig. 19). The median sclerite of opisthosomal tergite XIII is rectangular to trapezoid in *Alantakun*, but cup-shaped in *Bambara* (except *B. megahanseni*) (figs. 23A, 25C, 26C). The posteroventral and, to a lesser extent, posterodorsal margins of the opisthosoma are armed with posteriorly directed subspiniform granules, in *Alantakun*, whereas these granules are absent in *Bambara* (figs. 25C, D, 26C, D, 27B), *Gizoo*, *Ricinoides*, and

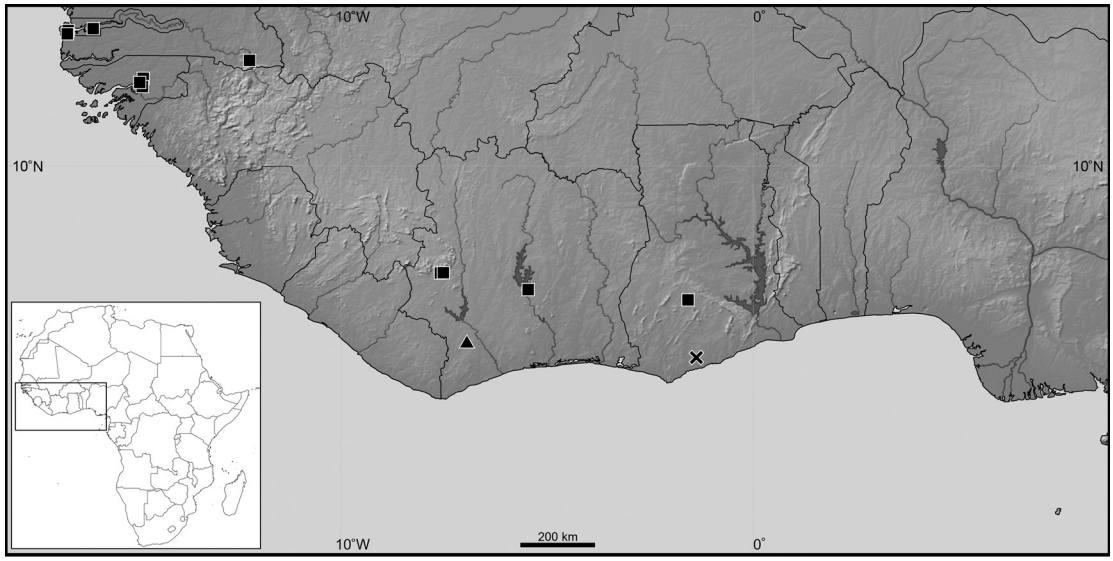

FIGURE 6. Map of West Africa, plotting known locality records of species of *Ricinoides* Ewing, 1929, based on material examined and verified identifications: *Ricinoides eburneus* Botero-Trujillo et al., 2021 (triangle); *Ricinoides kakum* Botero-Trujillo et al., 2021 (×); *Ricinoides* sp. (squares).

Tautau (figs. 30A, B, 31C). The opisthosomal dorsal and ventral pleural membranes are finely and densely granular in *Alantakun*, whereas the dorsal pleural membrane and, sometimes, the ventral pleural membrane, are moderately to sparsely granular in *Bambara*. The basal segment of the pygidium is parallel to the longitudinal axis of the opisthosoma in *Alantakun* (fig. 23C, D), but slightly tilted dorsally in *Bambara* (figs. 25C, 26C), *Gizoo*, and *T. ziama* (fig. 30C). The posterior margin of the basal segment of the pygidium is entirely broad in *Alantakun*, more markedly so ventrally (fig. 23C, D), whereas it is only broad ventrally in *Gizoo* (fig. 23E, F), and narrow in *Bambara*, *Ricinoides*, and *Tautau*. The opening of the basal segment of the pygidium is at least half the lateral width of the segment at its base, in *Alantakun*, but distinctly narrow, its width two-fifths to one-third the lateral width of the segment, in *Ricinoides*.

Etymology: The generic name means "spider" in Yorùbá, an indigenous language spoken in several West African countries. Gender feminine.

Included Species: *Alantakun*, gen. nov., is hereby created to accommodate a species formerly assigned to *Ricinoides*, *Alantakun karschii* (Hansen and Sørensen, 1904), comb. nov.

Distribution: *Alantakun* has been recorded from Cameroon, Congo, Equatorial Guinea, and Gabon (fig. 3).

Alantakun karschii
(Hansen and Sørensen, 1904), comb. nov.

Figures 3, 8F, 11A, B, 13A, 14A, 19, 22A, 23C, D, 24A, table 1

Cryptostemma westermanni Guérin-Méneville: Karsch, 1892a: 32, unpaginated, pl. 4, figs. 1–3; 1892b: 64 (misidentifications).

Cryptostemma karschii Hansen and Sørensen, 1904: 153, 154, unpaginated, pl. VIII, figs. 4a, b, unpaginated, pl. IX, figs. 1a–l; Lankester, 1904: 257, 258, figs. 73–76; Petrunkevitch, 1913: 76, fig. 41; Hansen, 1930: unpaginated, pl. XV, fig. 9c; Moritz and Fischer, 1980: 139.

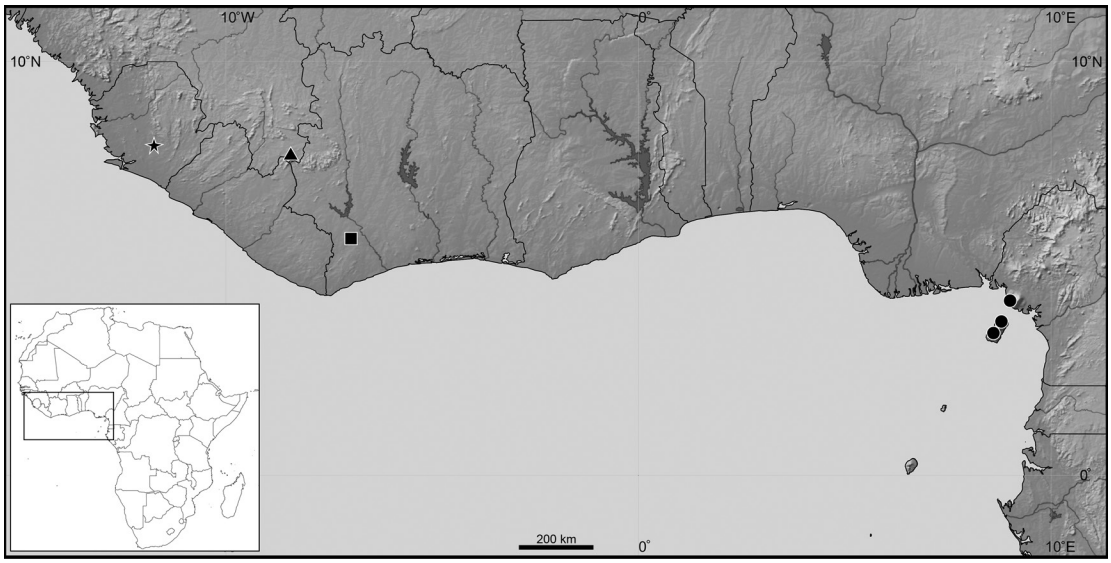

FIGURE 7. Map of West Africa, plotting known locality records of species of *Gizoo*, gen. nov., and *Tautau*, gen. nov., based on material examined and verified identifications: *Gizoo crassipalpe* (Hansen and Sørensen, 1904), comb. nov. (circles); *Tautau leonensis* (Legg, 1978), comb. nov. (star); *Tautau ziama*, sp. nov. (triangle); *Tautau* sp. (square).

Ricinoides karschii (Hansen and Sørensen, 1904): Ewing, 1929: 597; Kästner, 1932: 100, 101, 103, 107, 111, figs. 132, 133, 138, 139, 143, 152; Bolívar y Pieltain, 1942: 201; Petrunkevitch, 1955: 160, fig. 114(2); Pittard, 1970: 26; Pittard and Mitchell, 1972: 13; Legg, 1976b: 2, 54; Hammen, 1979: 5, 10, 13, 33, 34, 36–52, 55–58, figs. 2, 3, 5–21, 24–27; Harvey, 1984: 205, 208, 209, fig. 11; Hammen, 1989: 435, 454, 461, figs. 230, 231, 233–249, 252–255; Shultz, 1989: 18; Harvey, 2003: 183; Talarico and Michalik, 2010: 384–388, figs. 1–3, 4a, b; Talarico et al., 2011: 90; Murienne et al., 2013: 2, 4, 5, figs. 1, 2; Tourinho et al., 2014: 82; Fernández and Giribet, 2015: 2, 3, 6, 8, 11, figs. 1b, 3a–c; Salvatierra and Tourinho, 2016: 2, 3; Ballesteros et al., 2019: 6, figs. 3a, c; Lozano-Fernández et al., 2019: 4, fig. 2; Whalen and Selden, 2021: 605–608; Benavides et al., 2021: 3, 7, 10–12, 14, 15, figs. 1a, 3a, b, 4a, 5; Botero-Trujillo et al., 2021a: 12.

Ricinoides karschi: Tuxen, 1974: 87–89, 91, 100, 101, figs. 1c, 29–33; Legg, 1976a: 243–248, figs. 1–21; 1978a: 91, 93, 99; 1982: 295.

Ricinoides cf. *karschii*: Murienne et al., 2013: 2, 4, 5, figs. 1, 2; Fernández and Giribet, 2015: 6; Sato et al., 2024: 2, 8, figs. 1a, 4a.

Ricinoides olounoua Legg, 1978a: 89–93, 99, figs. 1–8; Selden, 1992: 599; Harvey, 2003: 183; Benavides et al., 2021: 3, 12, fig. 1b; Botero-Trujillo et al., 2021a: 12; Král et al., 2025: 6, 10, 26, 29, 41, 59, figs. 16A, 22 (misidentifications); syn. nov.

Ricinoides cf. *olounoua*: Murienne et al., 2013: 2, 4, 5, figs. 1, 2; Fernández and Giribet, 2015: 6; Benavides et al., 2021: 7, 11, 12, 14, 15, figs. 3b, 4a, 5; Sato et al., 2024: 2, 8, figs. 1a, 4a (misidentifications).

Type Material Examined: *Cryptostemma karschii*: Lectotype ♂ (BMNH 13588959), **CONGO:** Benita River, G.L. Bates. Paralectotypes: 2 ♀, in same vial and with same data as lectotype; 1 ♂, 1 ♀ (ZMB 7833), **CAMEROON:**

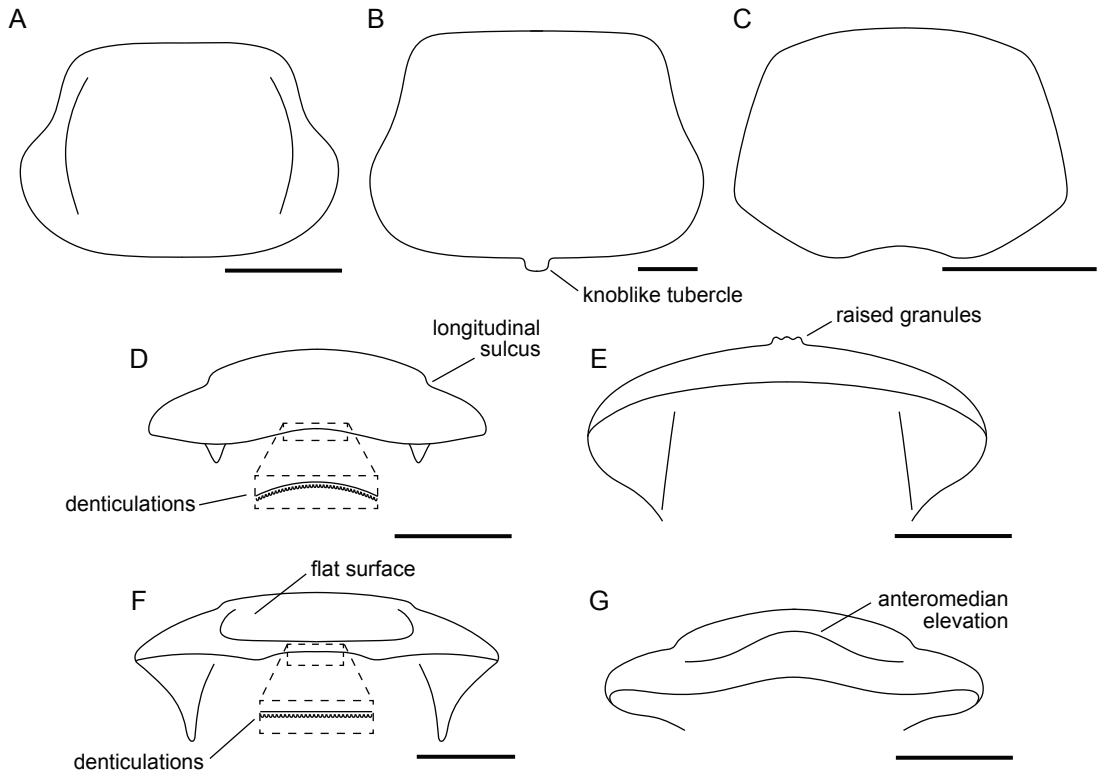

FIGURE 8. *Alantakun*, gen. nov., *Bambara*, gen. nov., and *Ricinoides* Ewing, 1929, cucullus, **A–C.** anterior, **D, G.** ventral, and **E, F.** posteroventral aspects. **A, D.** *Ricinoides westermannii* (Guérin-Méneville, 1838), neotype ♂ (ZMB 7013), illustrating median row of denticulations on ventral margin (**D**). **B.** *Ricinoides afzelii* (Thorell, 1892), ♂ (BMNH 13588948). **C.** *Bambara jocquei*, gen. et sp. nov., holotype ♂ (MRAC 209.284), illustrating bilobate ventral margin and truncate ventrolateral margins. **E.** *Ricinoides atewa* Naskrecki, 2008, holotype ♂ (AMNH IZC 324855). **F.** *Alantakun karschii* (Hansen and Sørensen, 1904), comb. nov., ♂ (CAS CASENT 9080643), illustrating median row of denticulations on ventral margin. **G.** *Ricinoides iita* Botero-Trujillo et al., 2021, holotype ♂ (USNM). Scale bars = 1 mm (**A, D, E, G**), 0.5 mm (**B, C, F**).

South Region: Kribi [02°56′N 09°55′E], x.1988. *Ricinoides olounoua*: Holotype ♂ (MRAC 141.310), **CAMEROON:** *South Region*: Olounou [02°49′N 12°05′E], 11–19.ix.1971, F. Puylaert.

Diagnosis: As for the genus.

Distribution: *Alantakun karschii* is known from several localities in Cameroon, Congo, Equatorial Guinea, and Gabon (fig. 3).

Remarks: The precise locality at which the lectotype of *A. karschii* was collected is unclear and the specimen is severely damaged, lacking the opisthosoma, cucullus, chelicerae, and fourth pair of legs. Both copulatory apparatuses are missing from the paralectotype male. A nontype male specimen from an accurate locality in the province of Woleu-Ntem, Gabon, is similar morphologically to what remains of the lectotype. This specimen, as well as a conspecific female and some immatures from the same locality, are in good condition. In the circumstances, these specimens from Gabon shall serve as reference materials of *A. karschii*, despite lacking type status.

The adult morphology of *R. olounoua* (here synonymized with *A. karschii*) was known only from the male. Differences between *R. olounoua* and *A. karschii* are entirely morphometric and appear to represent intraspecific rather than interspecific variation. The possibility that *R.*

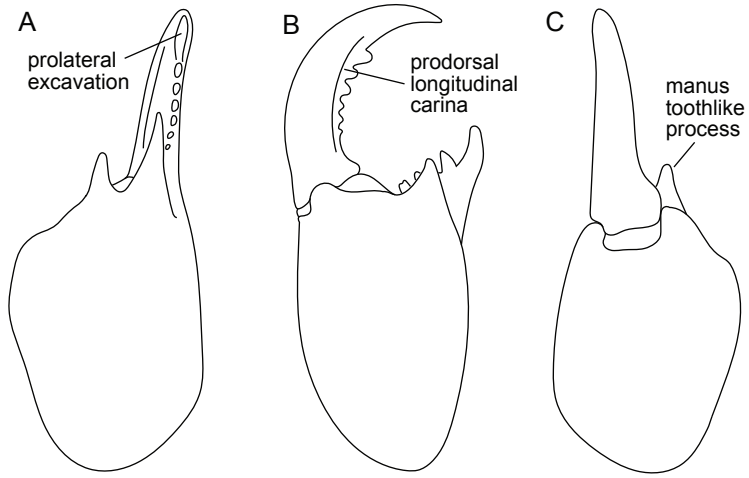

FIGURE 9. *Ricinoides westermannii* (Guérin-Méneville, 1838), neotype ♂ (ZMB 7013), chelicera, **A.** prolateral, **B.** dorsal, and **C.** retrolateral aspects. Scale bar = 0.5 mm.

olounoua could be a synonym of *A. karschii* was previously considered by Benavides et al. (2021: 12), based on molecular species delimitation; however, the specimens were identified as "*R.* cf. *olounoua*."

Additional Material Examined: **CAMEROON:** Cameroons, G.L. Bates, 1 ♂ (BMNH 13588960), 1 ♀ (BMNH 13588961). *East Region*: Dja Reserve [03°09′N 13°00′E], 19.iv.2005, I. Deblauwe, old secondary forest, pitfall, 1 ♀ (MRAC 219.781); north of Dja Reserve [03°09′N 13°00′E], 8.iii.2005, I. Deblauwe, old secondary forest, pitfall, 1 ♀ (MRAC 220.670), same data, except: 10.xi.2004, 1 ♀ (MRAC 216.492). Ja River [02°37′N 14°09′E], G.L. Bates, 1 ♂ (BMNH 13588946 old 08.8.11.43-44), 1 ♀ (BMNH 14041440 old 08.8.11.43-44). *South Region*: Province Sud: Bondé Forest N'kolo village, 27.5 km 155° SSE Elogbatindi, 03°13′18″N 10°14′48″E, 40 m, 12.iv.2000, B.L. Fisher, rainforest sifted litter [BLF 2323], 1 ♂ (CAS CASENT 9042979); Réserve de Faune de Campo: Massif des Mamelles, 15.1 km 84° E Ébodjé, 02°35′39″N 09°57′34″E, 180 m, 4.iv.2000, B.L. Fisher, rainforest, sifted litter, 1 deutonymph, 1 larva (CAS CASENT 9080571), 2.16 km 106° ESE Ébodjé, 02°34′04″N 09°50′40″E, 10 m, 9.iv.2000, B.L. Fisher, littoral rainforest, sifted litter, 1 deutonymph (CAS CASENT 9062627). Kribi, road towards Bipindi, near Bidou [03°01′N 10°05′E], 12.x.2014, A. Henrard and D. van den Spiegel, forested mountain ridge, primary forest, 1 ♀ (MRAC 243.798), 1 protonymph (MRAC 243.797), same data, except: 15.x.2014, 1 tritonymph, 2 protonymphs (MRAC 243.888), 2 deutonymphs, 1 protonymph (MRAC 243.907); Kribi, road towards Bipindi, Bidou [03°01′N 10°05′E], 12.x.2014, D. van den Spiegel and A. Henrard, in degraded forest near cacao plantation, disturbed vegetation near secondary forest, 1 deutonymph (MRAC 243.854). *West Region*: Province Sud-Ouest: Korup National Park, 6.9 km 317° NW Mundemba, 05°00′58″N 08°51′50″E, 110 m, 19.iv.2000, B.L. Fisher, rainforest, sifted litter, 2 protonymphs (CAS CASENT 9080570). **EQUATORIAL GUINEA:** Span. Guinea, Afrika, 1 ♀ (SMF 1262). **GABON:** *Estuaire*: F.C. Mondah, 21 km 331° NNW Libreville, 00°34′36″N 09°20′06″E, 10 m, 24.ii.1998, B.L. Fisher, rotten wood rainforest, sifted leaf litter, 1 larva (CAS CASENT 9080642). *Ogooué-Maritime*: Aire d'Exploit, Rationnelle de Faune des Monts Doudou, 25.2 km 304° NW Doussala, 02°13′39″S 10°23′40″E, 640 m, 14.iii.2000, B.L. Fisher, rainforest, sifted litter, 1 tritonymph, 1 larva (CAS CASENT 9080569), same data,

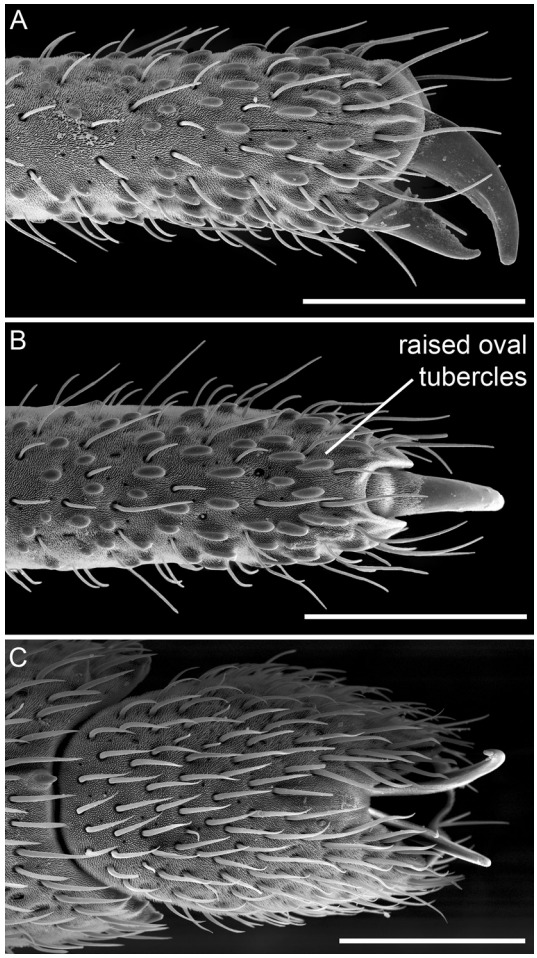

FIGURE 10. *Ricinoides* sp., tritonymph (AMCC [LP 4664]), scanning electron micrographs. **A, B.** Pedipalp tibia, distal part, **A.** retrolateral and **B.** dorsal aspects. **C.** Sinistral leg I tarsus, ventral aspect, illustrating absence of ventrodistal papillae. Scale bars = 0.2 mm.

except: 24.3 km 307° NW Doussala, 02°13′21″S 10°24′21″E, 375 m, 6.iii.2000, 1 ♀, 2 larvae (CAS CASENT 9062624), 1 tritonymph, 2 protonymphs, 8 larvae (CAS CASENT 9080568), 1 protonymph (CAS CASENT 9080641), 24.5 km 303° NW Doussala, 02°13′58″S 10°23′53″E, 630 m, 18.iii.2000, 2 larvae (CAS CASENT 9056956), 1 larva (CAS CASENT 9056956). *Woleu-Ntem Prov.*: 31.3 km 108° ESE Minvoul, 02°04′48″N 12°24′24″E, 600 m, 7.ii.1998, B.L. Fisher, rainforest, sifted leaf litter, mold, rotten wood, 1 ♂, 1 ♀, 1 tritonymph, 2 deutonymphs, 2 protonymphs (CAS CASENT 9080643), same data, except: 11.ii.1998, 1 tritonymph, 1 protonymph (CAS CASENT 9080567).

***Bambara*, gen. nov.**

Figures 1, 2, 4, 8C, 11C, 14B, C, 17, 18, 23A, 24B, 25–29, tables 1, 2

Type Species: *Bambara jocquei*, sp. nov., here designated.

Diagnosis: *Bambara* may be separated from other African genera of Ricinulei as follows. The tegument of *Bambara* bears polygonal setae (figs. 25, 26, 27B), which are absent in *Alantakun*, *Ricinoides*, and *Ududo* (figs. 34, 35, 36B), and lacks saucer-shaped granules, which are present in *Alantakun* and *Ududo*. The granules on the carapace and dorsal surface of the opisthosoma are separated in *Bambara* (figs. 25A, C, 26A, C), but distinctly clustered in *Alantakun*. The carapace of the female, but not the male, of *Bambara* (the male of *B. megahanseni* is unknown) exhibits a posteromedian moundlike excrescence (fig. 26A) which is absent in both sexes of *Alantakun*, *Ricinoides* (the females of *R. eburneus*, *R. iita*, and *R. westermannii* are unknown), and *Ududo* (the female of *U. sjostedtii* is unknown) (fig. 35A), whereas it is present in the male and female of *Gizoo*, and at least in the male of *Tautau* (the females of *T. leonensis* and *T. ziama* are unknown) (figs. 30A, 31A). The ventral part of the anterior surface of the cucullus (♂) is shallowly convex and does not bear particularly coarse granules in *Bambara* (figs. 8C, 27A), whereas it has an approximately flat surface and is coarsely granular in *Alantakun* (fig. 8F). The ventrolateral margins of the cucullus are truncate in *Bambara* (figs. 8C, 27A), except for *B. megahanseni* in which the margins are unmodified (at least in the female), but rounded in the other genera (figs. 8A, B, E, 31B, 36A). The tritosternum is vestigial, yet visible, in *Bambara* (figs. 25B, 26B), but extremely small, not exposed, in *Alantakun* (fig.

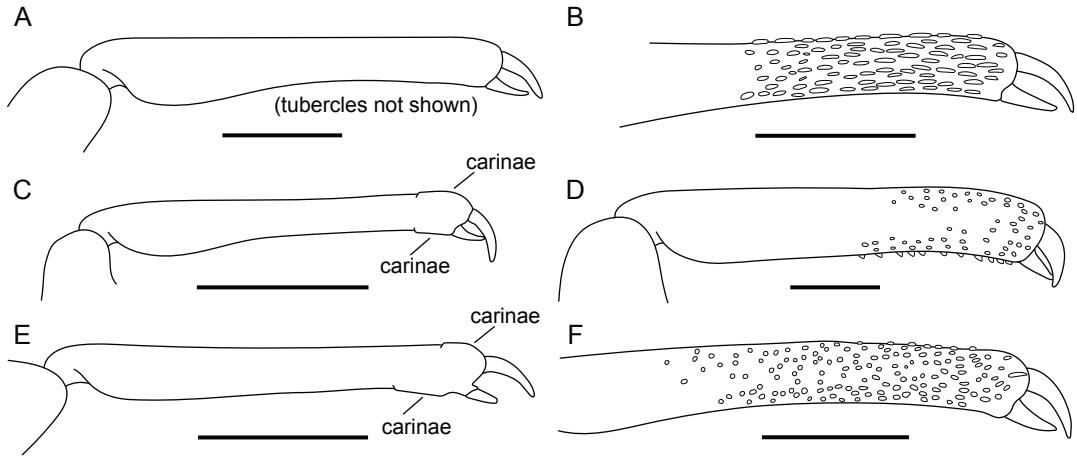

FIGURE 11. *Alantakun*, gen. nov., *Bambara*, gen. nov., *Ricinoides* Ewing, 1929, *Tautau*, gen. nov., and *Ududo*, gen. nov., pedipalp tibia, prolateral aspect. **A, B.** *Alantakun karschii* (Hansen and Sørensen, 1904), comb. nov., ♂ (CAS CASENT 9080643), illustrating raised elongate tubercles (**B**). **C.** *Bambara hanseni* (Legg, 1976), comb. nov., holotype ♂ (BMNH 13588962). **D.** *Ricinoides nzerekorensis* Botero-Trujillo et al., 2021, holotype ♂ (MRAC 209.266), illustrating raised oval tubercles. **E.** *Tautau ziama*, gen. et sp. nov., holotype ♂ (MRAC 209.517). **F.** *Ududo tuxeni*, gen. et sp. nov., holotype ♂ (BMNH 13588977 old 1953.3.28.71), illustrating raised oval tubercles. Scale bars = 0.5 mm.

22A). The pedipalp tibia is markedly swollen proximally compared to the rest of the segment, in *Bambara* (figs. 11C, 27C, D), but moderately swollen proximally in *Ududo* (figs. 11F, 36C, D), and robust along its entire length in most *Ricinoides* (except for *R. feae* and *R. westermannii*, in which it is not noticeably robust) (fig. 11D) and *T. leonensis*. The pedipalp tibia bears apical longitudinal carinae in *Bambara* (figs. 11C, 27C, D), which are absent in the other genera (except *T. ziama*) (figs. 11A, B, D, F, 36C, D). The distal region of the pedipalp tibia lacks raised tubercles in *Bambara* (figs. 11C, 27C, D) that are present and oval in *Ricinoides* (fig.11D) and *Ududo* (figs. 11F, 36C, D) or elongate in *Alantakun* (fig. 11B) and *Gizoo*. A dorsal longitudinal sulcus is absent on the leg femora in *Bambara*, but present in *Ricinoides*. The leg I femur (♂) is slender in *Bambara* (at least in *B. hanseni* and *B. jocquei*) but slightly swollen in *Alantakun, Ricinoides* (except *R. taii*), and *Ududo*. The leg I tibia (♂) lacks ventral apophyses in *Bambara*, which are present in *Ududo* (figs. 12A, C, 37C, D). The leg I metatarsus (♂) is sublinear in lateral aspect and subcircular in cross section in *Bambara*, but convex ventrally in lateral aspect and dorsoventrally elongate in cross section in *Ududo* (figs. 12C, 36E). The leg I metatarsus (♂) lacks a proventral proximal depression in *Bambara*, which is present in *Alantakun* and *Ricinoides* (fig. 12B). The leg II femur (♂) is slender in *Bambara* (fig. 28A, B), but moderately to markedly swollen and robust in *Alantakun* and *Ricinoides*. The leg II tibia (♂) lacks a ventromedian apophysis in *Bambara* (fig. 28C), which is present in *Ricinoides* (except *R. westermannii*) (fig. 12D). The leg II metatarsus (♂) of *Bambara* lacks a ventral subproximal depression (fig. 28D), which is present in *Ricinoides* (fig. 12E), and a ventrosubmedian concavity, which is present in *Alantakun*. The terminal (fifth) tarsomere of leg II is movable, not fused to the preceding tarsomere, in *Bambara* (fig. 28E), but fixed, fused to the preceding (fourth) tarsomere, in *Gizoo* and *Tautau* (fig. 32E). The leg III femur (♂) is slender in *Bambara*, but slightly swollen in *Alantakun*, *Ududo*, *R. afzelii*, and *R. iita*. The leg III metatarsus (♂) is relatively slender in *Bambara* (figs.

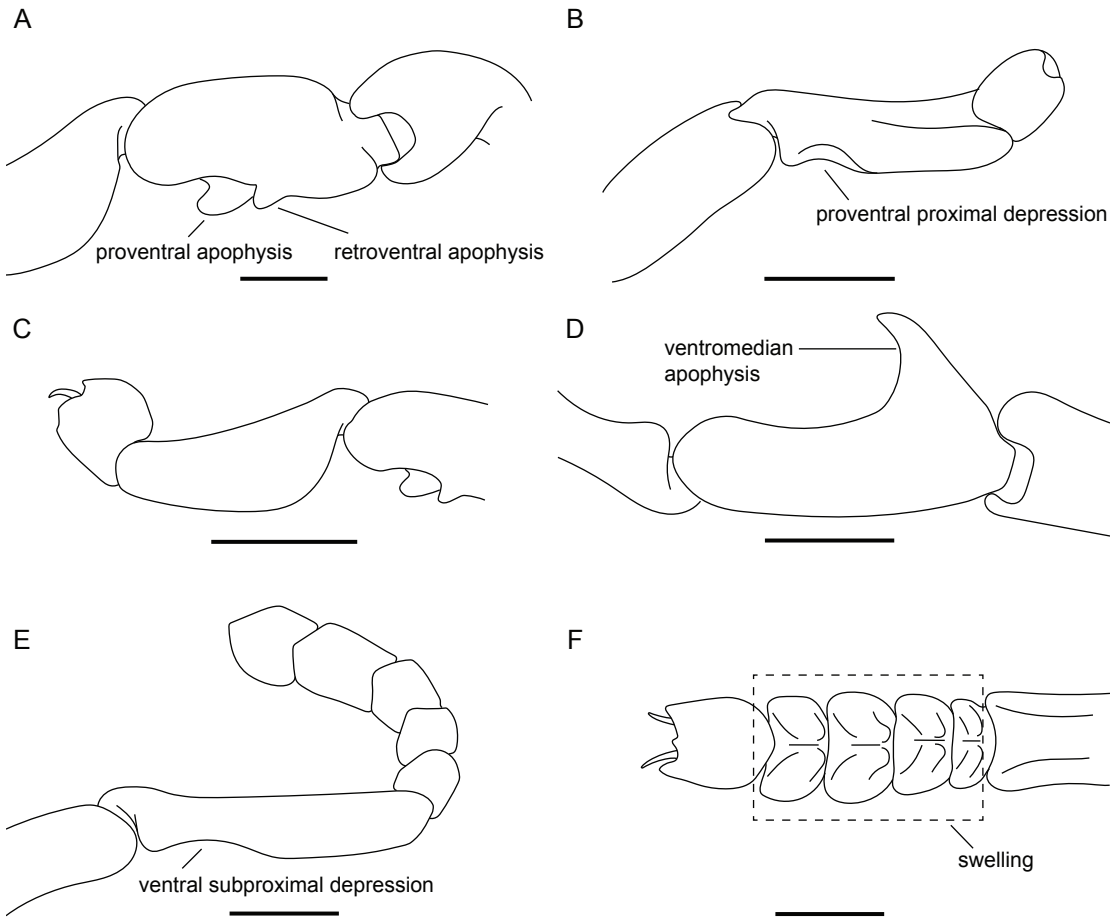

FIGURE 12. *Ricinoides* Ewing, 1929, and *Ududo*, gen. nov., leg segments. **A, C.** *Ududo sjostedtii* (Hansen and Sørensen, 1904), comb. nov., lectotype ♂ (NHRS JUST 519), **A.** leg I tibia, retrolateral aspect, and **C.** leg I metatarsus and tarsus, retrolateral aspect, illustrating metatarsus convex ventrally. **B.** *Ricinoides westermannii* (Guerin-Meneville, 1838), neotype ♂ (ZMB 7013), leg I metatarsus and tarsus, prodorsal aspect. **D, E.** *Ricinoides nzerekorensis* Botero-Trujillo et al., 2021, holotype ♂ (MRAC 209.266), **D.** leg II tibia, prolateral aspect, and **E.** leg II metatarsus and tarsus, prolateral aspect. **F.** *Ududo tuxeni*, gen. et sp. nov., holotype ♂ (BMNH 13588977 old 1953.3.28.71), sinistral leg IV tarsus, dorsal aspect. Scale bars = 0.5 mm (**A, F**), 1 mm (**B–E**).

14B, C, 29) but swollen in *Alantakun* (fig. 14A) and *Tautau* (figs. 14E, 33). The dorsal surface of the leg III metatarsus (♂) is not excavated basally in *Bambara* (figs. 14B, C, 29D), whereas it is moderately excavated in *Ududo* (figs. 14F, 38D) and markedly excavated in *Alantakun* (fig. 14A). The dorsal concavity of the leg III metatarsus (♂) is moderately deep, gradually becoming shallower proximally in *Bambara* (figs. 14B, C, 29D), whereas it is very deep and forms a well-defined chamber extending across the distal half of the segment in *Alantakun* (fig. 14A) and *Ududo* (figs. 14F, 38D) and to the attachment point of the metatarsal process in *Tautau* (figs. 14E, 33D). The prodorsal margin of the second tarsomere of leg III (♂) is sublinear to slightly curved proximally (in prolateral aspect) in *Bambara* (fig. 29B), but moderately angular in *Alan-*

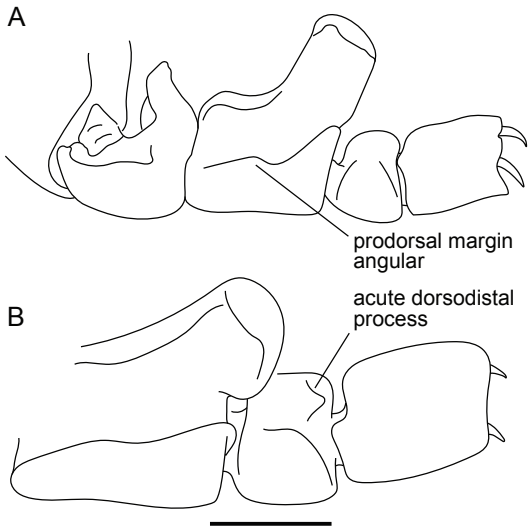

FIGURE 13. *Alantakun*, gen. nov., and *Ricinoides* Ewing, 1929, leg III (modified) tarsus (♂). **A.** *Alantakun karschii* (Hansen and Sørensen, 1904), comb. nov., ♂ (CAS CASENT 9080643), prolateral aspect. **B.** *Ricinoides nzerekorensis* Botero-Trujillo et al., 2021, holotype ♂ (MRAC 209.266), prodorsal aspect. Scale bar = 0.5 mm.

takun (fig. 13A). The third tarsomere of leg III (♂) lacks an acute dorsodistal process in *Bambara*, which is present in *Ricinoides* (fig. 13B). The second to fourth tarsomeres of leg IV (♂) are swollen in *Bambara* (fig. 28F) but unmodified in *Ricinoides*. The male copulatory apparatus fixed process is of the *hanseni* Type in *Bambara* (figs. 17, 18). The median sclerite of opisthosomal tergite XIII is cup shaped in *Bambara* (figs. 23A, 25C, 26C, 27B), except *B. megahanseni* in which, as in other genera, it is rectangular to trapezoid (figs. 23B, 34C, 35C). The tergal membranes of the opisthosoma are smooth in *Bambara*, but granular in *Ricinoides*, *Ududo*, and *T. ziama*. The posterodorsal and posteroventral margins of the opisthosoma lack subspiniform granules in *Bambara* (figs. 23A, 25C, D, 26C, D, 27B), which are present in *Alantakun* and *Ududo* (figs. 23B, 34C, D, 35C, D, 36B). The opisthosomal dorsal pleural membrane and, sometimes, the ventral pleural membrane are moderately to sparsely granular in *Bambara*, but finely and densely granular in the other genera. The basal segment of the pygidium is slightly tilted dorsally, relative to the longitudinal axis of the opisthosoma, in *Bambara* (figs. 25C, 26C, 27B), but parallel to the longitudinal axis in *Alantakun* (fig. 23C, D), *Ricinoides*, *Ududo* (figs. 23G, H, 34C, D, 35C, D, 36B), and *T. leonensis*. The posterior margin of the basal segment of the pygidium is narrow in *Bambara* (figs. 23A, 27B), whereas it is entirely broad in *Alantakun* (fig. 23C, D) and *Ududo* (fig. 23G, H), and only broad ventrally in *Gizoo* (fig. 23E, F). The opening of the basal segment of the pygidium is at least half the lateral width of the segment at its base, in *Bambara*, but distinctly narrow, its width two-fifths to one-third the lateral width of the segment, in *Ricinoides*.

Etymology: The generic name means "spider" in Mandinka, an indigenous language spoken in six West African countries, including Guinea and Côte d'Ivoire. Gender feminine.

Included Species: *Bambara*, gen. nov., is hereby created to accommodate three species, *Bambara jocquei*, sp. nov., and two species, *Bambara hanseni* (Legg, 1976), comb. nov., and *Bambara megahanseni* (Legg, 1982), comb. nov., formerly assigned to *Ricinoides*.

Distribution: Species of *Bambara* have been recorded from Côte d'Ivoire, Guinea, Liberia, and Sierra Leone (fig. 4).

Bambara hanseni (Legg, 1976), comb. nov.

Figures 4, 11C, 14B, 17, 23A, table 1

Ricinoides hanseni Legg, 1976b: 4–51, 52, 54, 55–58, figs. 1–43, unpaginated, pls. 1–6; Dumitresco and Juvara-Balş, 1977a: 174, 175, 178, 179; 1977b: 259–261, fig. 2; Legg, 1976a: 243; 1977: 51–61, figs. 1a–e, 2a–d, 3a–c, 4, 5, pls. Ia, b, IIa, b, III; 1978a: 93, 97–99; Barnes, 1980: 643, fig. 13.51; Legg, 1982: 290, 295, 296; Platnick and Pass, 1982: 2; Harvey, 1984: 209; Barnes, 1987: 533, fig. 13.40; Selden, 1992: 599, 618; Adis et al., 1999: 8; Harvey, 2003: 183; Talarico et al.,

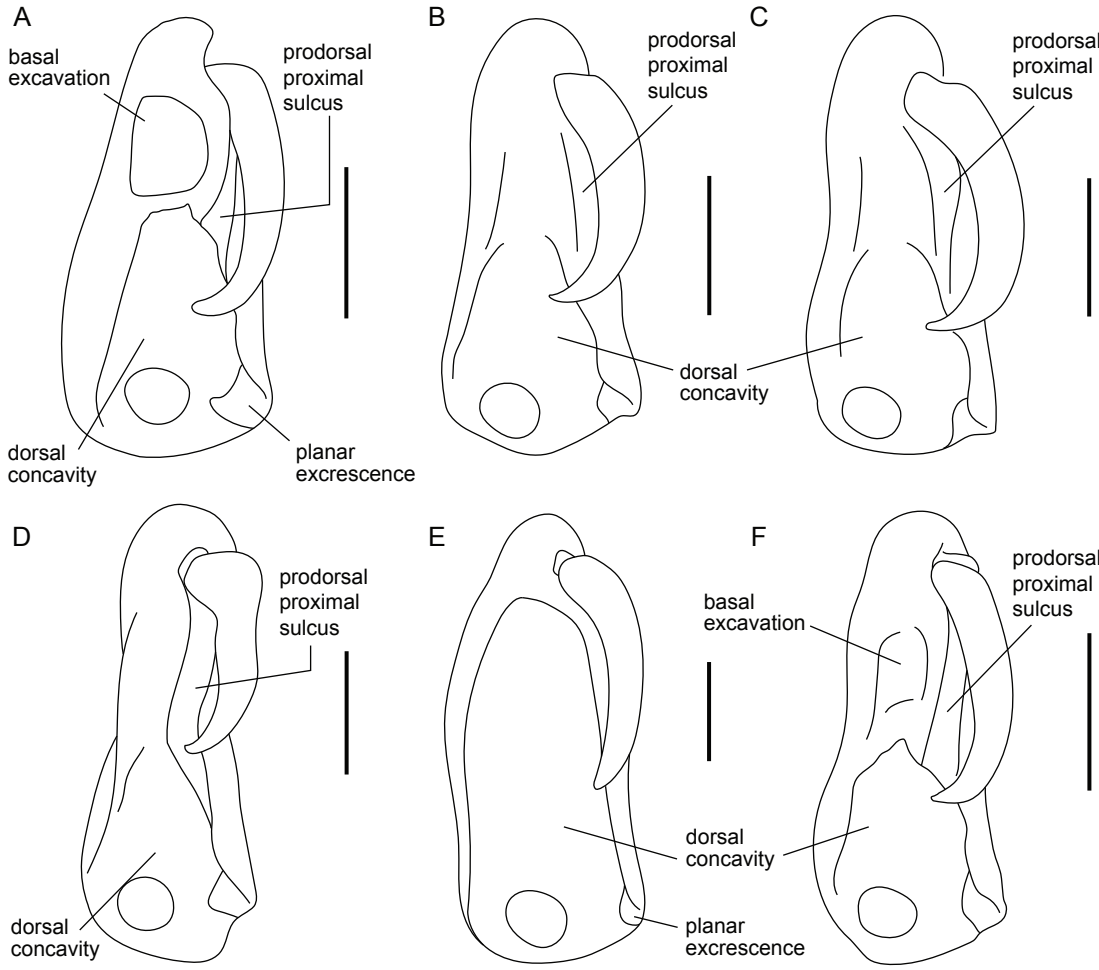

FIGURE 14. *Alantakun*, gen. nov., *Bambara*, gen. nov., *Ricinoides* Ewing, 1929, *Tautau*, gen. nov., and *Ududo*, gen. nov., sinistral (**A, D**) or dextral (**B, C, E, F**) leg III (modified) metatarsus (♂), dorsal aspect. **A.** *Alantakun karschii* (Hansen and Sørensen, 1904), comb. nov., ♂ (CAS CASENT 9080643). **B.** *Bambara hanseni* (Legg, 1976), comb. nov., paratype ♂ (BMNH 13588964). **C.** *Bambara jocquei*, gen. et sp. nov., paratype ♂ (MRAC 209.292). **D.** *Ricinoides westermannii* (Guérin-Méneville, 1838), neotype ♂ (ZMB 7013). **E.** *Tautau ziama*, gen. et sp. nov., holotype ♂ (MRAC 209.517), illustrating prodorsal proximal sulcus covered by metatarsal process. **F.** *Ududo tuxeni*, gen. et sp. nov., paratype ♂ (BMNH 13588981 old 1953.3.28.72-78). Scale bars = 0.5 mm (**A, D, F**), 0.25 mm (**B, C, E**).

2006: 455; 2008a: 403, 407; Beccaloni, 2009: 155; Tourinho et al., 2014: 82; Salvatierra and Tourinho, 2016: 2, 3; Whalen and Selden, 2021: 605, 607, 608; Botero-Trujillo et al., 2021a: 12.

Ricinoides ranseni: Legg, 1976b: 57, pl. 3 (caption).

Type Material Examined: Holotype ♂ (BMNH 13588962), **SIERRA LEONE:** *Western Area*: Freetown, University of Sierra Leone, Fourah Bay College [08°29′N 13°14′W], Botanical Garden, ix.1973, G. Legg, secondary forest. Paratypes: 1 ♀ (allotype, BMNH 13588963), same data as holotype; 2 ♂ (BMNH 13588964), 2 ♀ (BMNH

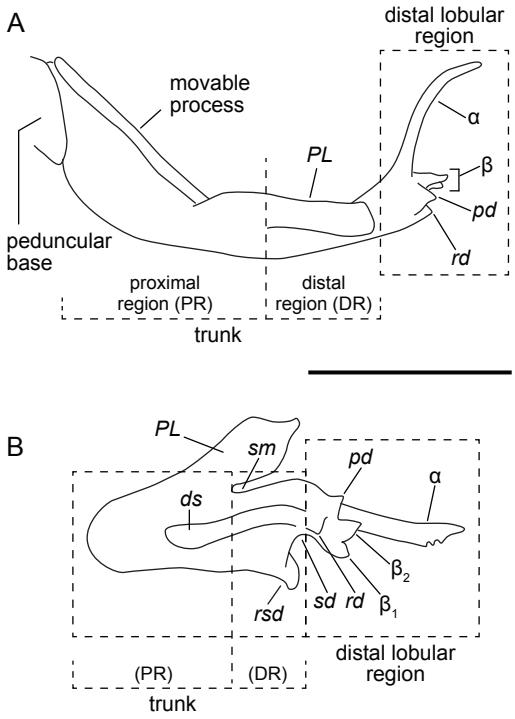

FIGURE 15. *Ricinoides kakum* Botero-Trujillo et al., 2021, holotype ♂ (MRAC 217.183), leg III copulatory apparatus, **A.** prolateral and **B.** ventral aspects, illustrating components of apparatus and structures of fixed process. Abbreviations: α, alpha lobe; β, beta lobe (bicuspid, $\beta_1 + \beta_2$); *ds*, dorsal longitudinal sulcus (translucent in ventral aspect); *pd*, prolateral distal lobe; *PL*, prolateral laminar lobe; *rd*, retrolateral distal lobe; *rsd*, retrolateral subdistal lobe; *sd*, subdistal emargination; *sm*, submedian emargination. Scale bar = 0.5 mm.

13588965), 2 tritonymphs (BMNH 13588966, 13588967), 2 deutonymphs (BMNH 13588968), 2 protonymphs (BMNH 13588969), 2 larvae (BMNH 13588970), same data, except: x.1973.

Diagnosis: *Bambara hanseni* most closely resembles *B. jocquei*, both of which differ from the other species in the genus, *B. megahanseni*, in the moderately truncate ventrolateral margins of the cucullus (figs. 8C, 27A) and the cup-shaped median sclerite of tergite XIII (figs. 23A, 25C, 26C, 27B). The ventral margin of the cucullus is sublinear in anterior aspect in *B. hanseni*, but bilobate in the male and, to a lesser extent, the female, in *B. jocquei* (fig. 8C). Furthermore, major differences in the morphology of the male copulatory apparatus exist between the two species. The *PL* lobe is curved, with a round apex, the α lobe completely bifid, the β lobe large and thumb shaped, and the *rsd* lobe pointed in *B. hanseni* (fig. 17) whereas the *PL* lobe is predominantly linear with an acute apex, the α lobe partially bifid, the β lobe medium sized and tuberculate, and the *rsd* lobe broad and laminar, in *B. jocquei* (fig. 18).

Distribution: *Bambara hanseni* is known only from two localities in the Western Area and Northern Province of Sierra Leone (fig. 4).

Additional Material Examined: **SIERRA LEONE:** *Western Area*: Freetown, University of Sierra Leone, Fourah Bay College [08°29′N 13°13′W], Botanical Garden, 21.iii.1974, G. Legg, leaf litter by stream, 1 ♀ (ZMUC). *Northern Province*: Port Loko, Freetown, Pepeltown [Pepel, 08°35′N 13°04′W], iv.1977, D. Olu-Pitt, 1 ♂ (MRAC 159.076).

***Bambara jocquei*,** gen. et sp. nov.

Figures 4, 8C, 14C, 18, 24B, 25–29, tables 1, 2

Type Material: Holotype ♂ (MRAC 209.284), **GUINEA:** *Nzérékoré Region*: Forêt Classée de Ziama [Ziama Forest Reserve, 07°42′N 08°25′W], 16.ix.1999, D. Flomo, rain forest, pitfall. The holotype lacks the fourth and fifth tarsomeres of sinistral leg IV. Paratypes: 1 ♂ (MRAC 247.305), 1 ♀ (MRAC 209.269), same data as holotype, except: 26.vii.1999; 2 ♀ (MRAC 209.271, 290), same data, except: 8.viii.1999; 1 ♂ (MRAC 209.292), 4.ix.1999; 1 ♂ (MRAC 209.268), 29.ix.1999; 2 ♀ (MRAC 209.512, 282), 10.x.1999; 1 ♂ (MRAC 209.519), 5.xi.1999.

Diagnosis: *Bambara jocquei* most closely resembles *B. hanseni*, both of which differ from the other species in the genus, *B. megahanseni*, in the moderately truncate ventrolateral margins of the cucullus (figs. 8C, 27A) and the cup-shaped median sclerite of tergite XIII (figs. 23A, 25C, 26C, 27B). The ventral margin of the cucul-

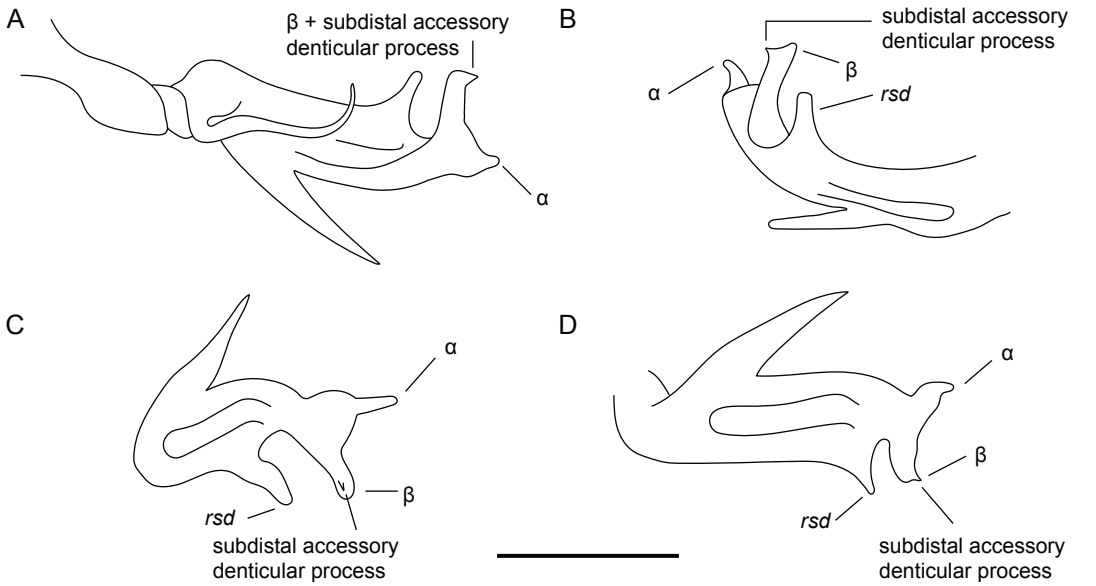

FIGURE 16. *Gizoo crassipalpe* (Hansen and Sørensen, 1904), comb. nov., ♂ (ZMUC), sinistral leg III copulatory apparatus, **A.** dorsal aspect, **B.** retroventral aspect, **C.** frontal (ventrally inclined) aspect, and **D.** ventral aspect. Abbreviations: α, alpha lobe; β, beta lobe; *rsd*, retrolateral subdistal lobe. Scale bar = 0.25 mm.

lus is bilobate in anterior aspect in the male and, to a lesser extent, the female (figs. 8C, 27A), in *B. jocquei*, but sublinear in anterior aspect in *B. hanseni*. Furthermore, major differences in the morphology of the male copulatory apparatus exist between the two species. The *PL* lobe is predominantly linear with an acute apex, the α lobe partially bifid, the β lobe medium-sized and tuberculate, and the *rsd* lobe broad and laminar (figs. 18, 29), in *B. jocquei* whereas the *PL* lobe is curved with a round apex, the α lobe completely bifid, the β lobe large and thumb shaped, and the *rsd* lobe pointed (fig. 17), in *B. hanseni*.

Etymology: The specific epithet is a patronym honoring the Belgian arachnologist, Rudy Jocqué, of the MRAC, in recognition of his many contributions to the advancement of African arachnology.

Description of Male: Based on the holotype (MRAC 209.284).

Measurements: Total length, 3.66 mm (table 2).

Coloration: Soma and appendages predominantly reddish, pedipalps paler (figs. 25, 27–29). Carapace lateral hyaline lines and semiocelli yellowish. Opisthosomal tergal and pleural membranes yellow, hyaline (figs. 25C, 27B). Cheliceral manus yellow (fig. 25B); fingers, finger dentition and manus toothlike process reddish.

Setation: Surfaces densely covered with moderately expanded navicular setae, except on ventral part of cucullus, coxosternal region, pedipalp femur lateral and ventral surfaces, pedipalp tibia, and leg tarsi (figs. 25, 27–29).

Tegument surface: Soma and appendages without cuticular pits. Except for pedipalps, tegument densely covered with iridescent granules evenly spaced apart, not clustered (figs. 25, 27–29). Pedipalp femur predominantly smooth, with sparse granules proximally and ventrally (fig. 27C); tibia entirely smooth, without raised tubercles (fig. 27C, D). Opisthosoma, pleural membranes sparsely granular (figs. 25C, 27B); tergal membranes smooth.

Carapace: Carapace wider than long, broadest between coxae of legs II and III; trapezoidal, lateral margins curved, narrowing anteriorly (fig. 25A); anterior margin linear in dorsal aspect; posterior margin slightly procurved; paired anterolateral longitudinal sulci shallow, median

longitudinal sulcus and paired posterior marginal transverse sulci obsolete; paired lateral depressions present, aligned with coxae of legs II; posteromedian moundlike excrescence absent; expansion of lateral hyaline lines present, entirely smooth, forming pair of semiocelli with well-defined borders; semiocelli medium sized, aligned with junction of coxae of legs I and II, visible in dorsolateral aspect (fig. 25A).

Cucullus: Cucullus broadened laterally, wider than long (table 2); ventrolateral margins moderately truncate, such that cucullus approximately hexagonal (figs. 8C, 27A); ventral margin distinctly bilobate in anterior aspect, linear in ventral aspect; posterior surface, median row of denticulations obsolete; pair of shallow sublateral longitudinal sulci; ventral part unmodified anteromedially.

Chelicerae: Manus dorsal surface with large toothlike process distally. Movable finger longer than fixed finger, tooth row comprising eight or nine small teeth; sharp prodorsal longitudinal carina parallel to tooth row (opposite fixed finger); mucron with shallow but distinct prolateral excavation (opposite fixed finger) delimited by two parallel longitudinal carinae. Fixed finger tooth row comprising five small teeth.

Coxosternal region: Tritosternum very small, barely visible, not abutting coxae of legs I (fig. 25B); coxae of legs II–IV abutting one another medially along entire length; coxae of legs II, anterior and posterior margins subparallel, not perpendicular to median axis, inclined anteriorly; coxae of legs II, posterior margin V-shaped medially; suture between coxae of legs II approximately twice length of suture between coxae of legs III and IV.

Opisthosoma: Opisthosoma oval, longer than wide (table 2), broadest at intersegmental membrane between tergites XI and XII (fig. 25C). Posterodorsal and posteroventral margins without spiniform granules (fig. 25C, D). Tergites X–XIII each comprising median and lateral sclerites; median sclerites of tergites XI–XIII wider than long (table 2), of XIII cup shaped, with round posterolateral margins (fig. 27B), each with paired, shallow submedian depressions near anterior margins, lateral margins converging posteriorly on XI and XII, subparallel on XIII; margins of lateral sclerites adjacent to tergal longitudinal membranes predominantly linear, tergal membranes broad. Sternites XI–XIII each with pair of shallow submedian depressions similar to tergites (fig. 25D). Pygidium basal segment slightly tilted dorsally (figs. 25C, 27B); opening broad, subcircular, width approximately half lateral width of segment at base; posterior margin narrow; dorsal surface with V-shaped notch; ventral surface entire.

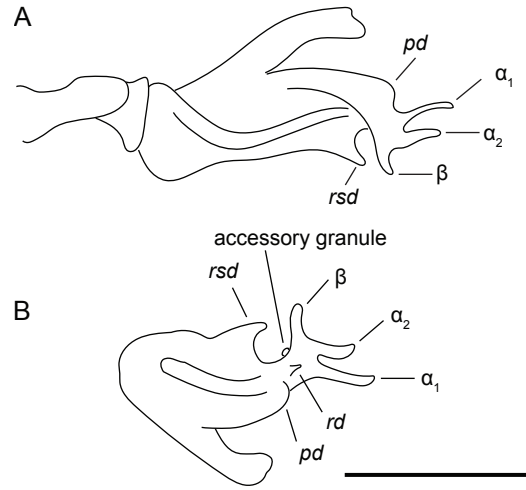

FIGURE 17. *Bambara hanseni* (Legg, 1976), comb. nov., paratype ♂ (BMNH 13588964), dextral leg III copulatory apparatus, **A.** dorsal aspect and **B.** frontal (ventrally inclined) aspect. Abbreviations: α, alpha lobe (bifid, $\alpha_1 + \alpha_2$); β, beta lobe; *pd*, prolateral distal lobe; *rd*, retrolateral distal lobe; *rsd*, retrolateral subdistal lobe. Scale bar = 0.25 mm.

Pedipalps: Femur globose, length approximately twice depth (table 2) (fig. 27C). Tibia longer than femur; entirely linear; moderately swollen proximally compared to rest of segment, which is noticeably narrower (fig. 27C, D); apical longitudinal carinae present. Movable finger approximately twice length of fixed finger.

Legs: Leg II longest; legs I–IV femora unmodified, all similar in width (table 2), dorsal surfaces without longitudinal sulci (fig. 28B). Leg I tibia without ventral apophyses; metatarsus subcircular in cross section, with-

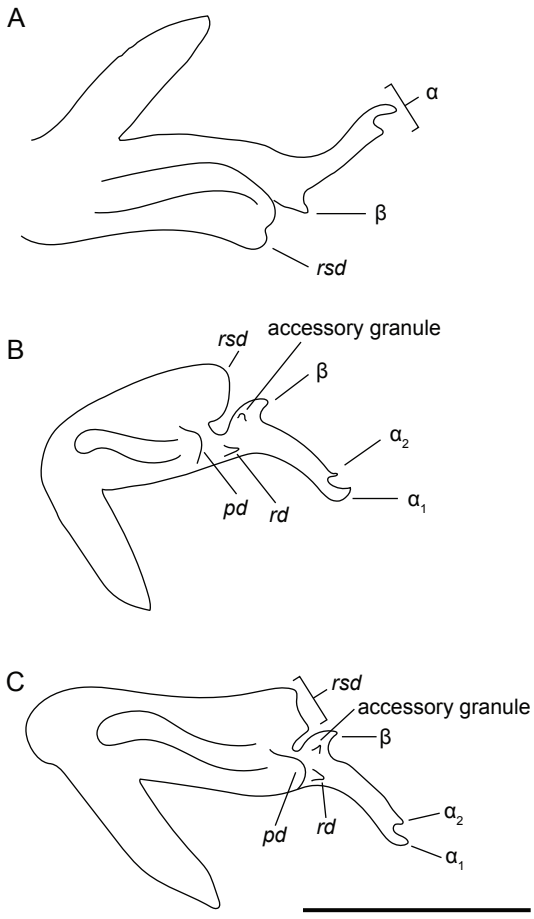

FIGURE 18. *Bambara jocquei*, gen. et sp. nov., paratype ♂ (MRAC 209.292), dextral leg III copulatory apparatus, **A.** dorsal aspect, **B.** frontal (ventrally inclined) aspect, and **C.** ventral aspect. Abbreviations: α, alpha lobe (bifid, $\alpha_1 + \alpha_2$); β, beta lobe; *pd*, prolateral distal lobe; *rd*, retrolateral distal lobe; *rsd*, retrolateral subdistal lobe. Scale bar = 0.25 mm.

out ventral excrescence or proventral proximal depression. Leg II tibia without ventral apophysis (fig. 28C); tibia and metatarsus without pad of long translucent setae ventrally (fig. 28C, D); metatarsus without ventral subproximal depression, submedian concavity, or submedian excrescence; first to third tarsomeres short, subequal, fourth approximately twice length of preceding tarsomeres (fig. 28E); all tarsomeres movable. Leg III metatarsus not swollen, with moderate concavity dorsodistally (figs. 14C, 29); proventral surface without apical brushlike row of setae; prodorsal proximal sulcus present; metatarsus, metatarsal process, and tarsus precisely fitting together to completely enclose copulatory apparatus when tarsus retracted; metatarsal process situated basally near tibia, moderately robust, tapering and curving retrolaterally, apex acute and dorsoventrally compressed, *lamina cyathiformis* of second tarsomere approximately as deep as long, with rounded or slightly pointed apex (fig. 29C); subdistal (third) tarsomere without acute dorsodistal process. Leg IV second to fourth tarsomeres swollen (fig. 28F). Legs III and IV terminal tarsomere apex, dorsal margin entire, medially projected, covering ungues. Leg I tarsus and legs II–IV terminal tarsomeres without ventrodistal papillae.

Copulatory apparatus: Fixed process, *PL* lobe moderately narrow, predominantly linear and dorsoventrally compressed (figs. 18, 29); apex acute. Distal lobular region, primary α lobe elongate and moderately large, partially bifid, with α_1 longer than α_2; retrolateral margin (i.e., on side of α_2) slightly irregular, prolateral margin smooth. Primary β lobe entire, medium sized, and tuberculate; retrolateral surface with small, subspiniform accessory granule basally. *rsd* lobe large, broad and laminar, associated with narrow U-shaped subdistal emargination. Secondary *pd* lobe forming moderately broad, raised surface. Secondary *rd* lobe small, forming pointed protrusion. Movable process slender, slightly flexible, narrowing distally; apex simple, entire.

Supplementary Description of Female: Based on paratypes (soma and appendages: MRAC 209.269; spermathecae: MRAC 209.512). Resembles male, except as noted.

Measurements: Total length, 3.66 mm (MRAC 209.269, table 2).

Tegument surface: Coxosternal region with fewer granules than male (fig. 26B).

Carapace: Posteromedian moundlike excrescence present (fig. 26A).

Cucullus: Ventrolateral margins moderately truncate, as in male; ventral margin more shallowly bilobate in anterior aspect, shallowly bilobate in ventral aspect.

Legs: Leg IV tarsus unmodified.

Spermathecae: Anterior wall of *bursa copulatrix* with pair of small, slightly pigmented, rounded areas (fig. 24B). Anterior surface with four small sacculiform structures sinistrally and six dextrally. Spermathecae follicular, each comprising soft, elongate tube terminating in tapering duct, situated sublaterally on anterior surface of *bursa copulatrix* adjacent to dorsal margin. Posterior genital lip as illustrated.

Additional Material Examined: **GUINEA:** *Nzérékoré Region*: Mount Nimba Strict Nature Reserve [07°38′N 08°25′W], Seringbara Forest, 599 m, 7–9.x.2008, D. van den Spiegel, Winkler trap, 1 ♂, 2 ♀, 1 deutonymph, 1 protonymph (MRAC 225.917), same data, except: 9.x.2008, collection method unspecified, 1 ♀ (MRAC 225.880).

Distribution: *Bambara jocquei* is known from the Mount Nimba Strict Nature Reserve and the Ziama Forest Reserve, in the Nzérékoré Region of Guinea (fig. 4). *Bambara jocquei* is one of three ricinuleid species known from the Ziama Forest Reserve, the others being *R. nzerekorensis* and *T. ziama*, and the second species known from the Mount Nimba Strict Nature Reserve, in addition to *R. nzerekorensis*.

Bambara megahanseni (Legg, 1982), comb. nov.

Figure 4, table 1

Ricinoides megahanseni Legg, 1982: 290–296, figs. 2–6; Harvey, 1984: 209; 2003: 183; Murienne et al., 2013: 3–5, figs. 1, 2; Botero-Trujillo et al., 2021a: 12, 33, 62; Sato et al., 2024: 2, 8, figs. 1a, 4a.

Type Material Examined: Holotype ♀ (MHNG), **CÔTE D'IVOIRE:** *Montagnes and Bas-Sassandra Districts*: Forêt de Taï [Taï National Park, 05°41′N 06°56′W], 17.x.1980, V. Mahnert and J.-L. Perret, sieving in rotten wood and dead leaves, [80/21]. Paratypes: 1 protonymph, 1 larva (MHNG), same data as holotype, except: near (scientific) station, sieving in dead leaves, [80/22]; 1 protonymph, 1 larva (MHNG), same data, except: sieving in dead wood, 20.x.1980, [80/25].

Diagnosis: *Bambara megahanseni* differs from the other species of the genus in the rounded ventrolateral margins of the cucullus and the rectangular median sclerite of tergite XIII. The ventrolateral margins of the cucullus are truncate (figs. 8C, 27A) and the median sclerite of tergite XIII cup shaped (figs. 23A, 25C, 26C), in *B. hanseni* and *B. jocquei*.

Distribution: *Bambara megahanseni* is known only from the type locality, Taï National Park, in the Montagnes and Bas-Sassandra districts of Côte d'Ivoire (fig. 4). It is one of four ricinuleid species recorded in the national park, the others being *Ricinoides eburneus*, *R. taii*, and an unidentified species of *Tautau*.

Remarks: The adult morphology of *B. megahanseni* is known only from the female.

Legg (1982: 292, figs. 4, 4e) reported the presence of an "unusual ampulliform seta" proximally on the pedipalp tibia of the holotype of *B. megahanseni*. The illustration provided closely resembles structures that have been found attached to the body parts of some South American forest arachnids, especially the coxae and pectines of scorpions such as the endogean (humicolous) Ecuadorian species *Troglotayosicus ballvei* Botero-Trujillo et al., 2021. These setalike structures are the thalli of fungi of the order Laboulbeniales Engler, 1898 (Ascomycota (Berk.) Caval.-Sm.: Laboulbeniomycetes Engler, 1898), a diverse group of obligate epibionts of arthropods that is remarkable for its high levels of host specificity (Santamaria, 2001; Haelewaters and Pfister, 2019). Although the alleged ampulliform seta is no longer attached to the holotype of *B. megahanseni*—preventing confirmation of its identity—the illustrations by Legg (1982: figs. 4, 4e) suffice to determine, with reasonable confidence, that it is a Laboulbeniales thallus. During the present investigation, a thallus was

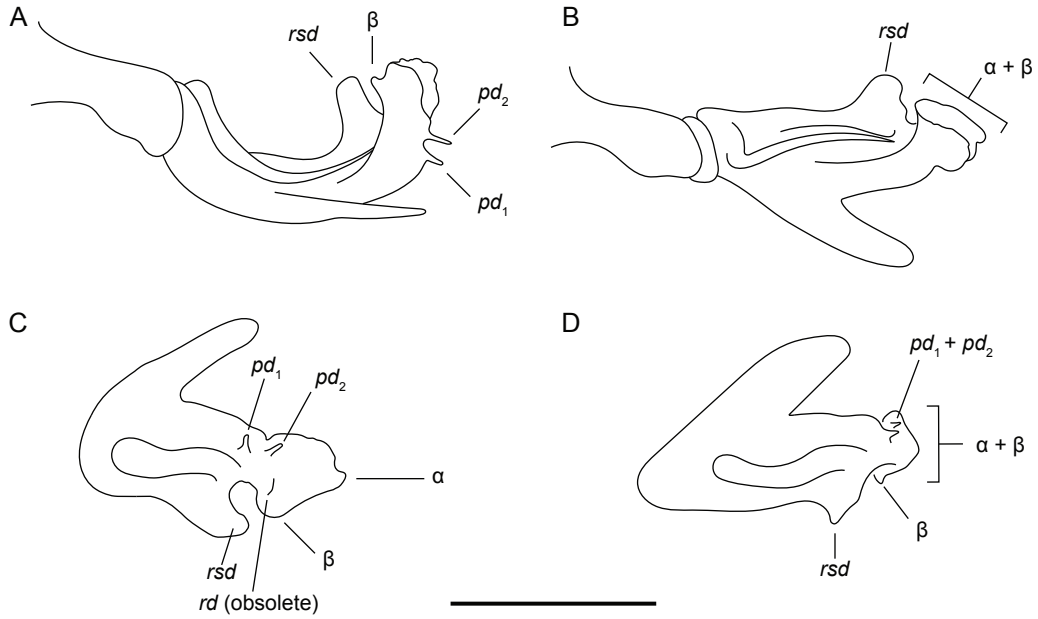

FIGURE 19. *Alantakun karschii* (Hansen and Sørensen, 1904), comb. nov., ♂ (CAS CASENT 9080643), sinistral leg III copulatory apparatus, **A.** prodorsal aspect, **B.** dorsal aspect, **C.** frontal (ventrally inclined) aspect, and **D.** ventral aspect. Abbreviations: α, alpha lobe; β, beta lobe; *pd*, prolateral distal lobe (divided into pd_1 and pd_2); *rd*, retrolateral distal lobe; *rsd*, retrolateral subdistal lobe. Scale bar = 0.5 mm.

also observed attached to the pedipalp tibia of a specimen of *Cryptocellus islacolon* Botero-Trujillo et al., 2021, from Panama. Among arachnids, a host relationship to Laboulbeniales has been recorded in Acari Leach, 1817 (mostly Mesostigmata Canestrini, 1891), Opiliones Sundevall, 1833, Schizomida Petrunkevitch, 1945, and Scorpiones C.L. Koch, 1837 (Weir and Hammond, 1997; Santamaria et al., 2017; Armas et al., 2021; Botero-Trujillo et al., 2021c). The present note is the first report of a Laboulbeniales thallus on Ricinulei.

Benavides et al. (2021) commented on the validity of *B. megahanseni* (as "*R. megahanseni*") based on the position of three specimens (two females and one juvenile) from Côte d'Ivoire (MCZ 130087–130089), allegedly belonging to that species, in their molecular phylogenetic and species delimitation analyses. According to MCZbase (https://mczbase.mcz.harvard.edu/SpecimenSearch.cfm), the database of collections at the Museum of Comparative Zoology, Harvard University, the three specimens were collected in Taï National Park, the type locality of *B. megahanseni* as well as two species of "giant" Ricinulei (i.e., *Ricinoides* as redefined herein), *R. eburneus* and *R. taii* (Botero-Trujillo et al., 2021a). Benavides et al. (2021: 12) cast doubt on the work of Botero-Trujillo et al. (2021a) after their molecular analyses allegedly failed to separate *R. megahanseni* (i.e., *B. megahanseni*) from *R. atewa*:

> Our molecular data are also unable to distinguish *R. atewa* from *R. megahanseni*. Instead of formalizing these synonymies, we see the need of a thorough integrative analysis of the whole *Ricinoides* to assess whether the characters currently used to recognize species (Botero-Trujillo et al., 2021), have a taxonomic basis.

The species of *Ricinoides* exhibit the largest body size among Ricinulei with most species of the genus reaching almost 10 mm in total length

TABLE 2

Measurements (mm) of Type Specimens of Three Species of African Ricinulei Thorell, 1876: *Bambara jocquei*, gen. et sp. nov., *Tautau ziama*, gen. et sp. nov., and *Ududo tuxeni*, gen. et sp. nov.

Material deposited in the Natural History Museum (BMNH), London, and the Musée Royal de l'Afrique Centrale (MRAC), Tervuren, Belgium. Abbreviations: H, height; L, length; W, width.

		Bambara jocquei		*Tautau ziama*	*Ududo tuxeni*	
Type / sex		Holotype ♂	Paratype ♀	Holotype ♂	Holotype ♂	Paratype ♀
Collection		MRAC	MRAC	MRAC	BMNH	BMNH
Number		209.284	209.269	209.517	13588977	13588978
Total body L[1]		3.66	3.66	4.14	6.31	5.88
Cucullus	L	0.75	0.78	0.86	1.35	1.26
	W[2]	1.00	1.02	1.26	2.02	1.83
Carapace	L	1.45	1.43	1.56	2.50	2.23
	W[2]	1.51	1.45	1.56	2.61	2.34
Opisthosoma	L[1]	2.21	2.23	2.58	3.81	3.64
	W[2]	1.91	1.99	1.91	2.94	2.94
Median sclerite XI	L	0.62	0.65	0.83	1.20	1.25
	W[2]	1.21	1.29	1.35	2.01	2.07
Median sclerite XII	L	0.65	0.62	0.73	1.03	1.09
	W[2]	1.05	1.02	0.94	1.47	1.63
Median sclerite XIII	L	0.67	0.67	0.81	1.20	1.14
	W[2]	0.78	0.78	0.62	1.41	1.36
Pedipalp	Femur L	0.70	0.75	0.81	1.18	1.08
	Femur H[3]	0.35	0.38	0.38	0.54	0.48
	Tibia L	1.13	1.13	1.18	1.80	1.72
	Tibia H[4]	0.09	0.09	0.11	0.24	0.24
Leg I	Femur L	0.75	0.69	0.83	1.35	1.13
	Femur W[4]	0.28	0.26	0.30	0.51	0.38
	Femur H[4]	0.32	0.32	0.32	0.54	0.43
	Patella L	0.56	0.58	0.65	0.97	0.83
	Tibia L	0.43	0.49	0.59	0.91	0.81
	Metatarsus L	0.86	0.82	0.97	1.61	1.37
	Tarsus L	0.39	0.34	0.32	0.56	0.51
Leg II	Femur L	1.29	1.27	1.61	2.42	2.21
	Femur W[4]	0.32	0.29	0.22	0.46	0.35
	Femur H[4]	0.43	0.37	0.38	0.62	0.48
	Patella L	0.88	0.84	0.91	1.32	0.94
	Tibia L	0.97	0.88	1.02	1.69	1.53
	Metatarsus L	1.38	1.29	1.56	2.42	2.13
	Tarsus L	1.42	1.33	1.35	2.13	1.88

TABLE 2 *continued*

		Bambara jocquei		*Tautau ziama*	*Ududo tuxeni*	
Type / sex		Holotype ♂	Paratype ♀	Holotype ♂	Holotype ♂	Paratype ♀
Collection		MRAC	MRAC	MRAC	BMNH	BMNH
Number		209.284	209.269	209.517	13588977	13588978
Leg III	Femur L	0.86	0.77	1.02	1.64	1.40
	Femur W[4]	0.32	0.28	0.30	0.51	0.38
	Femur H[4]	0.34	0.30	0.32	0.54	0.40
	Patella L	0.67	0.60	0.73	1.10	0.91
	Tibia L	0.58	0.45	0.62	0.97	0.83
	Metatarsus L	0.82	0.71	0.91	1.43	1.16
	Tarsus L	1.14	0.62	1.21	1.75	0.94
Leg IV	Femur L	0.95	0.84	1.10	1.78	1.72
	Femur W[4]	0.28	0.26	0.24	0.43	0.32
	Femur H[4]	0.34	0.29	0.32	0.51	0.40
	Patella L	0.62	0.56	0.70	0.86	0.91
	Tibia L	0.49	0.45	0.56	0.94	0.91
	Metatarsus L	0.80	0.73	0.86	1.37	1.29
	Tarsus L	0.88	0.69	0.78	1.61	1.13

[1] Excludes pygidium and cucullus.
[2] Maximum width.
[3] Maximum height.
[4] Midline.

(except for *R. feae*, which is slightly smaller) (Botero Trujillo et al., 2021a). Unlike *Ricinoides*, the species of *Bambara* are small, *B. jocquei* measuring <4 mm (table 2) and *B. megahanseni* <5 mm (Legg, 1982), for example. In addition to differences in size and habitus, *B. megahanseni* and *R. atewa* differ in several other conspicuous characters, as outlined in the identification key, species diagnoses, and illustrations presented herein. The possibility that Benavides et al. (2021) would consider these species potentially conspecific, taken together with their apparently close relationship in the authors' phylogenetic analysis, suggests that the specimens claimed to be *R. megahanseni* (i.e., *B. megahanseni*) were misidentified and instead belong to a species of *Ricinoides*, probably one of the two species of that genus previously recorded in Taï National Park.

This case serves to illustrate the importance of correctly identifying each sample included in a molecular phylogenetic analysis. The impact that misidentified samples (be that at the genus or species level) can have on the interpretation of phylogenies and downstream classifications is well known and can prove difficult to correct (e.g., Almeida et al., 2023). In the era of phylogenomics, accurate specimen identification and taxon-based expertise in the study group is more essential than ever, especially for understudied taxa like Ricinulei. The identity of the MCZ specimens alleged to be *B. megahanseni* should be verified before sequences derived from them are included in further studies.

Bambara sp.

Figure 4

Material Examined: **LIBERIA:** *Montserrado*: Mount Coffee [06°29′N 10°39′W], iii.1895,

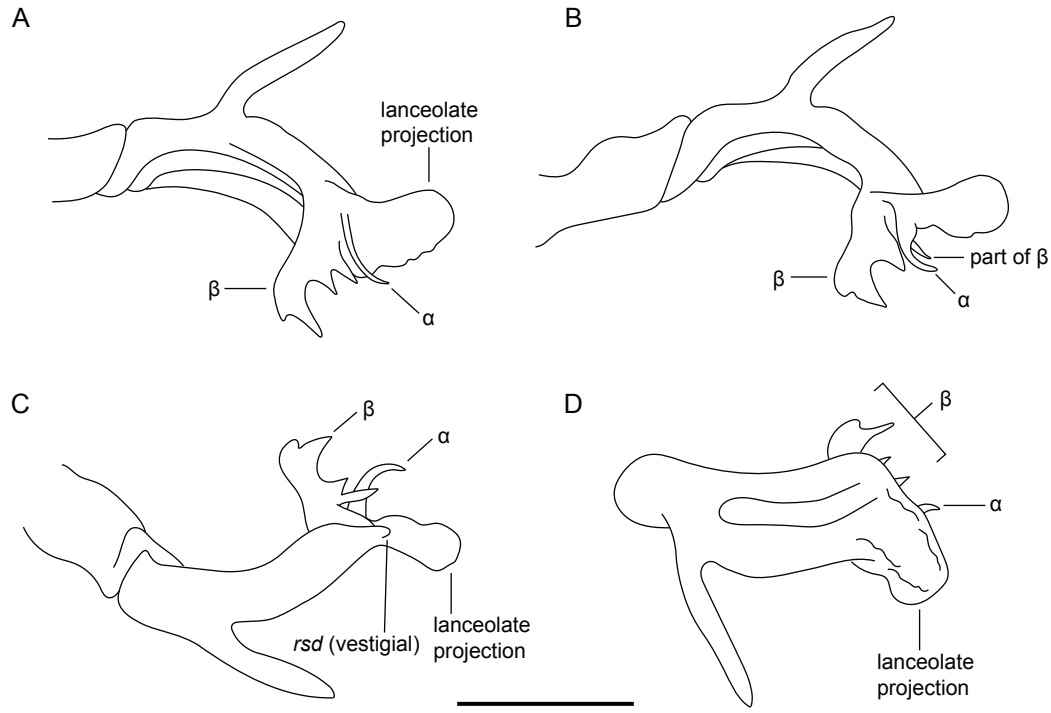

FIGURE 20. *Tautau ziama*, gen. et sp. nov., holotype ♂ (MRAC 209.517), dextral leg III copulatory apparatus, **A.** dorsal aspect, **B.** prodorsal aspect, **C.** retroventral aspect, and **D.** ventral aspect. Abbreviations: α, alpha lobe; β, beta lobe; *rsd*, retrolateral subdistal lobe. Scale bar = 0.25 mm.

O.F. Cook, under rotting wood in deep forest, 1 ♀ (AMNH IZC 324884).

Remarks: This single female may be an undescribed species, closely related to *B. megahanseni*.

***Gizoo*, gen. nov.**

Figures 1, 2, 7, 16, 23E, F, table 1

Type Species: *Cryptostemma crassipalpe* Hansen and Sørensen, 1904 [= *Gizoo crassipalpe* (Hansen and Sørensen, 1904), comb. nov.], by monotypy.

Diagnosis: *Gizoo* may be separated from other African genera of Ricinulei as follows. The tegument of *Gizoo* bears polygonal setae, which are absent in *Alantakun*, *Ricinoides*, and *Ududo* (figs. 34, 35, 36B), and lacks saucer-shaped granules, which are present in *Alantakun* and *Ududo* (figs. 34, 35, 36B). The granules on the carapace and dorsal surface of the opisthosoma are separated in *Gizoo* but distinctly clustered in *Alantakun*. The carapace of the male and female of *Gizoo* exhibits a posteromedian moundlike excrescence, which is absent in *Alantakun*, *Ricinoides* (the females of *R. eburneus*, *R. iita*, and *R. westermannii* are unknown), *Ududo* (the female of *U. sjostedtii* is unknown) (figs. 34A, 35A), and the male of *Bambara* (the male of *B. megahanseni* is unknown) (fig. 25A). The ventral part of the anterior surface of the cucullus (♂) is shallowly convex and not particularly coarsely granular, in *Gizoo*, whereas the surface is almost flat and coarsely granular, in *Alantakun* (fig. 8F). The ventrolateral margins of the cucullus are rounded in *Gizoo*, but moderately truncate in *Bambara* (except *B. megahanseni*, known only

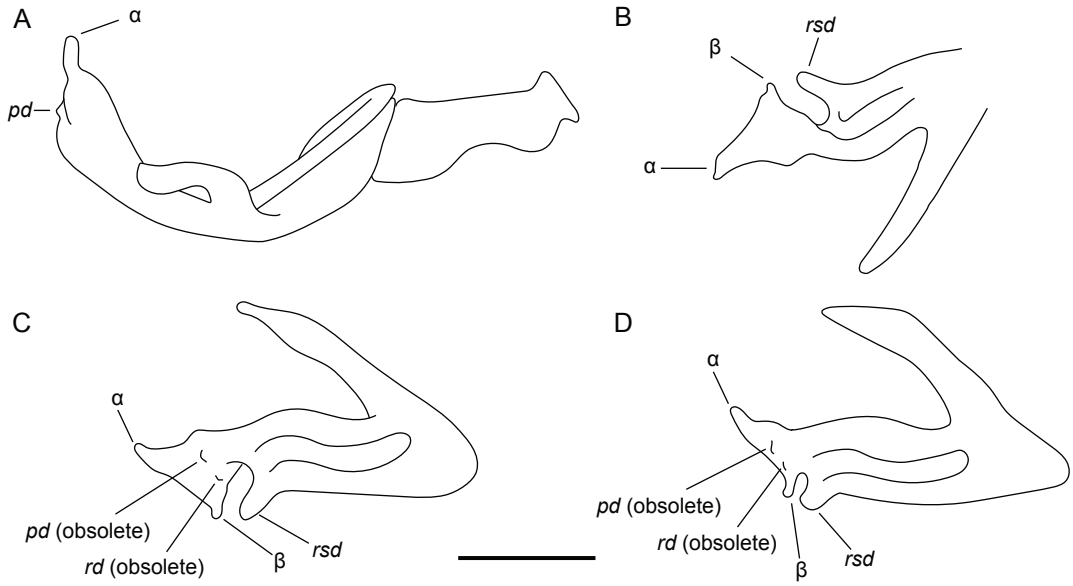

FIGURE 21. *Ududo tuxeni*, gen. et sp. nov., holotype ♂ (BMNH 13588977 old 1953.3.28.71), dextral leg III copulatory apparatus, **A.** prolateral aspect, **B.** dorsal aspect, **C.** frontal (ventrally inclined) aspect, and **D.** ventral aspect. Abbreviations: α, alpha lobe; β, beta lobe; *pd*, prolateral distal lobe; *rd*, retrolateral distal lobe; *rsd*, retrolateral subdistal lobe. Scale bar = 0.25 mm.

from the female) (figs. 8C, 27A). The ventral margin of the cucullus is linear or sublinear in *Gizoo*, but bilobate in the male and female of *Ududo* (at least in *U. tuxeni* as the female of *U. sjostedtii* is unknown), and bilobate in the male and, to a lesser extent, the female of *B. jocquei* (figs. 8C, 27A). The tritosternum is vestigial, yet visible, in *Gizoo*, but extremely small, not exposed, in *Alantakun* (fig. 22A). The pedipalp tibia is markedly swollen proximally compared to the rest of the segment, in *Gizoo*, whereas it is robust along its entire length in *Ricinoides* (except *R. feae* and *R. westermannii*, in which it is not noticeably robust) (fig. 11D), and moderately swollen proximally in *Ududo* (figs. 11F, 36C). The pedipalp tibia lacks apical longitudinal carinae in *Gizoo*, which are present in *Bambara* (figs. 11C, 27C, D) and *T. ziama* (figs. 11E, 31D, E). The distal region of the pedipalp tibia bears raised tubercles that are elongate in *Gizoo*, oval in *Ricinoides* (fig. 11D) and *Ududo* (fig. 11F), and absent in *Bambara* (figs. 11C, 27D) and *Tautau* (figs. 11E, 31D, E). A dorsal longitudinal sulcus is absent on the leg femora in *Gizoo*, but present in *Ricinoides*. The leg I femur (♂) is slender in *Gizoo* but slightly swollen in *Ricinoides* (except *R. taii*) and *Ududo*. The leg I tibia (♂) lacks ventral apophyses in *Gizoo*, which are present in *Ududo* (figs. 12A, C, 37C, D). The leg I metatarsus (♂) is sublinear in lateral aspect and subcircular in cross section, in *Gizoo*, but convex ventrally in lateral aspect and dorsoventrally elongate in cross section, in *Ududo* (figs. 12C, 36E). The leg I metatarsus (♂) lacks a proventral proximal depression in *Gizoo*, which is present in *Alantakun* and *Ricinoides* (fig. 12B). The leg II femur (♂) is slender in *Gizoo*, but moderately to markedly swollen and robust in *Alantakun* and *Ricinoides*. The leg II tibia (♂) lacks a ventromedian apophysis in *Gizoo*, which is present in *Ricinoides* (except *R. westermannii*) (fig. 12D). The leg II metatarsus (♂) lacks a ventral subproximal depression in *Gizoo*, which is present in *Ricinoides* (fig. 12E), and a ventrosubmedian concavity,

which is present in *Alantakun*. The terminal (fifth) tarsomere of leg II is fixed, fused to the preceding tarsomere, in *Gizoo*, but movable, not fused to the preceding (fourth) tarsomere, in *Alantakun*, *Bambara* (fig. 28E), *Ricinoides* (fig. 12E), and *Ududo*. The leg III femur (♂) is slender in *Gizoo*, but slightly swollen in *Alantakun*, *Ududo*, *R. afzelii*, and *R. iita*. The leg III metatarsus (♂) is relatively slender in *Gizoo*, but slightly to markedly swollen in *Alantakun* (fig. 14A) and *Tautau* (figs. 14E, 33A, C, D). The dorsal surface of the leg III metatarsus (♂) is not excavated basally in *Gizoo*, but moderately excavated in *Ududo* (figs. 14F, 38D), and markedly excavated in *Alantakun* (fig. 14A). The dorsal concavity of the leg III metatarsus (♂) is moderately deep, gradually becoming shallower proximally in *Gizoo*, whereas it is very deep and forms a well-defined chamber extending across the distal half of the segment, in *Alantakun* (fig. 14A) and *Ududo* (figs. 14F, 38D), and to the attachment point of the metatarsal process, in *Tautau* (figs. 14E, 33D). The prodorsal margin of the second tarsomere of leg III (♂) is sublinear to slightly curved proximally (in prolateral aspect) in *Gizoo*, but moderately angular in *Alantakun* (fig. 13A). The third tarsomere of leg III (♂) lacks an acute dorsodistal process in *Gizoo*, which is present in *Ricinoides* (fig. 13B). The leg IV femur (♂) is slender in *Gizoo*, but slightly swollen in *Alantakun* and *Ududo*. The second to fourth tarsomeres of leg IV (♂) are swollen in *Gizoo*, but unmodified in *Ricinoides*. The male copulatory apparatus fixed process is of the *crassipalpe* Type in *Gizoo* (fig. 16). The median sclerite of opisthosomal tergite XIII is rectangular to trapezoid in *Gizoo*, but cup shaped in *Bambara* (except *B. megahanseni*) (figs. 23A, 25C, 26C, 27B). The tergal membranes of the opisthosoma are smooth in *Gizoo*, but granular in *Ricinoides*, *Ududo*, and *T. ziama*. The posterodorsal and posteroventral margins of the opisthosoma lack subspiniform granules in *Gizoo*, which are present in *Alantakun* and *Ududo* (figs. 23B, 34C, D, 35C, D, 36B). The opisthosomal dorsal and ventral pleural membranes are finely and densely granular in *Gizoo*, whereas the dorsal pleural membrane and, occasionally, the ventral pleural membrane, are moderately to sparsely granular in *Bambara* (figs. 25C, 26C, 27B). The basal segment of the pygidium is slightly tilted dorsally, relative to the longitudinal axis of the opisthosoma, in *Gizoo*, but parallel to the longitudinal axis in *Alantakun* (fig. 23C, D), *Ricinoides*, *Ududo* (figs. 23G, H, 34C, D, 35C, D, 36B), and *T. leonensis*. The posterior margin of the basal segment of the pygidium is broad ventrally in *Gizoo* (fig. 23E, F), whereas it is entirely broad in *Alantakun* (fig. 23C, D) and *Ududo* (fig. 23G, H), and narrow in *Bambara* (figs. 23A, 27B), *Ricinoides*, and *Tautau* (figs. 30C, 31C). The opening of the basal segment of the pygidium is at least half the lateral width of the segment at its base, in *Gizoo*, but distinctly narrow, its width two-fifths to one-third the lateral width of the segment, in *Ricinoides*.

Etymology: The generic name is taken from the word Gízòo, meaning "spider" in Hausa, an indigenous language spoken in eight West African countries, including Cameroon. Gender masculine.

Included Species: *Gizoo*, gen. nov., is hereby created to accommodate a species formerly assigned to *Ricinoides*, *Gizoo crassipalpe* (Hansen and Sørensen, 1904), comb. nov.

Distribution: *Gizoo* has been recorded from Bioko Island, Equatorial Guinea, and a single locality on the adjacent mainland in Cameroon (fig. 7).

Gizoo crassipalpe
(Hansen and Sørensen, 1904), comb. nov.

Figures 7, 16, 23E, F, table 1

Cryptostemma crassipalpe Hansen and Sørensen, 1904: 147, unpaginated, pl. VII, figs. 1a–y; Hansen, 1921: 23–26, unpaginated, pl. II, figs. 2a–h; Barrows, 1925: 487, pl. XXXVI, fig. 9; Ewing, 1929: 583; Roewer, 1932: 4, fig. 1.

Ricinoides crassipalpe (Hansen and Sørensen, 1904): Ewing, 1929: 597; Kästner, 1932: 101, 102, 107–110, 113, figs. 134, 136, 137, 145–149, 154, 155; Bolívar y Pieltain, 1942: 200, 201; Savory, 1964: 195, 197, figs. 97–99; Kennaugh, 1968: 396; Lawrence, 1969: 130; Pittard, 1970: 26; Pittard and Mitchell, 1972: 8, 10, 13; Tuxen, 1974: 87–89, 95, 103–105, figs. 1e, 39–44; Legg, 1976b: 2, 51, 54; Savory, 1977: 212–214, 216, figs. 84–86; Brusca and Brusca, 1990: 501, fig. 4k; 2003: 661, fig. 19.4m; Harvey, 2003: 183; Botero-Trujillo et al., 2021a: 12.

Ricinoides crassipalpis: Legg, 1978a: 97–99, fig. 15.

Type Material Examined: Syntypes [1 deutonymph, 1 tritonymph(?) (otherwise ♀, markedly damaged)] (NHRS JUST 517), **CAMEROON:** *South-West Region*: Bibundi [04°13′N 08°59′E], 1891, Y. Sjöstedt.

Diagnosis: As for the genus.

Distribution: *Gizoo crassipalpe* is known from Bioko Island, Equatorial Guinea, and a single locality on the adjacent mainland in Cameroon (fig. 7).

The precise type locality of *G. crassipalpe* was not reported in the original description and it has remained unknown since (Hansen and Sørensen, 1904; Tuxen, 1974; Harvey, 2003). However, the original labels accompanying the syntypes indicate the type locality as Bibundi, a coastal locality in Cameroon. One paralectotype of *U. sjostedtii* shares the same collection data as the syntypes of *G. crassipalpe*, i.e., "Cameroon, Bibundi, 1891, Y. Sjöstedt," suggesting that the two species may be sympatric at that locality.

Remarks: Additional material examined, deposited in the MSNG, contains labels that identify the specimens as types (see below). However, these specimens were not mentioned in the original description and are therefore not part of the type series. These specimens, from Musola and Basilé, on the island of Bioko, were used by Hansen (1921) to describe the adult morphology of *G. crassipalpe* (as "*Cryptostemma crassipalpe*"). The other material examined from Musola, deposited in the ZMUC, was used by Tuxen (1974) to augment the description of this species. As neither syntype enables the species to be unambiguously characterized according to modern standards, designating a lectotype was deemed pointless. The nontype material from Bioko, examined by Hansen (1921), will remain the foundation of the existing knowledge on the morphology of *G. crassipalpe*.

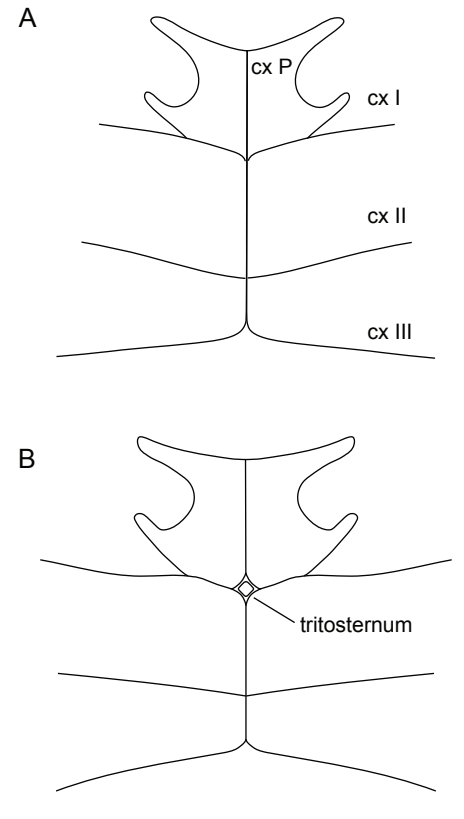

FIGURE 22. *Alantakun*, gen. nov., and *Ududo*, gen. nov., coxosternal region except coxae of leg IV (not shown), ventral aspect. **A.** *Alantakun karschii* (Hansen and Sørensen, 1904), comb. nov., ♂ (CAS CASENT 9080643), tritosternum not visible. **B.** *Ududo sjostedtii* (Hansen and Sørensen, 1904), comb. nov., lectotype ♂ (NHRS JUST 519). Abbreviations: cx, coxae of pedipalp (P) and legs I–III. Scale bar = 0.5 mm.

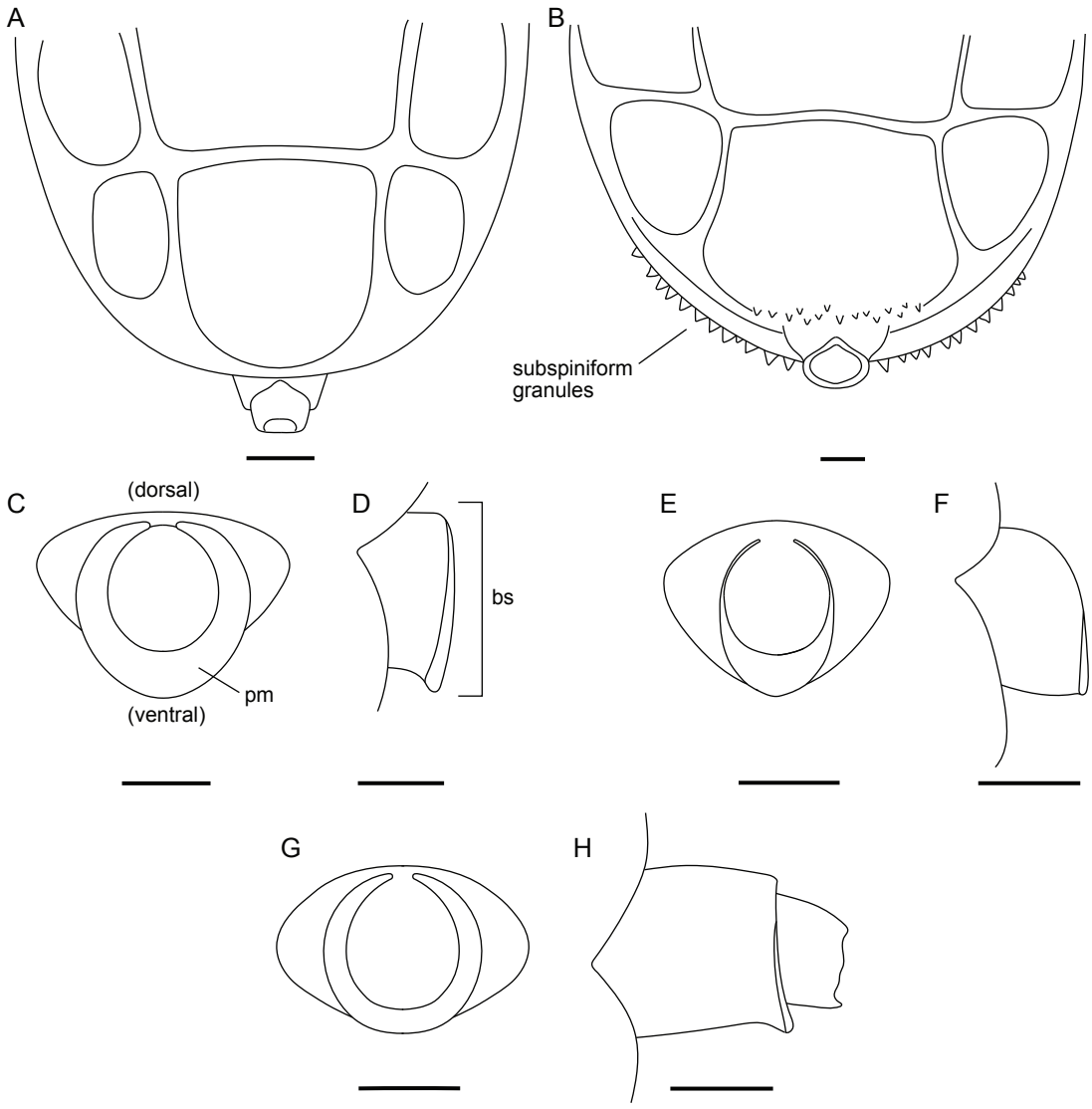

FIGURE 23. *Alantakun*, gen. nov., *Bambara*, gen. nov., *Gizoo*, gen. nov., and *Ududo*, gen. nov. **A, B.** Opisthosoma, posterior half, dorsal aspect. **C–H.** Pygidium, posterior (**C, E, G**) and lateral (**D, F, H**) aspects, illustrating posterior margin of basal segment entirely broadened (**C, G**) vs. only broadened ventrally (**E**). **A.** *Bambara hanseni* (Legg, 1976), comb. nov., holotype ♂ (BMNH 13588962). **B.** *Ududo tuxeni*, gen. et sp. nov., holotype ♂ (BMNH 13588977 old 1953.3.28.71). **C, D.** *Alantakun karschii* (Hansen and Sørensen, 1904), comb. nov., ♂ (CAS CASENT 9080643). **E, F.** *Gizoo crassipalpe* (Hansen and Sørensen, 1904), comb. nov., ♀ (ZMUC). **G, H.** *Ududo tuxeni*, gen. et sp. nov., paratype ♀ (BMNH 13588978 old 1953.3.28.61). Abbreviations: bs, basal segment of pygidium; pm, posterior margin of bs. Scale bars = 0.25 mm.

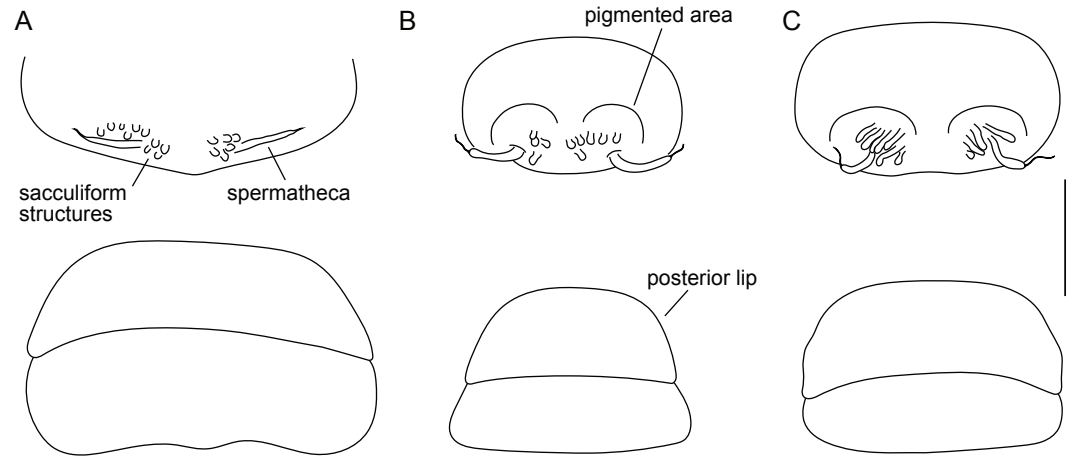

FIGURE 24. *Alantakun*, gen. nov., *Bambara*, gen. nov., and *Ududo*, gen. nov., female genital sclerites, anterior wall of *bursa copulatrix*, anterior aspect (above), posterior genital lip and wall of *bursa copulatrix*, posterior aspect (below). **A.** *Alantakun karschii* (Hansen and Sørensen, 1904), comb. nov., ♀ (BMNH 14041440 old 08.8.11.43-44). **B.** *Bambara jocquei*, gen. et sp. nov., paratype ♀ (MRAC 209.512). **C.** *Ududo tuxeni*, gen. et sp. nov., paratype ♀ (BMNH 13588934 old 1953.3.28). Scale bar = 0.25 mm.

Additional Material Examined: **EQUATORIAL GUINEA:** *Bioko Island* [formerly Fernando Póo]: Basilé [03°42′N 08°48′E], 400–600 m, viii–ix.1901, L. Fea, 1 deutonymph (MSNG, labeled "cotypus"); Musola [03°26′N 08°37′E], 400–500 m, i.1902, L. Fea, 1 ♂, 2 ♀, 1 tritonymph (MSNG, labeled "typi"), 1 ♂, 1 ♀ (ZMUC).

Ricinoides Ewing, 1929

Figures 1, 2, 5, 6, 8A, B, D, E, G, 9, 10, 11D, 12B, D, E, 13B, 14D, 15, table 1

Cryptostemma Guérin-Méneville, 1838: 11 [junior homonym of *Cryptostemma* Herrich-Schäffer, 1835 (Insecta: Hemiptera)], type species by monotypy: *Cryptostemma westermannii* Guérin-Méneville, 1838; Gervais, 1844: 130, 131; Westwood, 1874: 201; Karsch, 1892a: 30–32; 1892b: 64; Thorell, 1892: 7, 8, 10; Börner, 1902: 438, 443, 453, 454, 457, 462; Hansen and Sørensen, 1904: 146; Fage, 1921: 526; Ewing, 1929: 584–586; Kästner, 1932: 100, 112, 114, 115, fig. 156; Fage, 1938: 370; Bolívar y Pieltain, 1942: 198, 199; Savory, 1964: 200; Tuxen, 1974: 86; Savory, 1977: 218; Dunlop, 1996: 193; Benavides et al., 2021: 2; Prendini, 2025: 409.

Cryptostema: Frič, 1904: 32, 33.

Ricinoides Ewing, 1929: 586 [replacement name for *Cryptostemma* Guérin-Méneville, 1838]; Gertsch and Mulaik, 1939: 1; Bolívar y Pieltain, 1942: 199, 201; Petrunkevitch, 1955: 160; Cloudsley-Thompson, 1958: 129; Savory, 1964: 199, 200; Cooke, 1967: 31; Cloudsley-Thompson, 1968: 161; Kaestner, 1968: 207; Kennaugh, 1968: 394, 396; Mitchell, 1969: 136, 137; 1970: 63; Pittard, 1970: 1, 23; Cooke, 1971: 2, 3; Pittard and Mitchell, 1972: 3, 17; Cooke and Shadab, 1973: 1; Tuxen, 1974: 86–91, 98, 105; Cooreman, 1976: 25; Legg, 1976a: 243; 1976b: 1, 2, 53, 55; Platnick and Shadab, 1976: 2; Dumitresco and Juvara-Balş, 1977a: 148, 159, 166, 171, 172, 174, 178, 179; 1977b: 259; Legg, 1977: 51, 57; Platnick and Shadab, 1977: 2, 3, 17; Savory, 1977: 218, 219; Legg, 1978a: 89, 90, 98; 1978b: 124; Hammen, 1979: 8;

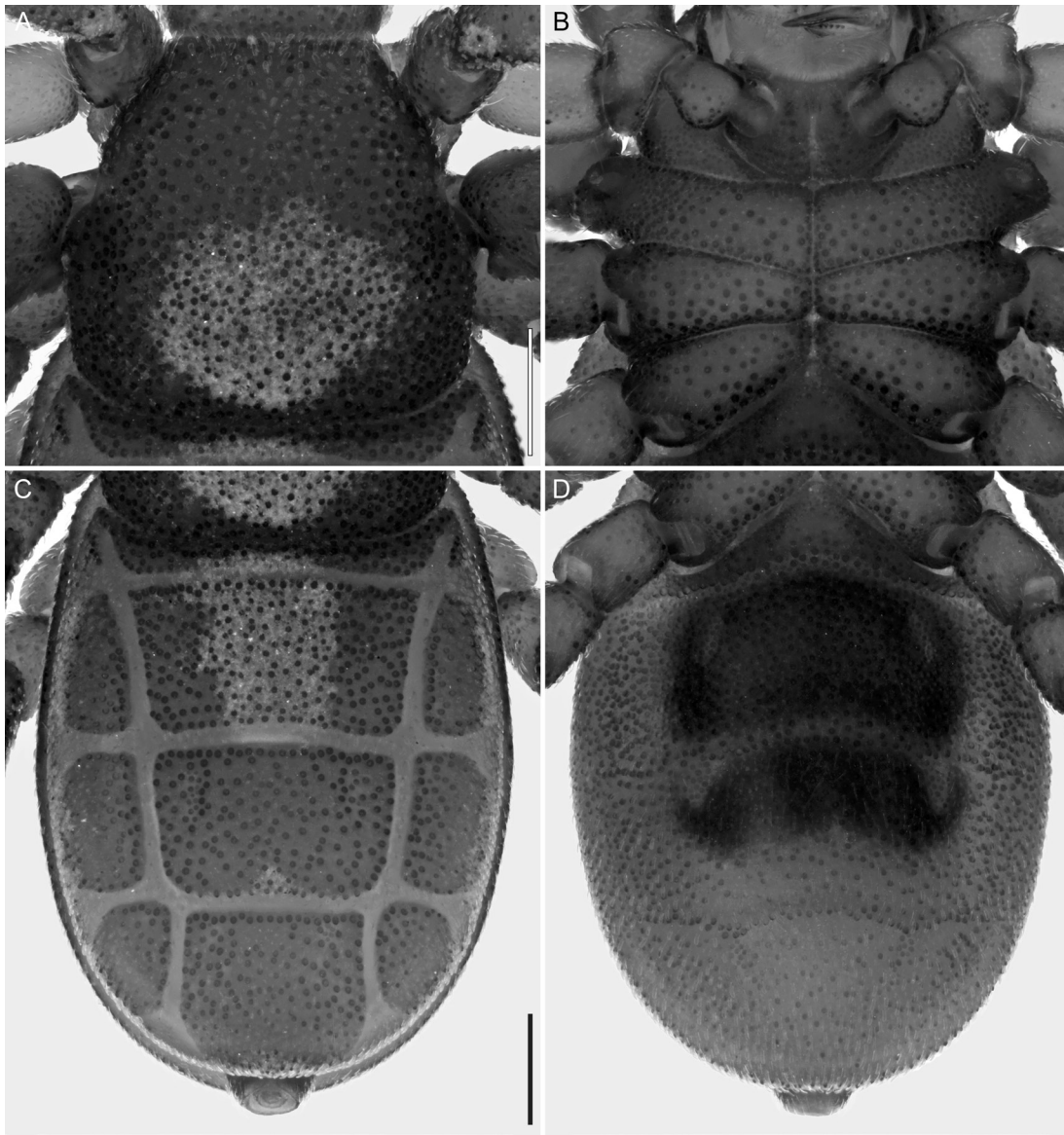

FIGURE 25. *Bambara jocquei*, gen. et sp. nov., holotype ♂ (MRAC 209.284). **A.** Carapace, dorsal aspect (posteromedian moundlike excrescence absent). **B.** Coxosternal region, ventral aspect. **C, D.** Opisthosoma, **C.** dorsal and **D.** ventral aspects. Scale bars = 0.5 mm.

Platnick and Paz, 1979: 2; Barnes, 1980: 642, fig. 13.50; Platnick, 1980: 349–352; Platnick and Shadab, 1981: 2; Legg, 1982: 287, 293; Harvey, 1984: 205, 209; Barnes, 1987: 530; Platnick, 1988: 363; Hammen, 1989: 441; Brusca and Brusca, 1990: 496; Selden, 1992: 201; Dunlop, 1996: 197, 198; Judson and Hardy, 2001: 290; Harvey, 2002: 361; Platnick, 2002: 383; Bonaldo and Pinto-da-Rocha, 2003: 103; Brusca and Brusca, 2003: 655; Harvey, 2003: 182; Barreiros et al., 2005: 2; Talarico et al., 2005: 604; 2006: 441;

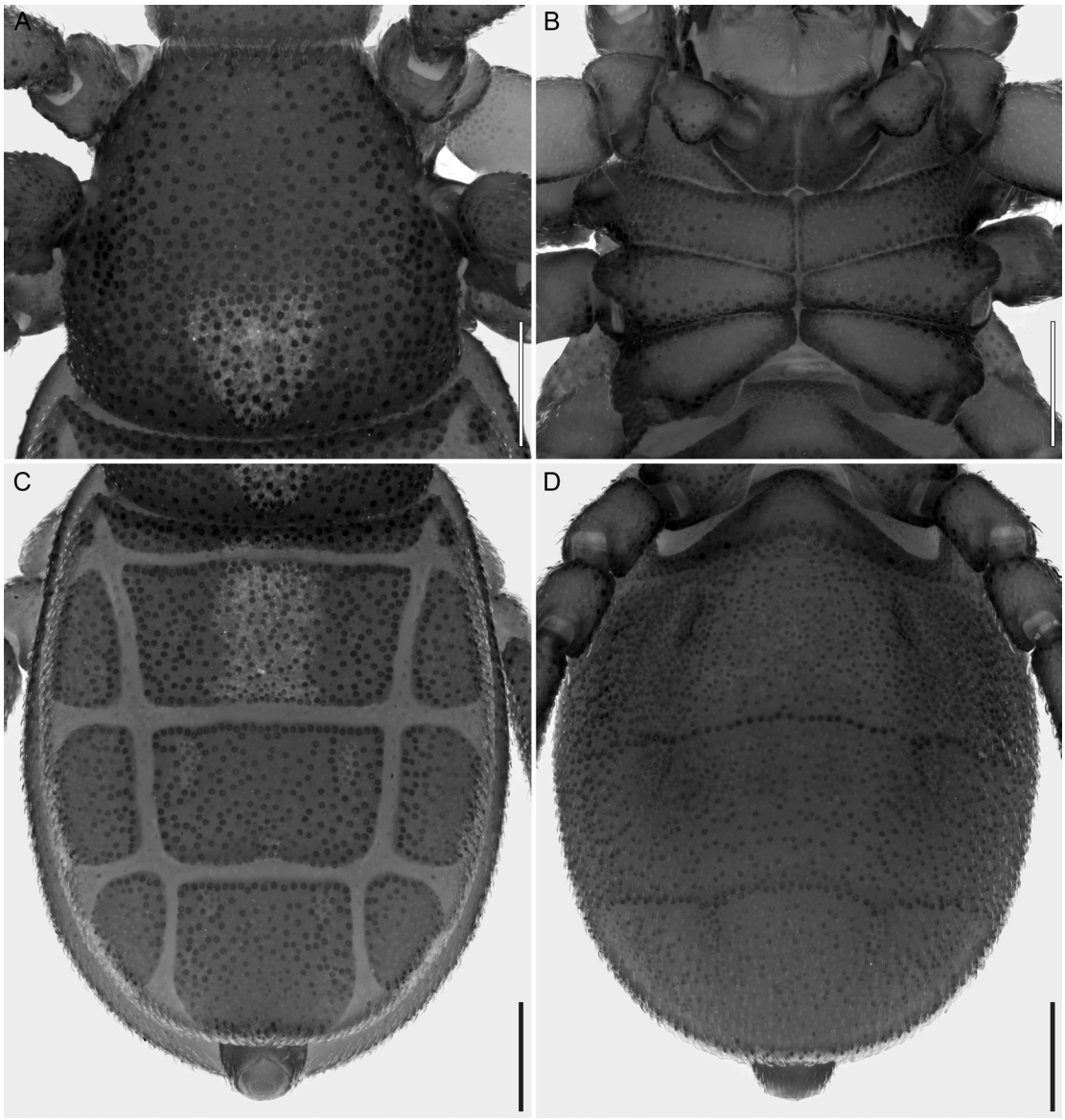

FIGURE 26. *Bambara jocquei*, gen. et sp. nov., paratype ♀ (MRAC 209.269). **A.** Carapace, dorsal aspect, illustrating posteromedian moundlike excrescence. **B.** Coxosternal region, ventral aspect. **C, D.** Opisthosoma, **C.** dorsal and **D.** ventral aspects. Scale bars = 0.5 mm.

Shultz, 2007: 225, 228, 234, 235, 255, figs. 5, 6; Tourinho and Azevedo, 2007: 55; Botero-Trujillo and Pérez, 2008: 468; Naskrecki, 2008: 57, 63; Platnick and García, 2008: 145; Talarico et al., 2008a: 396, 407; 2008b: 48; Beccaloni, 2009: 147, 153; Botero-Trujillo and Pérez, 2009: 56; Penney et al., 2009: 66; Talarico et al., 2009: 1374; Talarico and Michalik, 2010: 384, 389; Talarico et al., 2011: 89, 112; Valdez-Mondragón and Francke, 2011: 365; Wunderlich, 2012: 238; Murienne et al., 2013: 4, 6; Salvatierra et al.,

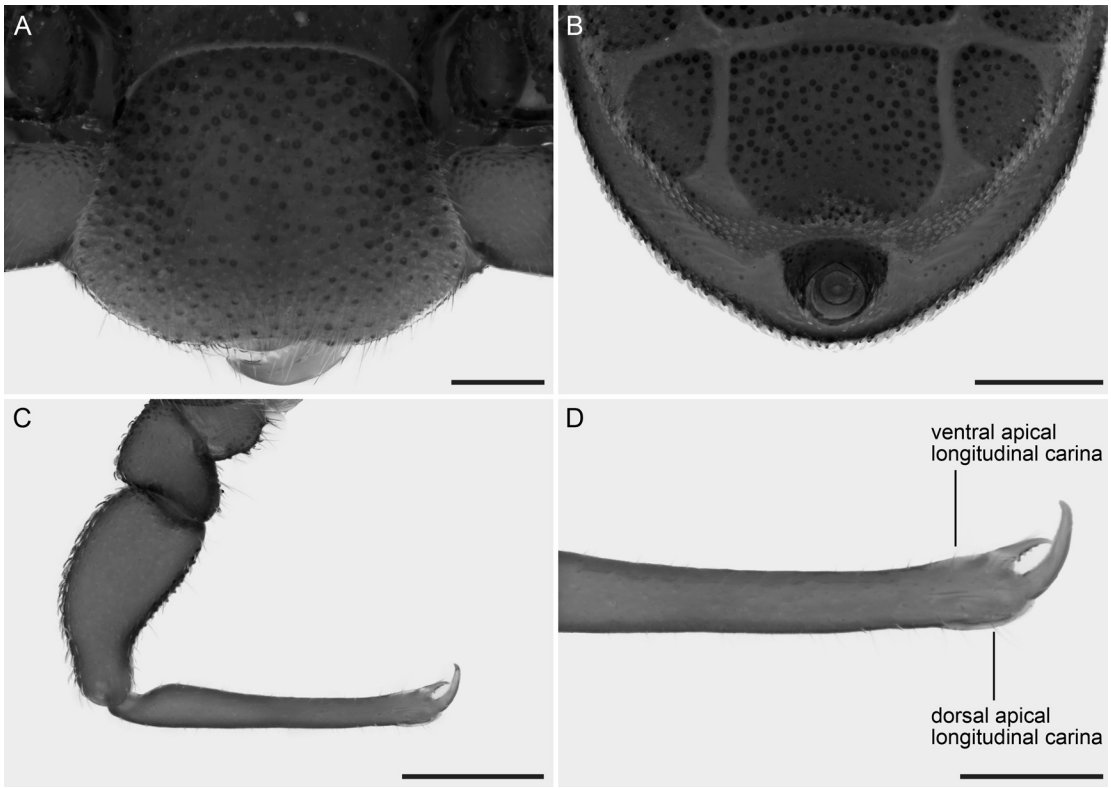

FIGURE 27. *Bambara jocquei*, gen. et sp. nov., holotype ♂ (MRAC 209.284). **A.** Cucullus, anterior aspect, illustrating bilobate ventral margin and truncate ventrolateral margins. **B.** Opisthosoma, posterior end, posterodorsal aspect. **C, D.** Pedipalp, **C.** prolateral aspect, with **D.** closeup. Scale bars = 0.25 mm (**A, D**), 0.5 mm (**B, C**).

2013: 149; Valdez-Mondragón and Francke, 2013: 545; Botero-Trujillo, 2014: 121, 130; Sharma et al., 2014: 2976, 2979, figs. 10, 12; Tourinho et al., 2014: 81; Fernández and Giribet, 2015: 2, 3, 9, 10, fig. 2c; Armas and Agreda, 2016: 79; Botero-Trujillo and Valdez-Mondragón, 2016: 321, 322, 332, 335; Salvatierra and Tourinho, 2016: 1, 9, 10, 17; Botero-Trujillo and Flórez, 2017: 483; Valdez-Mondragón and Francke, 2017: 12; Valdez-Mondragón et al., 2018: 114, 131; 2020: 2; Whalen and Selden, 2021: 606, 608; Benavides et al., 2021: 2–4, 11, 12, 14, 15, figs. 2–5; Botero-Trujillo et al., 2021a: 3, 4, 6, 8–10, 12–17, 20–24, 26–28, 30–32, 36–41, 46–49, 53, 55, figs. 2, 4–25, 28–31, 33, 34; 2021b: 2; Valdez-Mondragón and Juárez-Sánchez, 2021: 329; Botero-Trujillo et al., 2022: 493; Sato et al., 2024: 1–4, 6, 7, figs. 1c, d, 2a, c–e, 3b,c; Král et al., 2025: 29, 40, 41; Prendini, 2025: 408, 409; Valdez-Mondragón et al., 2025: 30.

Diagnosis: *Ricinoides*, as redefined herein, may be separated from other African genera of Ricinulei as follows. The tegument of *Ricinoides* lacks polygonal (calyxlike to navicular) setae and saucer-shaped granules, whereas polygonal setae are present in *Bambara* (figs. 25, 26, 27B), *Gizoo*, and *Tautau* (figs. 30, 31), and saucer-shaped granules

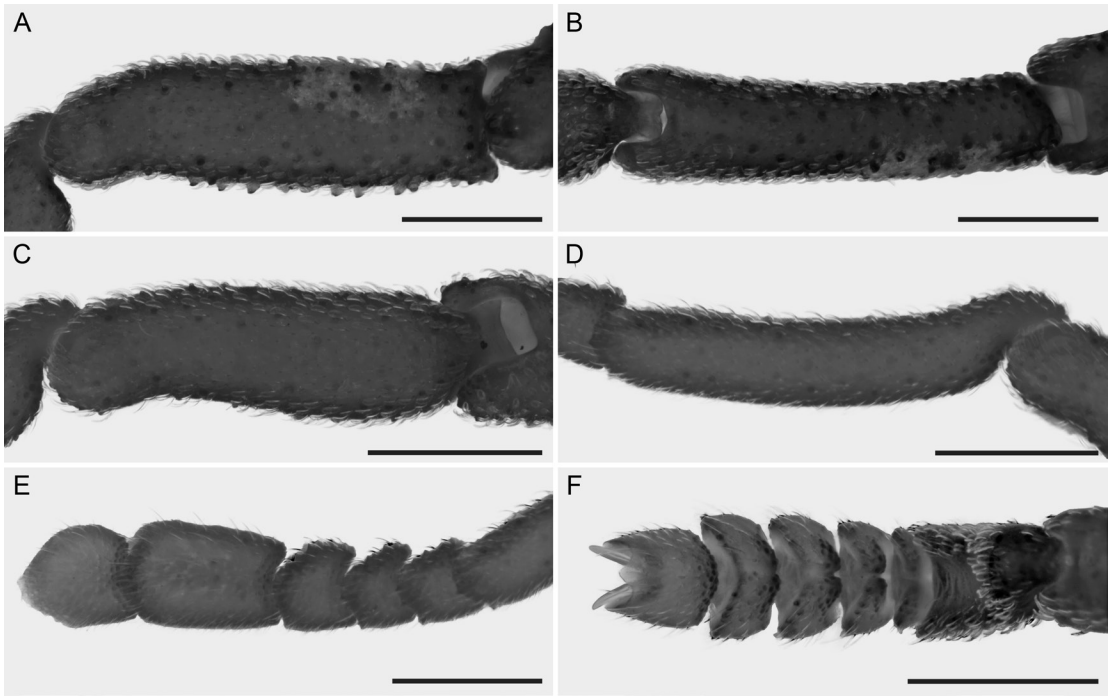

FIGURE 28. *Bambara jocquei*, gen. et sp. nov., holotype ♂ (MRAC 209.284). **A B.** Leg II femur, **A.** prolateral and **B.** dorsal aspects. **C.** Leg II tibia, prolateral aspect. **D.** Leg II metatarsus, prolateral aspect. **E.** Leg II tarsus, prolateral aspect. **F.** Dextral leg IV tarsus, dorsal aspect, illustrating swollen second to fourth tarsomeres. Scale bars = 0.5 mm.

are present in *Alantakun* and *Ududo*. The granules on the carapace and dorsal surface of the opisthosoma are separated in *Ricinoides*, but distinctly clustered in *Alantakun*. The carapaces of male and female *Ricinoides* (the females of *R. eburneus*, *R. iita*, and *R. westermannii* are unknown) lack a posteromedian moundlike excrescence that is present in the male of *Gizoo* and *Tautau* (figs. 30A, 31A) and the females of *Bambara* (fig. 26A) and *Gizoo*. The ventral part of the anterior surface of the cucullus (♂) is shallowly convex and does not bear particularly coarse granules in *Ricinoides* (fig. 8A, B, D), whereas it is almost flat and coarsely granular in *Alantakun* (fig. 8F). The ventrolateral margins of the cucullus are rounded in *Ricinoides* (fig. 8A, B) but moderately truncate in *Bambara* (except *B. megahanseni*, known only from the female) (figs. 8C, 27A). The ventral margin of the cucullus is linear or sublinear in *Ricinoides* (fig. 8A, B) but bilobate in the male and female of *Ududo* (at least in *U. tuxeni*, as the female of *U. sjostedtii* is unknown) and the male and, to a lesser extent, the female of *B. jocquei* (fig. 27A). The tritosternum is vestigial, yet visible, in *Ricinoides*, but extremely small, not exposed, in *Alantakun* (fig. 22A). The pedipalp tibia is robust along its entire length in *Ricinoides*, except *R. westermannii* and *R. feae*, in which it is not noticeably robust (fig. 11D), but markedly swollen proximally compared to the rest of the segment, in *Alantakun* (fig. 11A), *Bambara* (fig. 11C), *Gizoo*, and *T. ziama* (fig. 11E), and moderately swollen proximally, in *Ududo* (figs. 11F, 36C). The pedipalp tibia lacks apical longitudinal carinae in *Ricinoides* (figs. 10A, B, 11D), which are present in *Bambara* (figs. 11C, 27C, D) and *T. ziama* (figs. 11E, 31D, E). The distal region

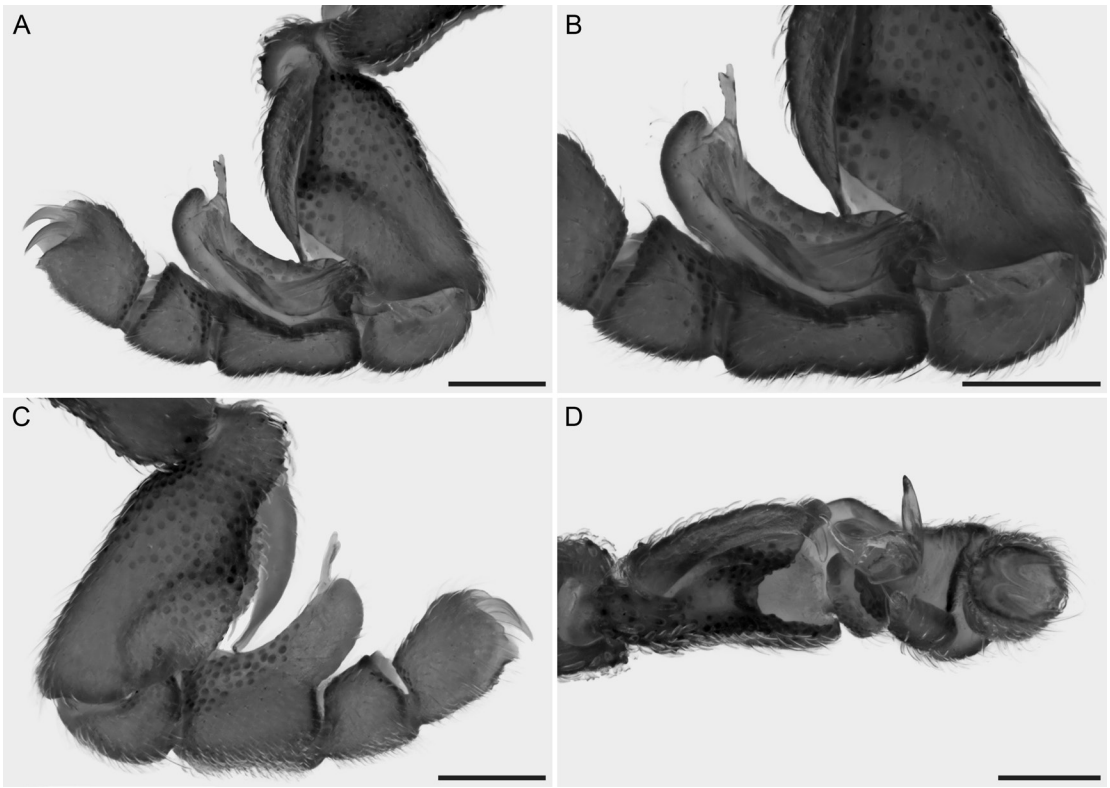

FIGURE 29. *Bambara jocquei*, gen. et sp. nov., holotype ♂ (MRAC 209.284), leg III (modified) distal segments, **A.** prolateral aspect, with **B.** closeup of copulatory apparatus, **C.** retrolateral aspect, and **D.** dorsal (relative to metatarsus) or frontal (relative to tarsus) aspect. Scale bars = 0.25 mm.

of the pedipalp tibia bears raised tubercles that are oval in *Ricinoides* (figs. 10A, B, 11D), elongate in *Alantakun* (fig. 11B) and *Gizoo*, and absent in *Bambara* (figs. 11C, 27C, D) and *Tautau* (figs. 11E, 31D, E). A longitudinal sulcus is present dorsally on the leg femora in *Ricinoides* but absent in the other genera. The leg I femur (♂) is slightly swollen and moderately robust in *Ricinoides*, except *R. taii*, in which it is unmodified, but slender in *Bambara*, *Gizoo*, and *Tautau*. The leg I tibia (♂) lacks ventral apophyses in *Ricinoides* (fig. 12B), which are present in *Ududo* (figs. 12A, C, 37C, D). The leg I metatarsus (♂) is sublinear in lateral aspect and subcircular in cross section, in *Ricinoides* (fig. 12B), but convex ventrally in lateral aspect and dorsoventrally elongate in cross section, in *Ududo* (figs. 12C, 36E). The leg I metatarsus (♂) exhibits a proventral proximal depression in *Ricinoides* (fig. 12B), which is absent in *Bambara*, *Gizoo*, *Tautau*, and *Ududo* (fig. 36E). The leg II femur (♂) is markedly swollen and noticeably robust in *Ricinoides* (slightly swollen and moderately robust in *R. taii*), but slender in *Bambara* (fig. 28A, B), *Gizoo*, *Tautau* (fig. 32A, B), and *Ududo* (fig. 37A, B). The leg II tibia (♂) bears a ventromedian apophysis in *Ricinoides*, except *R. westermannii* (fig. 12D), which is absent in the other genera (figs. 28C, 32C). The leg II metatarsus (♂) of *Ricinoides* exhibits a shallow to deep, ventral subproximal depression (fig. 12E), which is absent in the other genera (figs. 28D, 32D, 37E), and lacks a ventrosubmedian concavity, which is present in *Alantakun*. The terminal (fifth) tarsomere of leg II is movable, not fused to the preceding tarsomere, in

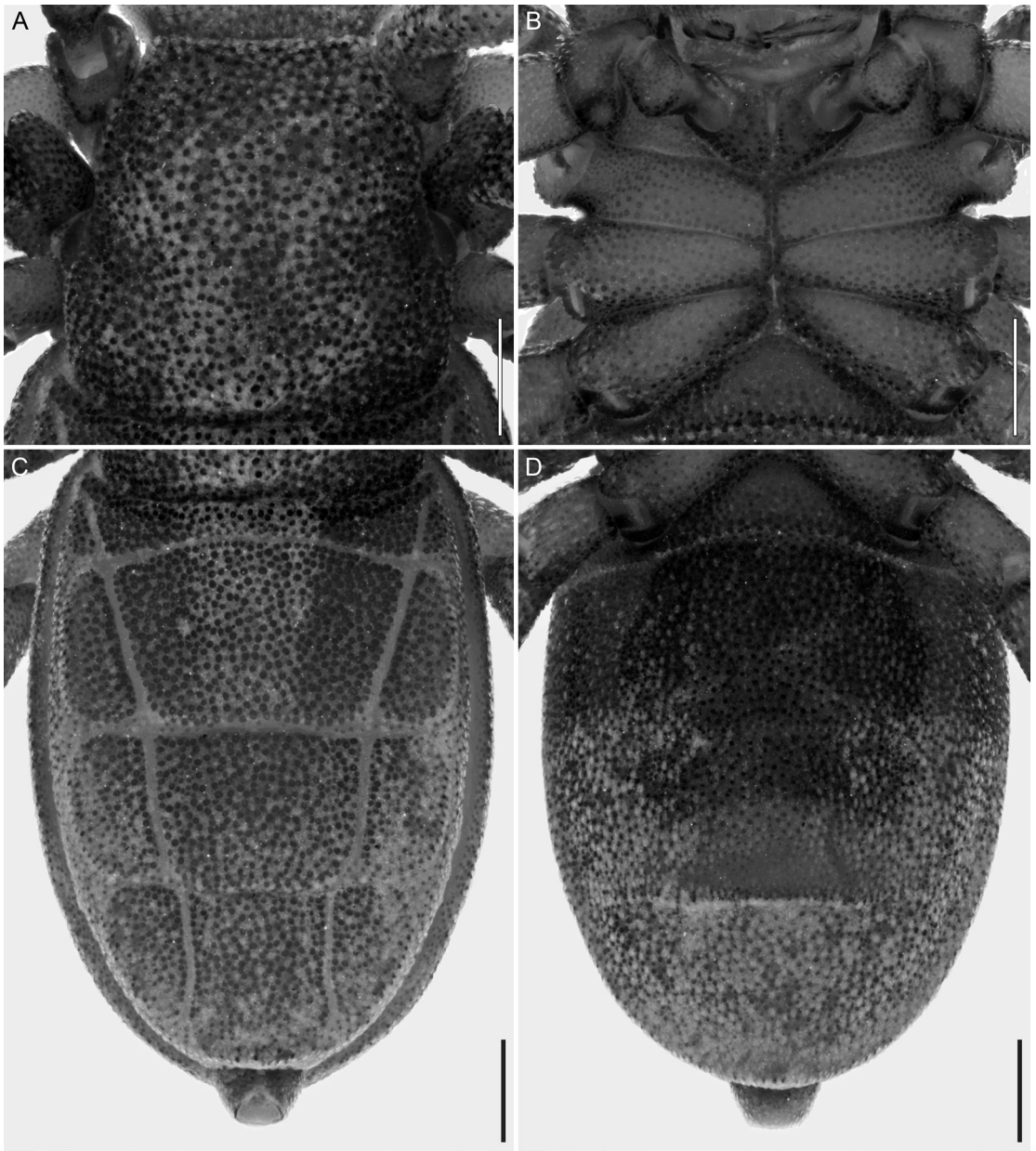

FIGURE 30. *Tautau ziama*, gen. et sp. nov., holotype ♂ (MRAC 209.517). **A.** Carapace, dorsal aspect, illustrating posteromedian moundlike excrescence. **B.** Coxosternal region, ventral aspect. **C, D.** Opisthosoma, **C.** dorsal and **D.** ventral aspects. Scale bars = 0.5 mm.

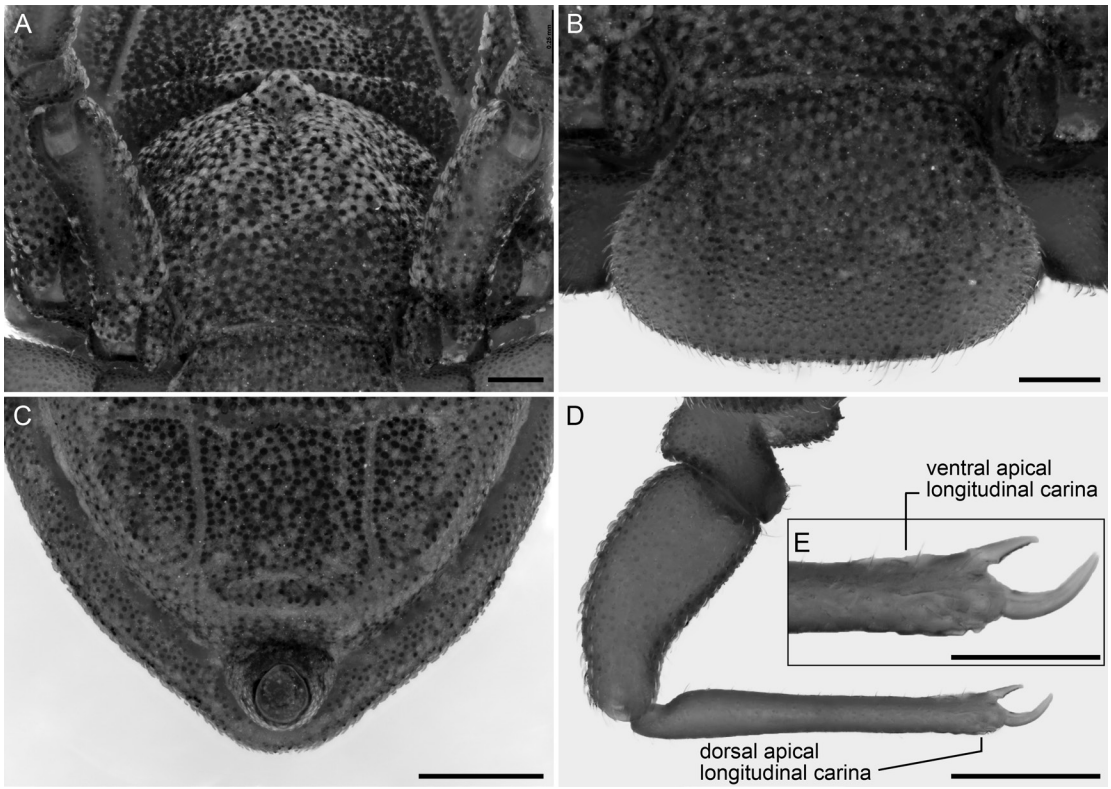

FIGURE 31. *Tautau ziama*, gen. et sp. nov., holotype ♂ (MRAC 209.517). **A.** Carapace, anterodorsal aspect, illustrating posteromedian moundlike excrescence. **B.** Cucullus, anterior aspect. **C.** Opisthosoma, posterior end, posterodorsal aspect. **D, E.** Pedipalp, **D.** prolateral aspect, with **E.** closeup of distal part of tibia. Scale bars = 0.25 mm (**A, B, E**), 0.5 mm (**C, D**).

Ricinoides (fig. 12E), but fixed, fused to the preceding (fourth) tarsomere, in *Gizoo* and *Tautau* (fig. 32E). The leg III femur (♂) is slender in *Ricinoides*, except *R. afzelii* and *R. iita*, in which, as in *Alantakun* and *Ududo*, it is slightly swollen. The leg III metatarsus (♂) is relatively slender in *Ricinoides* (fig. 14D) but swollen in *Alantakun* (fig. 14A) and *Tautau* (fig. 14E). The dorsal surface of the leg III metatarsus (♂) is not excavated basally in *Ricinoides* (fig. 14D), whereas it is moderately excavated in *Ududo* (figs. 14F, 38D) and markedly excavated in *Alantakun* (fig. 14A). The dorsal concavity of the leg III metatarsus (♂) is moderately deep distally and gradually becomes shallower proximally, in *Ricinoides* (fig. 14D), whereas it is very deep and forms a well-defined chamber extending across the distal half of the segment, in *Alantakun* (fig. 14A) and *Ududo* (figs. 14F, 38D), and to the attachment point of the metatarsal process, in *Tautau* (fig. 14E). The prodorsal margin of the second tarsomere of leg III (♂) is sublinear to slightly curved proximally (in prolateral aspect) in *Ricinoides* (fig. 13B), but moderately angular in *Alantakun* (fig. 13A). The third tarsomere of leg III (♂) bears an acute dorsodistal process in *Ricinoides* (fig. 13B), which is absent in the other genera (fig. 13A). The second to fourth tarsomeres of leg IV (♂) are unmodified in *Ricinoides*, but swollen in *Bambara* (fig. 28F), *Gizoo*, *Tautau* (fig. 32F), and *Ududo* (figs. 12F, 37F). The male copulatory apparatus fixed process is of the *atewa* Type in *Ricinoides* (fig. 15). The median sclerite of opisthosomal tergite

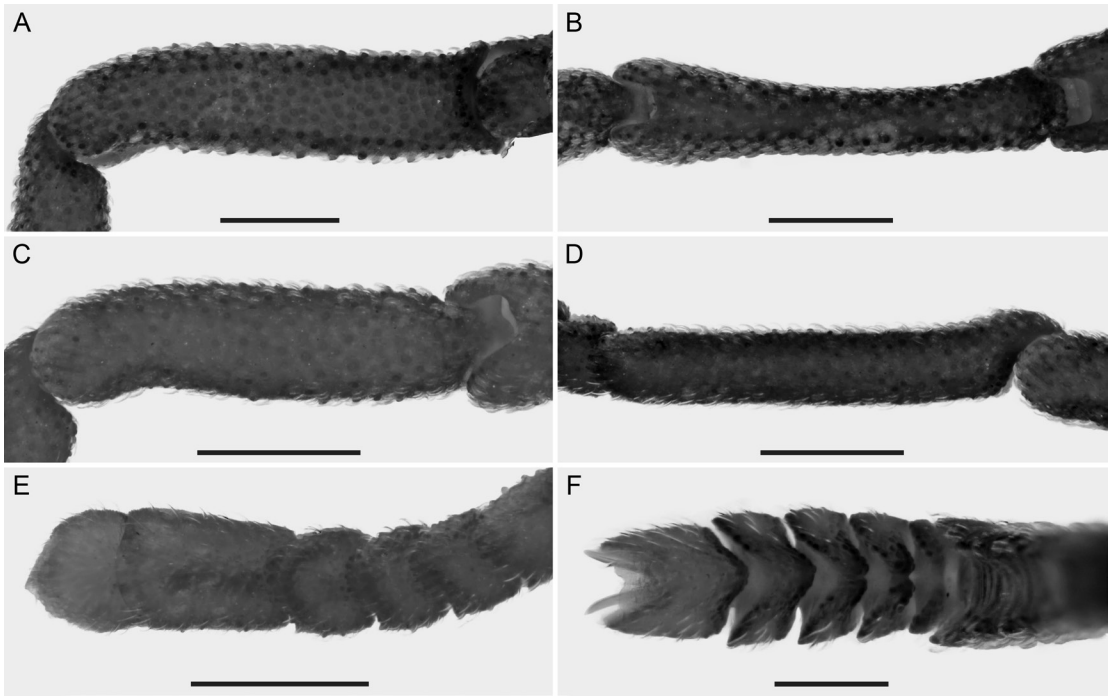

FIGURE 32. *Tautau ziama*, gen. et sp. nov., holotype ♂ (MRAC 209.517). **A, B.** Leg II femur, **A.** prolateral and **B.** dorsal aspects. **C.** Leg II tibia, prolateral aspect. **D.** Leg II metatarsus, prolateral aspect. **E.** Leg II tarsus, prolateral aspect, illustrating fifth tarsomere fixed, fused to fourth. **F.** Leg IV (dextral) tarsus, dorsal aspect, illustrating swollen second to fourth tarsomeres. Scale bars = 0.5 mm (**A–E**), 0.25 mm (**F**).

XIII is rectangular to trapezoid in *Ricinoides*, but cup shaped in *Bambara* (except *B. megahanseni*) (figs. 23A, 25C, 26C, 27B). The tergal membranes of the opisthosoma are granular in *Ricinoides*, but smooth in *Bambara*, *Gizoo*, and *T. leonensis*. The posterodorsal and posteroventral margins of the opisthosoma lack subspiniform granules in *Ricinoides*, which are present in *Alantakun* and *Ududo* (figs. 23B, 34C, D, 35C, D, 36B). The opisthosomal dorsal and ventral pleural membranes are finely and densely granular in *Ricinoides*, whereas the dorsal and, sometimes, the ventral pleural membrane are moderately to sparsely granular in *Bambara*. The basal segment of the pygidium is parallel to the longitudinal axis of the opisthosoma in *Ricinoides*, but slightly tilted dorsally in *Bambara* (figs. 25C, 26C), *Gizoo* (fig. 23E, F), and *T. ziama* (figs. 30C, 31C). The posterior margin of the basal segment of the pygidium is narrow in *Ricinoides*, entirely broad in *Alantakun* (fig. 23C, D) and *Ududo* (fig. 23G, H), and only broad ventrally in *Gizoo* (fig. 23E, F). The opening of the basal segment of the pygidium is distinctly narrow, its width two-fifths (*R. feae* and *R. westermannii* only) to one-third the lateral width of the segment at its base, in *Ricinoides*, but broad, its width at least half the lateral width of the segment, in the other genera.

Included Species: *Ricinoides*, as redefined herein, accommodates nine species: *Ricinoides afzelii* (Thorell, 1892); *Ricinoides atewa* Naskrecki, 2008; *Ricinoides eburneus* Botero-Trujillo et al., 2021; *Ricinoides feae* (Hansen, 1921); *Ricinoides iita* Botero-Trujillo et al., 2021; *Ricinoides kakum* Botero-Trujillo et al., 2021; *Ricinoides nzerekorensis* Botero-Trujillo et al., 2021; *Ricinoides taii* Botero-Trujillo et al., 2021; and *Ricinoides westermannii* (Guérin-Méneville, 1838).

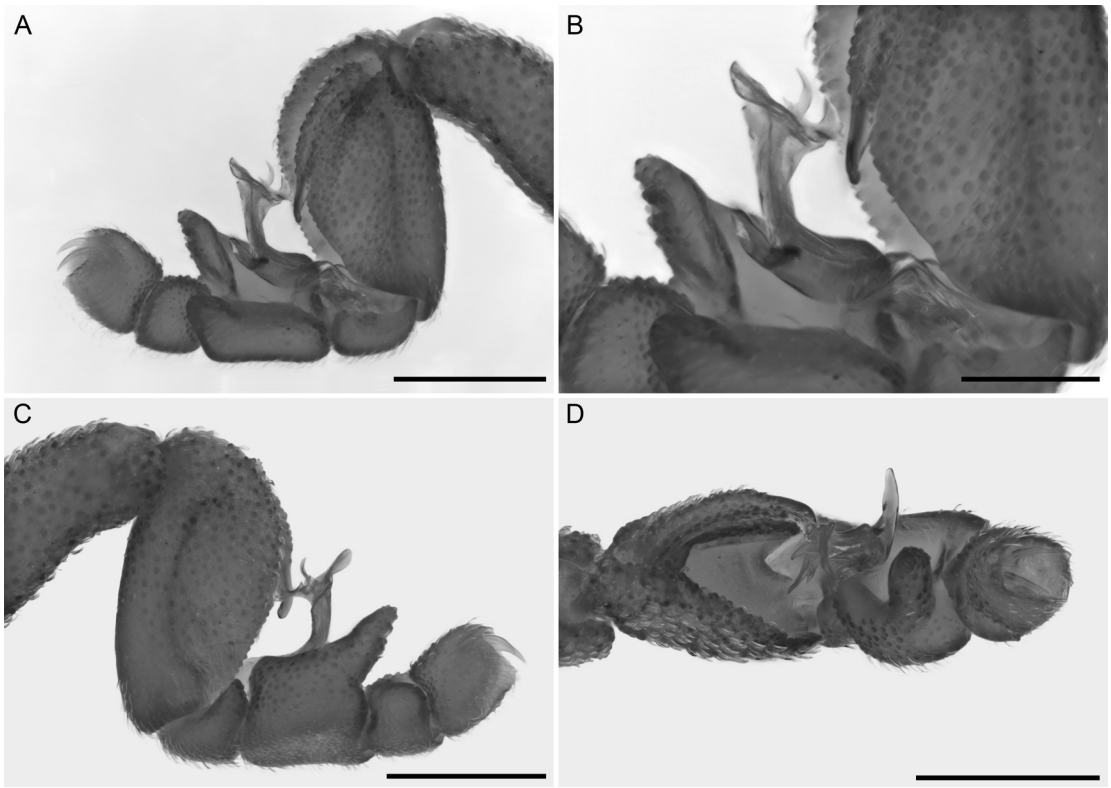

FIGURE 33. *Tautau ziama*, gen. et sp. nov., holotype ♂ (MRAC 209.517), leg III (modified) distal segments, **A.** prolateral aspect, with **B.** closeup of copulatory apparatus, **C.** retrolateral aspect, and **D.** dorsal (relative to metatarsus) or frontal (relative to tarsus) aspect. Scale bars = 0.5 mm (**A, C, D**), 0.25 mm (**B**).

Distribution: Species of *Ricinoides* have been recorded in Côte d'Ivoire, the Gambia, Ghana, Guinea, Guinea-Bissau, Nigeria, Senegal, Sierra Leone, and Togo (figs. 5, 6).

Remarks: Fernández and Giribet (2015: 6) referred to a specimen used in their COI phylogenetic analysis as "*Ricinoides gemmifera*." This name is a nomen nudum (ICZN, 1999).

Ricinoides afzelii (Thorell, 1892)

Figures 5, 8B, table 1

Cryptostemma afzelii Thorell, 1892: 10–17, figs. 1–8; Karsch, 1892b: 64; Hansen and Sørensen, 1904: 150, 151, unpaginated, pl. VIII, figs. 2a–g; Petrunkevitch, 1913: 77, fig. 43; Bolívar y Pieltain, 1942: 198; Tuxen, 1974: 86.

Ricinoides afzelii (Thorell, 1892): Ewing, 1929: 597; Kästner, 1932: 103, fig. 140; Bolívar y Pieltain, 1942: 201; Pollock, 1966: 402–405, unnumbered figs.; Cooke, 1967: 31, 35; Pollock, 1967: 19–22; Kaestner, 1968: 204, 207; Kennaugh, 1968: 394–396, 401, unpaginated, pls. IIb, IIIa, IVb, Vb, VI; Mitchell, 1969: 137; 1970: 64, 72; Pittard, 1970: 2, 11; Cooke, 1971: 4, 7, 18; Pittard and Mitchell, 1972: 4, 6; Tuxen, 1974: 86–89, 90–96 (part, material from Sierra Leone), figs. 5, 8; Legg, 1977: 58; Savory, 1977: 216, 219, fig. 88; Legg, 1978a: 89, 91, 93, 98, 99; 1978b: 124, 125, figs. 1, 2; Platnick and Pass, 1982: 2, 3; Harvey, 1984: 205, 207 (part), 208, 209, fig.

10; Selden, 1992: 598; Dunlop, 1994: 56, unnumbered fig.; 1996: 195, 200, fig. 11 (misidentification); Harvey, 2003: 183 (part); Beccaloni, 2009: 147, 154, 155, 157; Penney et al., 2009: 66; García et al., 2015: 455; Botero-Trujillo et al., 2021a: 4, 6, 8, 10–20, 22, 23, 26, 27, 30, 31, 36–38, 44, 46, 53, 55, 59, 65, figs. 5, 6A, 7A, 9A, 11A, 12A, 14A, 15A, 17A, 18A, 20A, 21A, 22A, C, E, G, 28A, C, E, G, I, 33A, 34A.

Ricinoides afzeli: Savory, 1964: 198, fig. 101; Valdez-Mondragón and Francke, 2017: 14.

Ricinoides afzelli: Legg, 1976b: 54; García et al., 2015: 455.

Ricinoides afzellii: Legg, 1976b: 1, 2, 51 (material from Sierra Leone).

Ricinoides cf. *afzelii*: Murienne et al., 2013: 2, 4, 5, figs. 1, 2 (misidentification).

Type Material Examined: Holotype ♀ (NHRS JUST 518, Thorell Collection), **SIERRA LEONE**, Afzelius. A microvial contains the following detached fragments: sinistral chelicera, dextral pedipalp femur, and second trochanter, and two pieces of the tarsi of legs III or IV. The following body parts are missing: cucullus, dextral chelicera, sinistral pedipalp femur, and tibia, dextral pedipalp first trochanter and tibia, tarsus of leg III or IV, and second to fifth tarsomeres of both legs II.

Diagnosis: The male of *Ricinoides afzelii* resembles the males of *R. atewa*, *R. iita*, and *R. kakum* in the modified ventral part of the cucullus. It further resembles the male of *R. iita* in possessing an apical brushlike row of yellowish setae on the proventral surface of the metatarsus of leg III, and in the dimensions of the femur of leg IV, which is wider than the femur of leg III and deeper than the femur of leg I, characters uniquely shared by the two species. On the other hand, the male of *R. afzelii* resembles the males of *R. atewa* and *R. kakum* in the presence of enlarged tubercles on the distal half of the ventral surface of the pedipalp tibia. The male of *R. afzelii* differs from the males of *R. atewa*, *R. iita*, and *R. kakum* in the following respects: the cucullus bears a pronounced anteromedian knoblike tubercle (fig. 8B); the distal retroventral tubercles of the pedipalp tibia are greatly enlarged; the femur of leg I is wider than the femur of leg IV, which in turn is wider than the femur of leg III; and the metatarsus of leg I bears a prominent ventral excrescence. *Ricinoides afzelii* may be further recognized by the structure of the fixed process of the male copulatory apparatus, in which the β lobe is entire and the *pd* lobe dorsoventrally expanded and laterally compressed.

Distribution: *Ricinoides afzelii* is known only from Bo in the Southern Province of Sierra Leone (fig. 5), where it is codistributed with *T. leonensis*.

Additional Material Examined: **SIERRA LEONE:** E.E. Austen, 1 ♀ (BMNH 13588947). *Southern Province*: Bo [07°57′N 11°44′W], vi–x.1964, J. Pollock, beneath log, 1 ♂ (BMNH 13588948), same data, except: viii.1965, 2 ♂ (BMNH 13588950), 1 ♂ (BMNH 13588953), 3 ♀ (BMNH 13588949, 13588951, 13588952), 1 tritonymph (BMNH 13588954), 2 deutonymphs (BMNH 13588958), 1 deutonymph (BMNH 13588956), 1 protonymph (BMNH 13588955), 1 larva (BMNH 13588957), same data, except: 19.x.1965, 1 ♀ (AMNH IZC 324954).

Ricinoides atewa Naskrecki, 2008

Figures 5, 8E, table 1

Ricinoides westermannii (Guérin-Méneville, 1838): Harvey, 1984: 205–208, figs. 1–9 (misidentification); 2003: 184 (misidentification, material from Ghana).

Ricinoides atewa Naskrecki, 2008: 58–64, figs. 1–13, 20–28; Beccaloni, 2009: 156; Murienne et al., 2013: 2, 4–6, figs. 1, 2; Sharma et al., 2014: 2964, 2966–2968, 2971, 2973, 2978, figs. 1f, 2, 3, 6, 8, 11; Fernández and Giribet, 2015: 2, 3, 7, 8, 11, figs. 1a, 2b, 3a–c; Sharma et al., 2015: 4, fig. 2c; Santibáñez-López et al., 2018: 8, fig. 1a; Sharma et al., 2018: 40, fig. 2; Ballesteros and Sharma, 2019: 902, fig. 1; Ballesteros et al., 2019: 3, 6,

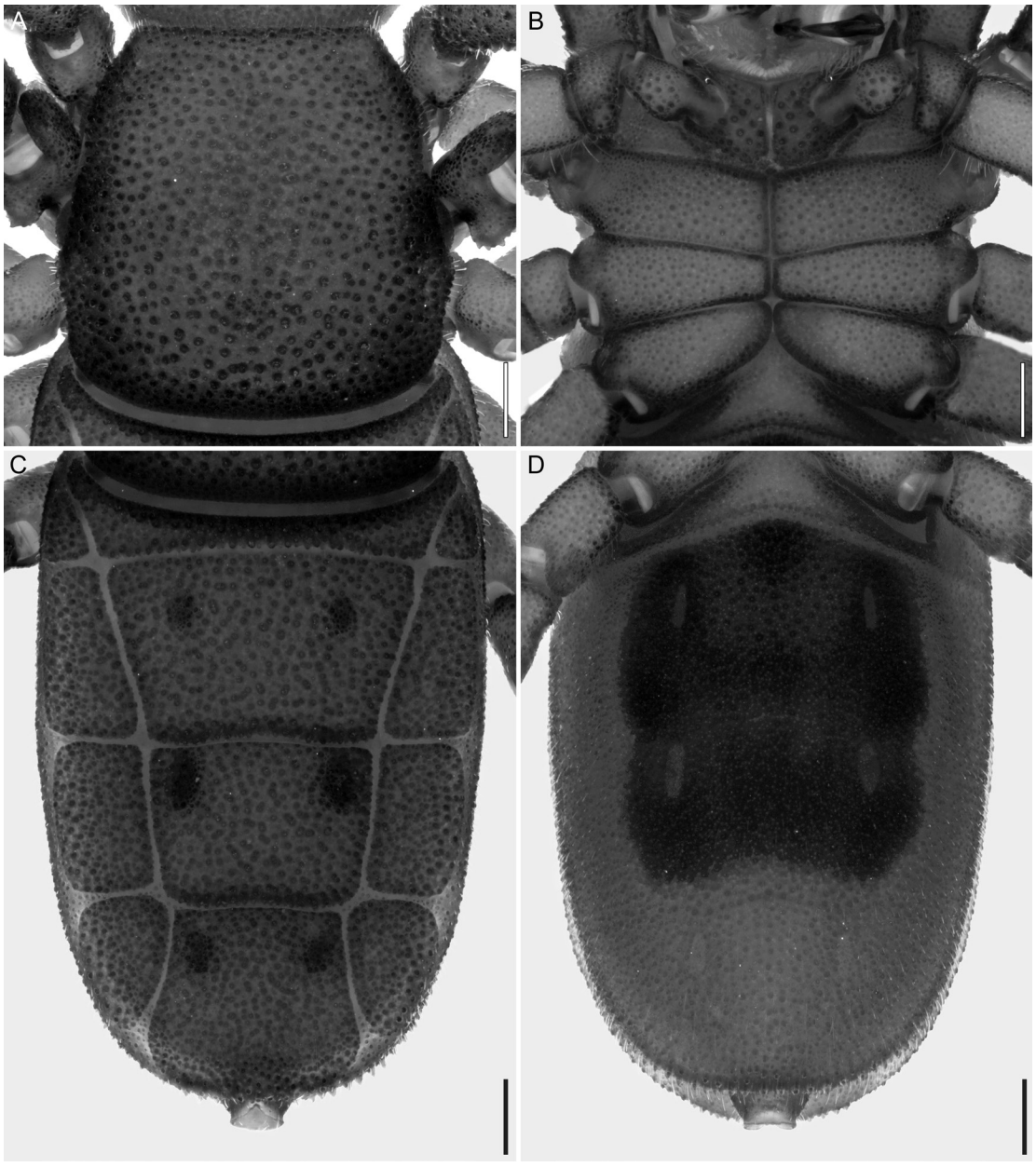

FIGURE 34. *Ududo tuxeni*, gen. et sp. nov., holotype ♂ (BMNH 13588977 old 1953.3.28.71). **A.** Carapace, dorsal aspect. **B.** Coxosternal region, ventral aspect. **C, D.** Opisthosoma, **C.** dorsal and **D.** ventral aspects, illustrating subspiniform granules posteriorly. Scale bars = 0.5 mm.

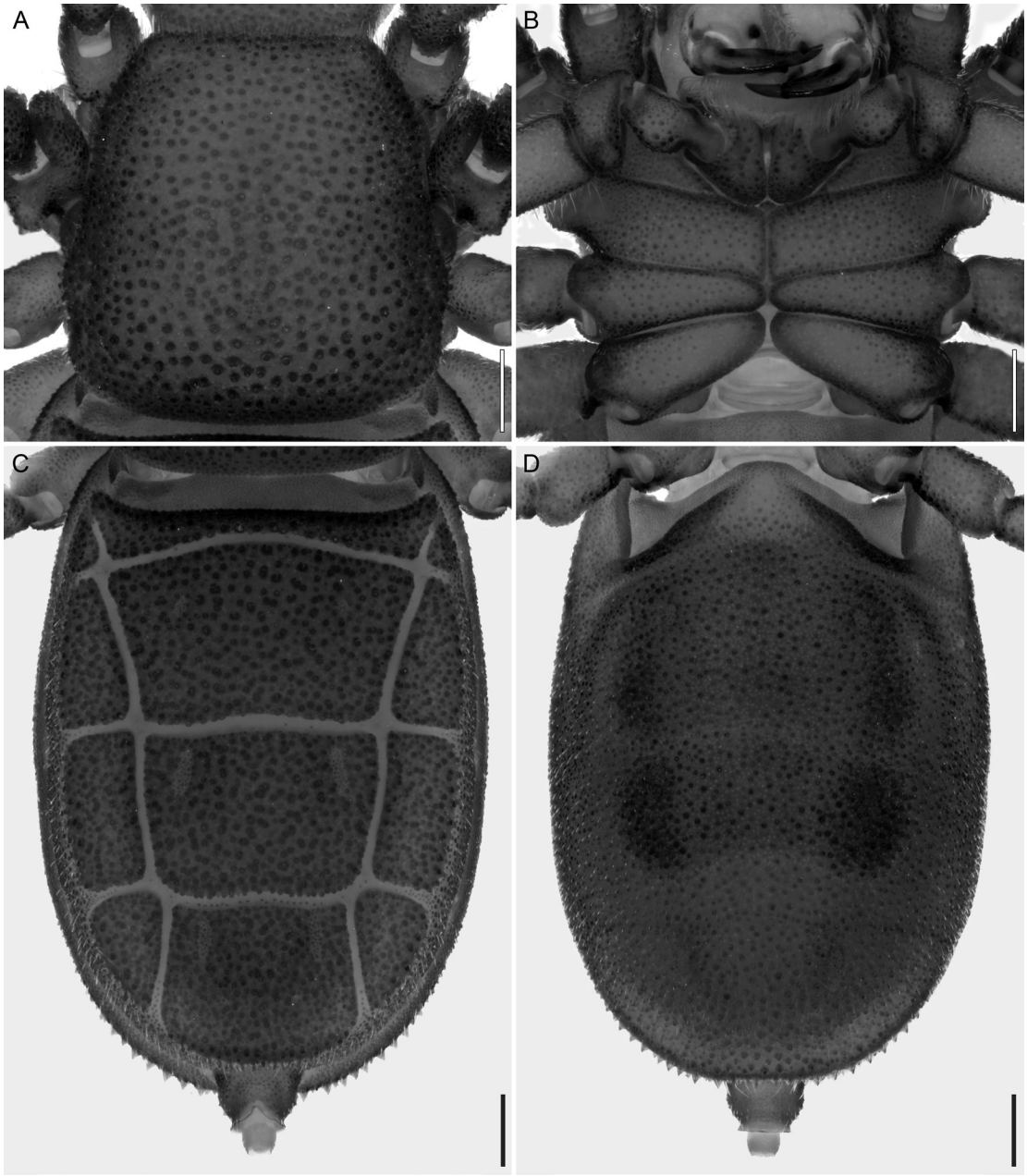

FIGURE 35. *Ududo tuxeni*, gen. et sp. nov., paratype ♀ (BMNH 13588978 old 1953.3.28.61). **A.** Carapace, dorsal aspect. **B.** Coxosternal region, ventral aspect. **C, D.** Opisthosoma, **C.** dorsal and **D.** ventral aspects, illustrating subspiniform granules posteriorly. Scale bars = 0.5 mm.

figs. 1a, 3a, c; Lozano-Fernández et al., 2019: 4, fig. 2; Benavides et al., 2021: 3, 7, 10–12, 14, 15, figs. 1c, 3a, 3b, 4a, 5; Botero-Trujillo et al., 2021a: 4, 11–15, 17–31, 36–38, 44, 46, 51, 53, 55, 64, figs. 5, 6B, 7B, 9B, 10B, 11B, 12B, 14B, 15B, 17B, 18B, 20B, 21B, 22B, D, F, H, 28B, D, F, H, J, 33B, 34B.

Type material: Holotype ♂ (AMNH IZC 324855), **GHANA:** *Eastern Region*: Atewa Range Forest Reserve, Asiakwa, main road, 06°15′00.7″N 00°33′53.7″W, 817 m, 7–11.xii.2007 [reported as "06°15′43.9″N 00°33′16.5″W, 827 m, 8.xii.2007" in original description], P. Naskrecki, V. Awotwe-Pratt, and N. Jengre [examined]. The vial containing the holotype includes a microvial with the detached dextral copulatory apparatus. Paratypes: 1 ♂, 2 ♀ (AMNH/MCZ), same data as holotype; 1 ♀ (MCZ), same data as original description, except: 11–16.vi.2006, P. Naskrecki; 2 ♀ (AMNH/MCZ), same data, except: along main reserve road, 06°15′00.7″N 00°33′53.7″W, 817 m, 7–11.xii.2007, P. Naskrecki, V. Awotwe-Pratt, and N. Jengre. Ajenjua Bepo Forest Reserve, 06°22′02.3″N 01°01′58″W, 300–330 m, 26–30.viii.2006, P. Naskrecki, 4 ♀ (AMNH/MCZ). Only the holotype, two males, and one female, labelled as paratypes although not listed as such in the original description (see Additional Material Examined), are present in the AMNH and there is no record confirming that additional specimens were deposited.

Diagnosis: *Ricinoides atewa* most closely resembles *R. kakum*. The males of both species share several characters, including a group of slightly raised granules anteromedially on the ventral part of the cucullus (fig. 8E), and moderately enlarged tubercles in the distal half of the ventral surface of the pedipalp tibia. The fixed process of the male copulatory apparatus of *R. atewa* resembles that of *R. kakum* in the laterally expanded *PL* lobe, a character also shared with *R. eburneus*, and the distinct subdistal serrations on the retrolateral margin of the α lobe, which is unique to *R. atewa* and *R. kakum*. The lateral sclerites of tergite X are well developed and the tergal membranes narrow in *R. atewa*, whereas the lateral sclerites of tergite X are obsolete and the tergal membranes broad, in *R. kakum*. Additionally, the moderately enlarged tubercles in the distal half of the ventral surface of the pedipalp tibia comprise two (proventral and retroventral) rows in the male of *R. atewa*, unlike the male of *R. kakum*, in which the tubercles comprise a single retroventral row.

Distribution: *Ricinoides atewa* has been recorded from several localities south of Lake Volta in the Eastern Region of Ghana (fig. 5).

Additional Material Examined: **GHANA:** *Eastern Region*: Akim Abuakwa region, NW of Asiakwa [06°16′N 00°30′W], Kibi hills, Pusa Pusa River, vii.1968, N.D. Jaga, 1 ♂, 1 ♀ (FMNH INS 3821310); Asamankese [05°51′N 00°40′W], 21.xii.1969, D. Leston, in rotten wood, dense shade on edge of coeva farm, 1 ♂ (AMNH IZC 324885); Mamang Forest Reserve, camp 2, 06°15′01.4″N 01°02′25.4″W, 130 m, 30.viii–5.ix.2006, P. Naskrecki and V. Awotwe-Pratt, 1 ♂, 1 ♀ (AMNH IZC 324883) [labeled "paratypes" but not mentioned in original description].

None of the following specimens, mentioned in the original description (Naskrecki, 2008), were located in the AMNH and there is no record confirming they were ever deposited: **GHANA:** *Eastern Region*: Ajenjua Bepo Forest Reserve, 06°22′02.3″N 01°01′58″W, 300–330 m, 26–30.viii.2006, P. Naskrecki, 3 ♂, 2 tritonymphs, 1 deutonymph, 1 protonymph (AMNH/MCZ) [1 ♂ (AMNH IZC 324951), labeled "paratype" but not mentioned as such in original description, examined]; Atewa Range Forest Reserve, Asiakwa, along main reserve road, 06°15′00.7″N 00°33′53.7″W, 817 m, 7–11.xii.2007, P. Naskrecki, V. Awotwe-Pratt, and N. Jengre, 4 ♂, 6 tritonymphs, 3 deutonymphs (AMNH/MCZ), same data, except: 06°15′43.9″N 00°33′16.5″W, 827 m, 8.xii.2007, 2 tritonymphs, 1 deutonymph (AMNH/MCZ).

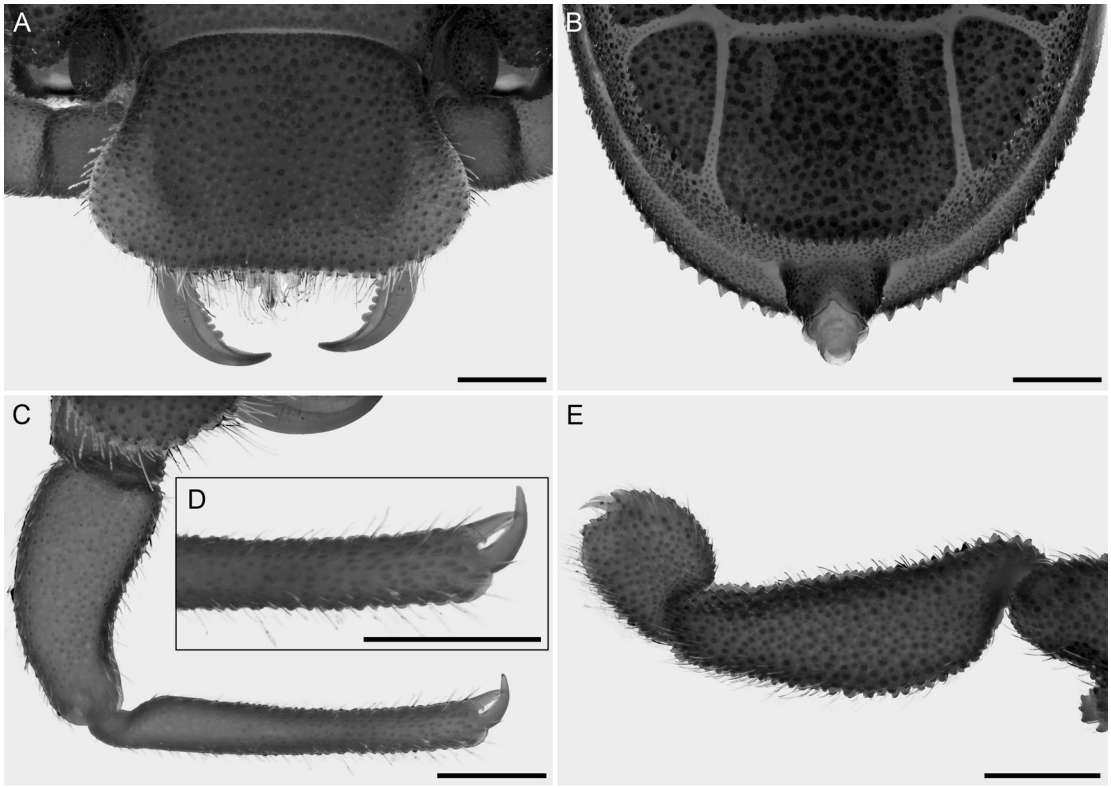

FIGURE 36. *Ududo tuxeni*, gen. et sp. nov., **A, C–E.** holotype ♂ (BMNH 13588977 old 1953.3.28.71), and **B.** paratype ♀ (BMNH 13588978 old 1953.3.28.61). **A.** Cucullus, anterior aspect. **B.** Opisthosoma, posterior end, posterodorsal aspect, illustrating subspiniform granules. **C.** Pedipalp, prolateral aspect, with **D.** closeup of distal part of tibia, illustrating raised oval tubercles. **E.** Leg I metatarsus and tarsus, prolateral aspect, illustrating metatarsus convex ventrally. Scale bars = 0.5 mm.

Ricinoides eburneus Botero-Trujillo et al., 2021

Figure 6, table 1

Ricinoides eburneus Botero-Trujillo et al., 2021a: 4, 12–14, 17, 18, 20–22, 26, 29–33, 36, 37, 39, 47, 51, 53, 62, figs. 5, 6C, 9C, 11C, 14C, 17C, 20C, 21C, 23A, C, E, G, 29A, C, E, G, I, 33C.

Type Material Examined: Holotype ♂ (MRAC 230.162), **CÔTE D'IVOIRE:** *Montagnes and Bas-Sassandra Districts*: Forêt de Taï [Taï National Park, 05°41′N 06°56′W], C.R.E., road near Chimpanzee Camp, 20.ii.2010, M. Diarassouba, forest across river, on clayey soil, near pitfalls III, manual capture. Two microvials contain the following detached pieces: sinistral leg I and dextral copulatory apparatus.

Diagnosis: *Ricinoides eburneus* resembles *R. nzerekorensis* in possessing a distinct pad of bristlelike setae on the ventral surfaces of the tibia and metatarsus of leg II in the male, and *R. atewa* and *R. kakum* in the laterally expanded *PL* lobe of the male copulatory apparatus. The ventromedian apophysis on the tibia of leg II is smooth dorsally and prolaterally in the male of *R. eburneus* unlike all other species of the genus, in which the apophysis is entirely covered with granules (the apophysis is absent in *R. westermannii*). *Ricinoides eburneus* differs further from

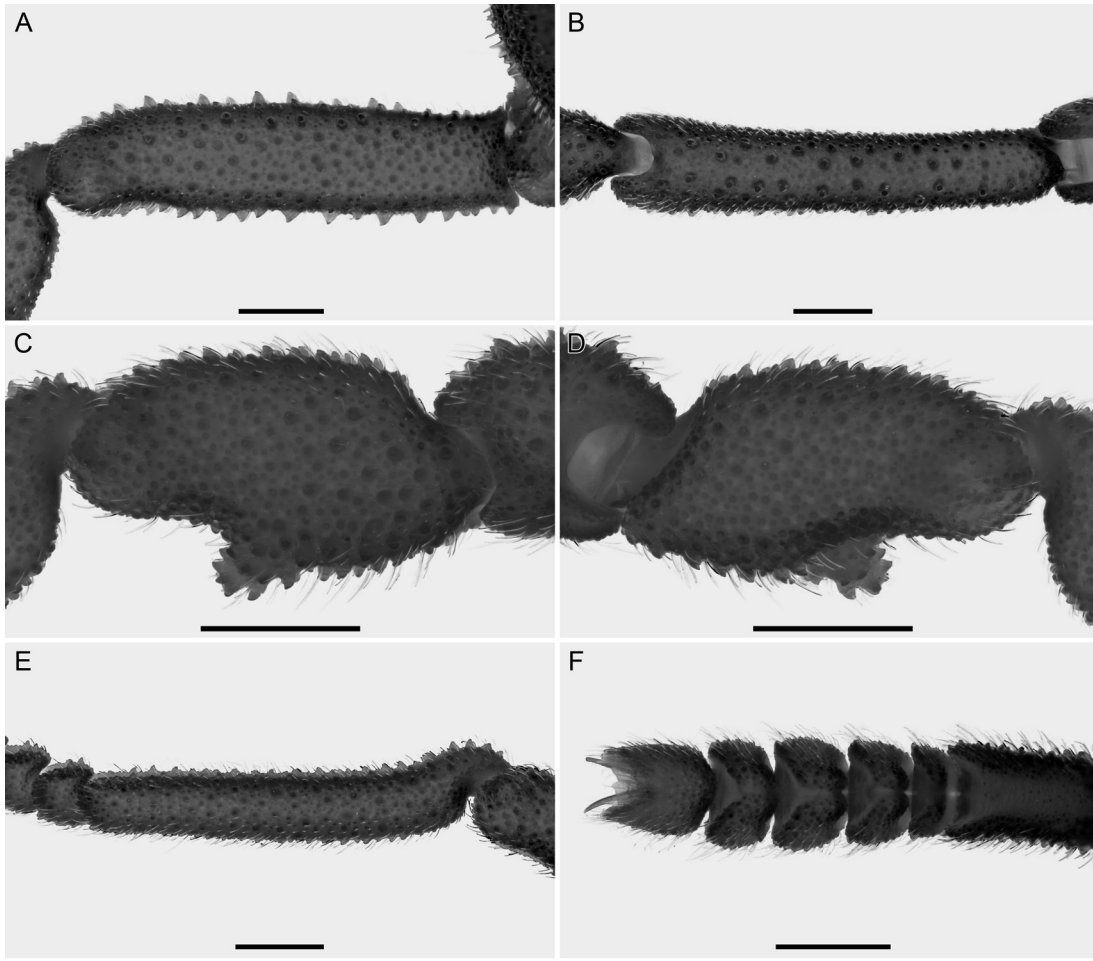

FIGURE 37. *Ududo tuxeni*, gen. et sp. nov., holotype ♂ (BMNH 13588977 old 1953.3.28.71). **A, B.** Leg II femur, **A.** prolateral and **B.** dorsal aspects. **C, D.** Leg I tibia, **C.** prolateral and **D.** retrolateral aspects. **E.** Leg II metatarsus, prolateral aspect. **F.** Sinistral leg IV tarsus, dorsal aspect. Scale bars = 0.5 mm.

R. nzerekorensis in the structure of the ventral pad of setae on the tibia of leg II in the male, which is more distinct and comprises longer setae, more than half the depth of the metatarsus of leg II. Other differences among the four species are evident in the structure of the male copulatory apparatus.

Distribution: *Ricinoides eburneus* is known only from the type locality, Taï National Park, in the Montagnes and Bas-Sassandra districts of Côte d'Ivoire (fig. 6). It is one of four ricinuleid species recorded in the national park, the others being *B. megahanseni*, *R. taii*, and an unidentified species of *Tautau*.

Remarks: The adult morphology of *R. eburneus* is known only from the male.

Ricinoides feae (Hansen, 1921)

Figure 5, table 1

Cryptostemma feae Hansen, 1921: 26–31, unpaginated, pl. II, figs. 3a–c, unpaginated, pl. III, figs. 1a–i; Hansen, 1930: unpaginated, pl. I,

fig. 11, unpaginated, pl. XV, fig. 9b; Bolívar y Pieltain, 1942: 199; Tuxen, 1974: 86.

Ricinoides feae (Hansen, 1921): Kästner, 1932: 112, 113, fig. 153; Bolívar y Pieltain, 1942: 201; Millot, 1945a: 72–74, figs. 1–3; 1945b: 1–29, figs. 1–34; 1949a: figs. 54a–c, 62, 79, 83, 90, 92; 1949b: 744–758, figs. 529–551; Zakhvatkin, 1952: 43, fig. 29b; Dubinin, 1962: 443, fig. 1287; Mitchell, 1969: 137; 1970: 63; Pittard and Mitchell, 1972: 10, 13; Tuxen, 1974: 86–89, 91, 94–98, 100, 105, figs. 18–23; Legg, 1976b: 2, 54; Dumitresco and Juvara-Balş, 1977a: 174–179, figs. 12a, b, 13a–e; 1977b: 259–261, fig. 1; Platnick and Shadab, 1977: 17; Legg, 1978a: 98, 99; Harvey, 1984: 209; Selden, 1992: 597; Selden and Dunlop, 1998: 305, fig. 7.1; Adis et al., 1999: 4; Harvey, 2003: 183; Naskrecki, 2008: 58; Talarico et al., 2008a: 396, 403; Penney et al., 2009: 66; Botero-Trujillo et al., 2021a: 4–6, 8, 12–15, 17, 20, 22, 23, 26, 27, 30, 31, 33–44, 47, 53, 55, 62, 65, figs. 1, 4C, 5, 6D, 7C, 9D, 11D, 12C, 14D, 15C, 17D, 18C, 20D, 21D, 23B, D, F, H, 29B, D, F, H, J, 33D, 34C.

Type Material Examined: *Cryptostemma feae*: Lectotype ♂ (MSNG), **GUINEA-BISSAU:** *Tombali Region*: Rio Cassine [Rio Cacine, 11°00′N 15°09′W], Guinea Portoghese, i–iv.1900, L. Fea. The vial containing the lectotype includes a microvial with the detached sinistral copulatory apparatus. Paralectotypes: *Bolama Region*: 4 ♂, 6 ♀, 12 tritonymphs, 13 deutonymphs, 8 protonymphs (MSNG), Bolama [11°34′37″N 15°28′44″W], Guinea Portoghese, vi–xii.1899, L. Fea; 2 larvae (MSNG), Bolama, Guinea Portoghese, L. Fea. *Tombali Region*: 9 ♂, 13 ♀, 27 tritonymphs, 3 deutonymphs, 3 protonymphs (MSNG), same data as lectotype; 1 ♂ (MSNG), 3 ♂, 1 ♀, 5 tritonymphs, 1 deutonymph, 1 protonymph (ZMUC), Rio Cacine, Guinea Portoghese, i–iv.1900, L. Fea.

Diagnosis: *Ricinoides feae* differs from the other eight species of the genus in the unique structure of the fixed process of the male copulatory apparatus, which features several distinctive characters, none shared with the other species, including the laterally compressed α lobe, the wide separation of β_1 and β_2 of the β lobe, the *pd* lobe forming a moderately broad raised surface, and the *rd* lobe comprising a cluster of small spines. Additionally, *R. feae* is the only species in which the median sclerite of tergite XIII is noticeably longer than wide, the sclerite being wider than long or as long as wide in the other species. *Ricinoides feae* differs further from all other species, except *R. westermannii*, in the relatively unmodified pedipalp tibia, which is markedly robust in the other species, and in the width of the opening of the basal segment of the pygidium, which is approximately two-fifths the lateral width of the segment at its base, but narrower laterally in the other species. The male of *R. feae* differs from the male of *R. westermannii* in several respects, including the presence of a large ventromedian apophysis on the tibia of leg II in *R. feae*, which is absent in *R. westermannii*.

Distribution: *Ricinoides feae* is known from only two localities in the Bolama and Tombali regions of Guinea-Bissau (fig. 5).

Remarks: According to the phylogenetic analyses (figs. 1, 2), *R. feae* is the second most basal species of the genus, after *R. westermannii*. Based on morphology, *R. feae* appears to be closely related to an undescribed species of *Ricinoides* from Guinea-Bissau (Botero-Trujillo et al., 2021a: 65) with which it is presumed to constitute a basal clade of *Ricinoides*.

Ricinoides iita Botero-Trujillo et al., 2021

Figures 5, 8G, table 1

Ricinoides iita Botero-Trujillo et al., 2021a: 4, 11–14, 17, 20–22, 26, 30, 35–37, 40, 43–51, 53, figs. 5, 6E, 9E, 10C, 11E, 14E, 17E, 20E, 21E, 24A, C, E, G, 27, 30A, C, E, G, I, 33E.

Type Material Examined: Holotype ♂ (USNM), **NIGERIA:** *Oyo*: Ibaden [Ibadan],

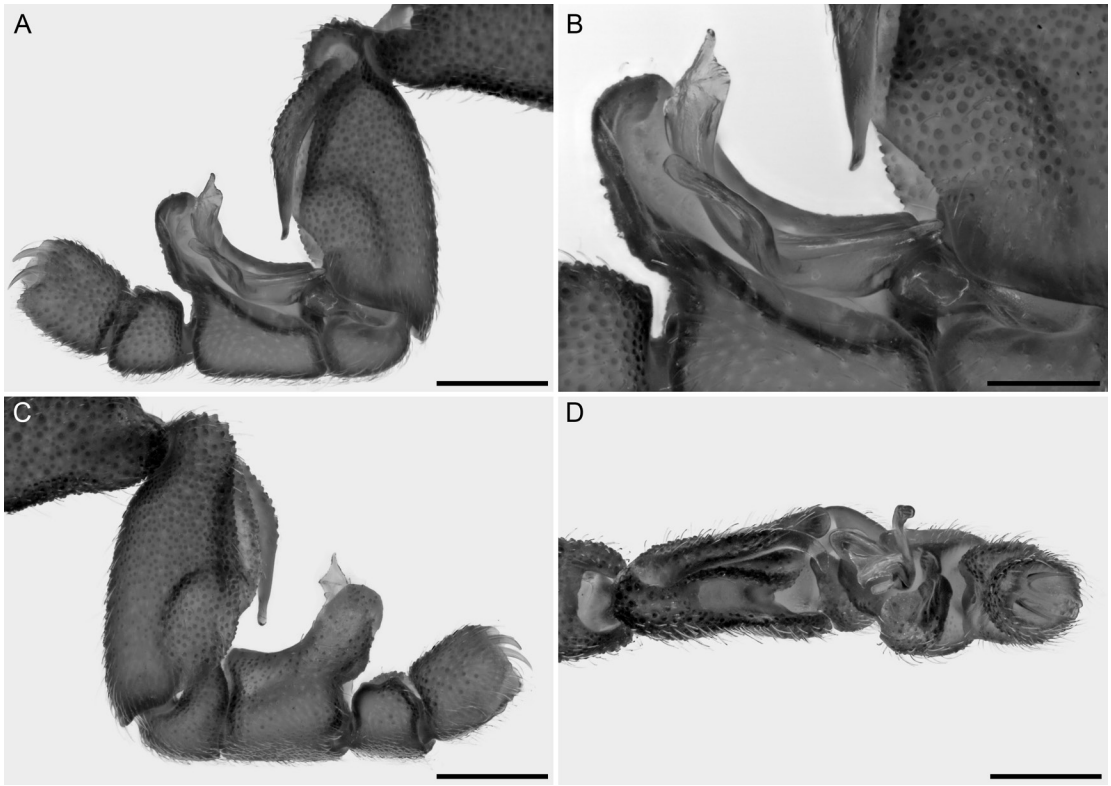

FIGURE 38. *Ududo tuxeni*, gen. et sp. nov., holotype ♂ (BMNH 13588977 old 1953.3.28.71), leg III (modified) distal segments, **A.** prolateral aspect, with **B.** closeup of copulatory apparatus, **C.** retrolateral aspect, and **D.** dorsal (relative to metatarsus) or frontal (relative to tarsus) aspect. Scale bars = 0.5 mm (**A, C, D**), 0.25 mm (**B**).

International Institute of Tropical Agriculture (IITA) [07°30′N 03°53′E], iv.1973, B. Critchley, pitfall. Two microvials contain the following detached pieces: sinistral leg I, dextral leg III, and copulatory apparatus.

Diagnosis: The male of *R. iita* resembles the males of *R. afzelii*, *R. atewa*, and *R. kakum* in the modified ventral part of the cucullus. It resembles the male of *R. afzelii* in possessing an apical brushlike row of yellowish setae on the proventral surface of the metatarsus of leg III and the femur of leg IV being wider than the femur of leg III, and deeper than the femur of leg I, characters unique to the two species. The male of *R. iita* is unique among the four species in the anteromedian elevation on the cucullus (fig. 8G), the tubercles on the ventral surface of the pedipalp tibia not being noticeably enlarged or arranged in distinct rows, the femur of leg IV being wider than the femur of leg I, and the femur of leg II less incrassate. Additionally, the structure of the fixed process of the male copulatory apparatus is unique in *R. iita*, as the α lobe is subcircular in cross section and curved retrolaterally, and β_2 of the β lobe is fingerlike and larger than β_1. Finally, the carapace of *R. iita* possesses the smallest semiocelli among the four species.

Distribution: *Ricinoides iita* is known only from the type locality, the International Institute of Tropical Agriculture (IITA) in the state of Oyo, Nigeria (fig. 5).

Remarks: The adult morphology of *R. iita* is known only from the male.

Ricinoides kakum Botero-Trujillo et al., 2021

Figures 6, 15, table 1

Ricinoides kakum Botero-Trujillo et al., 2021a: 4, 8, 11–15, 17, 20–23, 26, 27, 29–31, 35–37, 40, 44, 48, 51–55, figs. 4B, F, 5, 6F, 7D, 9F, 11F, 12D, 14F, 15D, 17F, 18D, 20F, 21F, 24B, D, F, H, 30B, D, F, H, J, 33F, 34D.

Type Material Examined: Holotype ♂, 2 ♀ paratypes (MRAC 217.183), **GHANA:** *Central Region*: Kakum Forest [Kakum National Park, 05°21′N 01°23′W], 8.xi.2005, L. Baert, R. Jocqué, and D. de Bakker, primary forest, pitfall. A microvial contains the following detached pieces of the holotype: sinistral leg III distal region with copulatory apparatus, and dextral copulatory apparatus.

Diagnosis: *Ricinoides kakum* most closely resembles *R. atewa*, with which it shares several characters of the male, including a group of slightly raised granules anteromedially on the ventral part of the cucullus and moderately enlarged tubercles in the distal half of the ventral surface of the pedipalp tibia. The fixed process of the male copulatory apparatus of *R. kakum* resembles that of *R. atewa* in the laterally expanded *PL* lobe (fig. 15), a character also shared by *R. eburneus*, and the distinct subdistal serrations on the retrolateral margin of the α lobe, which is unique to *R. kakum* and *R. atewa*. The lateral sclerites of tergite X are obsolete and the tergal membranes broad in *R. kakum*, whereas the lateral sclerites of tergite X are well developed and the tergal membranes narrow, in *R. atewa*. Additionally, the moderately enlarged tubercles in the distal half of the ventral surface of the pedipalp tibia comprise a single retroventral row in the male of *R. kakum*, unlike the male of *R. atewa*, in which the tubercles comprise two (proventral and retroventral) rows.

Distribution: *Ricinoides kakum* is known only from the type locality, Kakum National Park, in the Central Region of Ghana (fig. 6).

Additional Material Examined: **GHANA:** *Central Region*: Kakum Forest [Kakum National Park, 05°21′N 01°23′W], Kuntan trail, 159 m, 14–25.xi.2005, R. Jocqué, D. de Bakker, and L. Baert, secondary forest, pitfall, 1 ♀ (MRAC 217.210).

Ricinoides nzerekorensis
Botero-Trujillo et al., 2021

Figures 5, 11D, 12D, E, 13B, table 1

Ricinoides afzelii (Thorell, 1892): Tuxen, 1974: 90–96 (misidentification, material from Nzérékoré), figs. 2–4, 6–7, 9–17; Harvey, 1984: 207 (part); 2003: 183 (part); Naskrecki, 2008: 58, 62, figs. 14–19 (misidentification).

Ricinoides afzellii: Legg, 1976b: 1, 2 (misidentification, material from Guinea).

Ricinoides nzerekorensis Botero-Trujillo et al., 2021a: 4, 8, 12, 13, 15–17, 19, 20, 23, 24, 27–29, 31, 32, 36, 37, 41, 49, 53–60, figs. 4D, E, 5, 7E, 8A, 9G, 12E, 13A, 15E, 16A, 18E, 19A, 20G, 21G, 25A, C, E, G, 31A, C, E, G, I, 33G, 34E; Benavides et al., 2021: 7, 11, 12, 14, 15, figs. 3b, 4a, 5; Sato et al., 2024: 2, 4, 8, figs. 1a, 4a.

Type Material Examined: Holotype ♂ (MRAC 209.266), **GUINEA:** *Nzérékoré Region*: Forêt Classée de Ziama [Ziama Forest Reserve, 07°42′N 08°25′W], 31.iii.1999, D. Flomo, rainforest, pitfall. The vial containing the holotype includes a microvial with the detached sinistral leg III and copulatory apparatus. Paratypes: tritonymph (MRAC 209.265), same data as holotype; 1 ♂ (MRAC 209.280), same data, except: 13.iv.1999; 1 ♀ (MRAC 209.264), 22.v.1999; 1 ♂ (MRAC 209.293), 1 ♂, 1 ♀ (MRAC 209.273), 4 ♀ (MRAC 209.274, 278, 279, 283), 4.vi.1999; 1 ♂ (MRAC 209.263), 17.vi.1999; 1 ♂ (MRAC 209.270), tritonymph (MRAC 209.288), 30.vi.1999; 1 ♀ (MRAC 209.267), 13.vii.1999; 1 ♂ (MRAC 209.275), 2 ♀ (MRAC 209.262, 291), 26.vii.1999; 1 ♀ (MRAC 209.277), 4.ix.1999; 1 ♂ (MRAC 209.289), 2 ♀ (MRAC 209.281, 285), 16.ix.1999; 1 ♂ (MRAC 209.272), 29.ix.1999; 1 ♂ (MRAC 209.286), 1 ♀ (MRAC 209.518), 18.xi.1999; 1 ♂ (MRAC 209.506), 1 ♂, 1 ♀

(MRAC 209.507), 3 ♀ (MRAC 209.510, 511, 513), tritonymph (MRAC 209.276), 1.xii.1999; 1 ♂ (MRAC 209.509), 1 ♀ (MRAC 209.508), 14.xii.1999; 1 ♂ (MRAC 209.514), 9.i.2000; 1 ♀ (MRAC 209.505), 22.i.2000; 1 ♂ (MRAC 209.516), 4.ii.2000; tritonymph (MRAC 209.515), 17.ii.2000; 1 ♀ (MRAC 210.140), 18.iii.2000.

Diagnosis: *Ricinoides nzerekorensis* most closely resembles *R. taii*, with which it shares several unique characters of the fixed process of the male copulatory apparatus, including a thumb-shaped α lobe, with the prolateral margin sinuous and basally expanded, and the *pd* and *rd* lobes weakly developed. The male of *R. nzerekorensis* may be recognized from that of *R. taii* by the structure of leg II, specifically the moderate to very large ventromedian apophysis on the tibia (fig. 12D), the presence of a pad of bristlelike setae on the ventral surfaces of the tibia and metatarsus, and the markedly incrassate femur; and the copulatory apparatus, specifically the presence of a spiniform projection on the prolateral border of the subdistal emargination, and the small *pd* and *rd* lobes.

Distribution: *Ricinoides nzerekorensis* has been recorded from several localities in the Nzérékoré Region of Guinea (fig. 5). *Ricinoides nzerekorensis* is one of three ricinuleid species known from the Ziama Forest Reserve, the others being *B. jocquei* and *T. ziama*, and the second species known from the Mount Nimba Strict Nature Reserve, in addition to *B. jocquei*.

Additional Material Examined: **GUINEA:** *Nzérékoré Region*: Mount Nimba Strict Nature Reserve [07°38′N 08°25′W]: Bangala Forest, 609 m, 7.iii.2012, A. Henrard, C. Allard, P. Bimou, and M. Sidibé, soil litter, sieving, 1 tritonymph (MRAC 238.829); Fouenyi Forest, 573 m, 1.iii.2012, A. Henrard, C. Allard, P. Bimou, and M. Sidibé, soil litter, sieving, 2 ♂, 1 deutonymph (MRAC 239.116); Gbié, Miau River, 469 m, 15.iii.2012, A. Henrard, C. Allard, P. Bimou, and M. Sidibé, near clearance zone, near river, litter, sieving, 1 deutonymph (MRAC 238.761), same data, except: 16.iii.2012, 1 tritonymph (MRAC 238.765); Gouan Forest (mid-one), 2–11.x.2011, D. van den Spiegel and A. Henrard, soil litter near cliffs, pitfall, 1 ♀ (MRAC 238.168); Heyétouna Forest, 687 m, 18.iii.2012, A. Henrard, C. Allard, P. Bimou, and M. Sidibé, soil litter, sieving, 1 tritonymph (MRAC 238.767); Yeï Forest, 601 m, 5.iii.2012, A. Henrard, C. Allard, P. Bimou, and M. Sidibé, soil litter, sieving, 1 deutonymph (MRAC 238.763). Nzérékoré [07°45′N 08°49′W], 10–25.iv.1957, S. v. H. Olsen, on forest floor, 1 ♂ (ZMUC), same data, except: 15.v.1961 [or 15.iv.1961], 1 ♀ (ZMUC).

Ricinoides taii Botero-Trujillo et al., 2021

Figure 5, table 1

Ricinoides taii Botero-Trujillo et al., 2021a: 4, 12, 13, 15–17, 20, 23, 24, 27, 28, 31–33, 36, 37, 41, 49, 53, 55–57, 59–62, figs. 5, 7F, 8B, 9H, 12F, 13B, 15F, 16B, 18F, 19B, 20H, 21H, 25B, D, F, H, 31B, D, F, H, J, 33H, 34F.

Type Material Examined: Holotype ♂ (MRAC 233.458), paratype ♀ (MRAC 233.482), **CÔTE D'IVOIRE:** *Montagnes and Bas-Sassandra Districts*: Forêt de Taï [Taï National Park, 05°41′N 06°56′W], D. van den Spiegel and A. Kablan, pitfall. The membranous tissues of the specimens are weakened and some body parts broken. The vial containing the holotype includes the following detached pieces: both legs IV, opisthosoma, sinistral pedipalp, distal part of sinistral leg III, and copulatory apparatus. The dextral copulatory apparatus is missing. The female is in similar condition, with all fragments contained in the same vial.

Diagnosis: *Ricinoides taii* most closely resembles *R. nzerekorensis*, with which it shares several unique characters of the fixed process of the male copulatory apparatus, including a thumb-shaped α lobe, with the prolateral margin sinuous and basally expanded, and the *pd* and *rd* lobes weakly developed. The male of *R. taii* may be distinguished from that of *R. nzerekorensis* by the structure of leg II, specifically the small ventromedian apophysis on the tibia, the absence of a pad of bristlelike setae on the ventral surfaces of the tibia and metatarsus, and the less incras-

sate femur; and the copulatory apparatus, specifically the absence of a distinct spiniform projection on the prolateral border of the subdistal emargination, and the vestigial *pd* and *rd* lobes, represented by slightly raised ridges.

Distribution: *Ricinoides taii* is known only from the type locality, Taï National Park, in the Montagnes and Bas-Sassandra districts of Côte d'Ivoire (fig. 5). It is one of four ricinuleid species recorded in the national park, the others being *B. megahanseni*, *R. eburneus*, and an unidentified species of *Tautau*.

Ricinoides westermannii (Guérin-Méneville, 1838)

Figures 5, 8A, D, 9, 12B, 14D, table 1

Cryptostemma westermannii Guérin-Méneville, 1838: 11, 12; Lucas, 1838: 353, 354, unpaginated, pl. 539, figs. 7, 7a; Gervais, 1844: 131, unpaginated, pl. 47, fig. 4; Hansen and Sørensen, 1904: 149, 150, unpaginated, pl. VII, figs. 3a, b, unpaginated, pl. VIII, figs. 1a–f; Ewing, 1929: 583; Bolívar y Pieltain, 1942: 198; Pittard and Mitchell, 1972: 3; Moritz and Fischer, 1980: 139; Benavides et al., 2021: 2; Prendini, 2025: 409.

Cryptostemma westermani: Pittard, 1970: 1.

Cryptostemma westermanni: Thorell, 1892: 6, 7; Börner, 1902: 442, fig. 8; Frič, 1904: 32, fig. 36; Hansen, 1930: unpaginated, pl. XV, fig. 9a; Whittick, 1938: 479; Tuxen, 1974: 85, 86; Dunlop, 1996: 193.

Cryptostemma plebejum Hansen and Sørensen, 1904: 148, unpaginated, pl. VIII, figs. 2a–f; Moritz and Fischer, 1980: 139 (synonymized by Legg, 1978b: 124).

Ricinoides westermannii (Guérin-Méneville, 1838): Cooke, 1971: 1, 2, 7; Legg, 1976b: 1, 51, 54; Harvey, 2003: 184 (part, material from Togo only); Botero-Trujillo et al., 2021a: 3–6, 8, 12, 13, 16, 17, 21, 24, 28, 29, 32, 34, 36, 37, 42, 50, 53, 57, 62–64, figs. 4A, 5, 8C, 10A, 13C, 16C, 19C, 20I, 21I, 26, 32, 33I; Prendini, 2025: 409.

Ricinoides westermanni: Ewing, 1929: 597; Kästner, 1932: 100, 107, fig. 144; Bolívar y Pieltain, 1942: 201; Savory, 1964: 197, fig. 100; Mitchell, 1969: 136; Tuxen, 1974: 87–89, 100, 102, 103, figs. 1d, 34–38; Savory, 1977: 215, fig. 87; Legg, 1978a: 98, 99; 1978b: 124 (part, material from Togo only); 1982: 288–290, 295, figs. 1a–c, 6 (misidentification).

Ricinoides plebejum (Hansen and Sørensen, 1904): Ewing, 1929: 597; Bolívar y Pieltain, 1942: 201; Tuxen, 1974: 105; Harvey, 1984: 207.

Ricinoides phlebeium: Legg, 1976b: 2, 51, 53, 54.

Ricinoides plebeium: Kästner, 1932: 108.

Ricinoides plebejus: Legg, 1978a: 98; 1978b: 124; 1982: 287, 290.

Type Material Examined: *Cryptostemma westermannii*: Neotype ♂ (ZMB 7013), **TOGO:** *Centrale Region*: Bismarckbourg [08°11′N 00°41′E], 16.vii.1893, Büttner. Two microvials contain the following detached pieces: cucullus, both chelicerae and pedipalps, some segments and tarsomeres of legs II and III, and sinistral copulatory apparatus. The following body parts are missing: second to fifth tarsomeres of both legs IV, dextral leg III metatarsus, tarsus, and copulatory apparatus. *Cryptostemma plebejum*: Holotype tritonymph (ZMB 7834), **TOGO:** *Plateaux Region*: Misahöhe [Misahohé/Missahohé, 06°57′N 00°35′E], 24.vi.1894, E. Baumann.

Diagnosis: *Ricinoides westermannii* differs from the other eight species as the only species in which a ventromedian apophysis is absent on the tibia of leg II in the male and β_1 is noticeably larger than β_2 in the β lobe of the fixed process of the male copulatory apparatus. The male of *R. westermannii* differs further from the males of all other species, except *R. feae*, in the relatively unmodified pedipalp tibia, which is markedly robust in the other species, and in the width of the opening of the basal segment of

the pygidium, which is approximately two-fifths the lateral width of the segment at its base, but narrower laterally in the other species. The male of *R. westermannii* differs from that of *R. feae* in several respects, including the structure of the copulatory apparatus.

Distribution: *Ricinoides westermannii* is known from only two localities in the Centrale and Plateaux regions of Togo (fig. 5).

Remarks: The adult morphology of *R. westermannii* is known only from the male. According to the phylogenetic analyses (figs. 1, 2), *R. westermannii* is the basalmost species of the genus, suggesting an early origin in the *Ricinoides* clade.

Ricinoides sp.

Figures 6, 10

Material Examined: **CÔTE D'IVOIRE:** *Montagnes District*: Man, Centre Bethanie [07°25′N 07°34′W], 7.x.1980, V. Mahnert and J.-L. Perret, sifting dead leaves and rotten wood, 1 tritonymph, 2 deutonymphs (MHNG). Cascade nr. Man [07°25′N 07°35′W], 8.iii.1977, I. Löbl, in leaf litter, 1 tritonymph (MHNG). *Yamoussoukro Autonomous District*: Kossou [07°00′N 05°29′W], 25.xi.1974, R. Jocqué, secondary forest, 1 ♀ (MRAC 153.888). **THE GAMBIA:** *Lower River*: Kiang West, Keneba [13°20′N 16°01′W], 8.viii.1957, D.H. Murphy, moist litter in secondary forest, 1 ♂ (BMNH 13588975 old 1958.10.7.1), same data, except: 31.vii.1957, D.H. Murphy, deciduous litter in relict riverine forest, 1 ♀, 1 larva (BMNH 13588976 old 1958.10.7.2-3), 4. ix.1957, 1 ♀, 1 tritonymph, 1 larva (BMNH 14041443 old 1958.10.7.4-6), 19.i.1958, 2 protonymphs (BMNH 14041444 old 1958.10.7.7-8). *Western Region*: Brikama [13°16′N 16°38′W], 12.vii.1993, P. Olivier, border of primary forest, 2 ♀ (MRAC 177.186); Kiti [13°14′N 16°40′W], 14.vii.1993, P. Olivier, primary forest, under dead leaves, 1 protonymph (MRAC 177.187). **GHANA:** *Ashanti Region*: Fumes va., x.1971, M.B. Usher, litter of partially cleared forest scrub, 1 ♀, 1 deutonymph (MRAC 164.330); Tafo [06°45′N 01°36′W], viii.1945, A.H. Strickland, 1 tritonymph (AMNH IZC 324953). **GUINEA-BISSAU:** *Bafatá Region*: Bambadinca, property of Riverzoo Farm, 12°00′09″N 14°53′25.9″W, 29.vi.2005, J. Huff and V. Vignoli, secondary growth bordered by river and grass savannah, leaf litter sifting, 3 tritonymphs, 6 deutonymphs, 10 protonymphs (AMCC [LP 4664]); Bambadinca, 19 km S, 11°53′03.9″N 14°50′08.5″W, 1.vii.2005, J. Huff and V. Vignoli, wet savannah with marginal secondary rainforest, leaf litter sifting, 1 ♂ (AMCC [LP 4662]), 1 tritonymph, 1 deutonymph (AMCC [LP 4663]); Bambadinca, 22 km S, 12°04′53.6″N 14°48′03.7″W, 30.vi.2005, J. Huff and V. Vignoli, mango plantation behind village, leaf litter sifting, 1 ♂, 1 ♀ (AMCC [LP 4661]), 4 tritonymphs, 1 deutonymph, 5 protonymphs, 2 larvae (AMCC [LP 4658]), 12°04′53.6″N 14°48′03.7″W, 2.vii.2005, J. Huff and V. Vignoli, wet forest with permanent pond, under log, 1 ♀ (AMCC [LP 4660]). **SENEGAL:** *Kédougou Region*: Kédougou, W along road to Salemata, 12°33′10.6″N 12°13′39.4″W, 4.vii.2005, J. Huff and V. Vignoli, sparse forest with small boulders, hand collected under rocks and logs, 1 ♀ (AMCC [LP 4659]).

Remarks: These specimens cannot be identified to species due to the absence of adult males or, in the case of the specimens from Guinea-Bissau and the Gambia, because the adult males are damaged (Botero-Trujillo et al., 2021a).

Additional specimens, especially adult males, are needed to verify the identity of the species of *Ricinoides* discovered in Senegal, which represents the first record of Ricinulei from that country.

***Tautau*, gen. nov.**

Figures 1, 2, 7, 11E, 14E, 20, 30–33, tables 1, 2

Type Species: *Ricinoides leonensis* Legg, 1978 [= *Tautau leonensis* (Legg, 1978), comb. nov.], here designated.

Diagnosis: *Tautau* may be separated from other African genera of Ricinulei as follows.

The tegument of *Tautau* bears polygonal setae (figs. 30, 31), which are absent in *Alantakun*, *Ricinoides*, and *Ududo* (figs. 34, 35, 36B), and lacks saucer-shaped granules, which are present in *Alantakun* and *Ududo* (figs. 34, 35, 36B). The granules on the carapace and dorsal surface of the opisthosoma are separated in *Tautau* (figs. 30A, C, 31A, C) but distinctly clustered in *Alantakun*. The carapace (♂) of *Tautau* (females are unknown) exhibits a posteromedian moundlike excrescence (figs. 30A, 31A), which is absent in *Alantakun*, *Bambara* (the male of *B. megahanseni* is unknown) (fig. 25A), *Ricinoides*, and *Ududo* (fig. 34A). The ventral part of the anterior surface of the cucullus (♂) is shallowly convex and not particularly coarsely granular, in *Tautau* (fig. 31B), whereas the surface is almost flat and coarsely granular, in *Alantakun* (fig. 8F). The ventrolateral margins of the cucullus are rounded in *Tautau* (fig. 31B), but moderately truncate in *Bambara* (except *B. megahanseni*, known only from the female) (figs. 8C, 27A). The ventral margin of the cucullus is linear or sublinear in *Tautau* (fig. 31B), but bilobate in the male and female of *Ududo* (at least in *U. tuxeni* as the female of *U. sjostedtii* is unknown), and bilobate in the male and, to a lesser extent, the female of *B. jocquei* (figs. 8C, 27A). The tritosternum is vestigial, yet visible, in *Tautau* (fig. 30B), but extremely small, not exposed, in *Alantakun* (fig. 22A). The pedipalp tibia is markedly swollen proximally compared with the rest of the segment (*T. ziama*) (fig. 11E) or robust along its entire length (*T. leonensis*), in *Tautau*, but moderately swollen proximally in *Ududo* (figs. 11F, 36C). The distal region of the pedipalp tibia lacks raised tubercles in *Tautau* (figs. 11E, 31D, E), which are present and oval in *Ricinoides* (figs. 10A, B, 11D) and *Ududo* (figs. 11F, 36C, D) or elongate in *Alantakun* (fig. 11B) and *Gizoo*. A dorsal longitudinal sulcus is absent on the leg femora in *Tautau*, but present in *Ricinoides*. The leg I femur (♂) is slender in *Tautau* but slightly swollen in *Ricinoides* (except *R. taii*) and *Ududo*. The leg I tibia (♂) lacks ventral apophyses in *Tautau*, which are present in *Ududo* (figs. 12A, C, 37C, D). The leg I metatarsus (♂) is sublinear in lateral aspect and subcircular in cross section in *Tautau*, but convex ventrally in lateral aspect and dorsoventrally elongate in cross section in *Ududo* (figs. 12C, 36E). The leg I metatarsus (♂) lacks a proventral proximal depression in *Tautau*, which is present in *Alantakun* and *Ricinoides* (fig. 12B). The leg II femur (♂) is slender in *Tautau* (fig. 32A, B), but moderately to markedly swollen and robust in *Alantakun* and *Ricinoides*. The leg II tibia (♂) lacks a ventromedian apophysis in *Tautau* (fig. 32C), which is present in *Ricinoides* (except *R. westermannii*) (fig. 12D). The leg II metatarsus (♂) lacks a ventral subproximal depression in *Tautau* (fig. 32D), which is present in *Ricinoides* (fig. 12E), and a ventrosubmedian concavity, which is present in *Alantakun*. The terminal (fifth) tarsomere of leg II is fixed, fused to the preceding tarsomere, in *Tautau* (fig. 32E), but movable, not fused to the preceding (fourth) tarsomere, in *Alantakun*, *Bambara* (fig. 28E), *Ricinoides* (fig. 12E), and *Ududo*. The leg III femur (♂) is slender in *Tautau*, but slightly swollen in *Alantakun*, *Ududo*, *R. afzelii*, and *R. iita*. The leg III metatarsus (♂) is slightly to markedly swollen in *Tautau* (figs. 14E, 33), but relatively slender in *Bambara* (figs. 14B, C, 29), *Gizoo*, *Ricinoides* (fig. 14D), and *Ududo* (figs. 14F, 38). The dorsal surface of the leg III metatarsus (♂) is not excavated basally in *Tautau* (figs. 14E, 33D), moderately excavated in *Ududo* (figs. 14F, 38D), and markedly excavated in *Alantakun* (fig. 14A). The dorsal concavity of the leg III metatarsus (♂) is very deep and forms a well-defined chamber extending to the attachment point of the metatarsal process, in *Tautau* (figs. 14E, 33D), whereas it is moderately deep, gradually becoming shallower proximally in *Bambara* (fig. 14B, C), *Gizoo*, and *Ricinoides* (fig. 14D), and forms a well-defined chamber extending across the distal half of the segment, in *Alantakun* (fig. 14A) and *Ududo* (fig. 14F).

The prodorsal margin of the second tarsomere of leg III (♂) is sublinear to slightly curved proximally (in prolateral aspect) in *Tautau* (fig. 33A), but moderately angular in *Alantakun* (fig. 13A). The third tarsomere of leg III (♂) lacks an acute dorsodistal process in *Tautau*, which is present in *Ricinoides* (fig. 13B). The leg IV femur (♂) is slender in *Tautau*, but slightly swollen in *Alantakun* and *Ududo*. The second to fourth tarsomeres of leg IV (♂) are swollen in *Tautau* (fig. 32F), but unmodified in *Ricinoides*. The male copulatory apparatus fixed process is of the *leonensis* Type in *Tautau* (figs. 20, 33). The median sclerite of opisthosomal tergite XIII is rectangular to trapezoid in *Tautau* (figs. 30C, 31C), but cup shaped in *Bambara* (except *B. megahanseni*) (figs. 23A, 25C, 26C, 27B). The posterodorsal and posteroventral margins of the opisthosoma lack subspiniform granules in *Tautau* (figs. 30C, D, 31C), which are present in *Alantakun* and *Ududo* (figs. 23B, 34C, D, 35C, D, 36B). The opisthosomal dorsal and ventral pleural membranes are finely and densely granular in *Tautau* (fig. 31C), whereas the dorsal pleural membrane and, sometimes, the ventral pleural membrane, are moderately to sparsely granular in *Bambara* (figs. 25C, 26C, 27B). The posterior margin of the basal segment of the pygidium is narrow in *Tautau* (figs. 30C, 31C), whereas it is broad ventrally in *Gizoo* (fig. 23E, F), and entirely broad in *Alantakun* (fig. 23C, D) and *Ududo* (fig. 23G, H). The opening of the basal segment of the pygidium is at least half the lateral width of the segment at its base, in *Tautau*, but distinctly narrow, its width two-fifths to one-third the lateral width of the segment, in *Ricinoides*.

Etymology: The generic name is taken from the word Tàùtáù, meaning "spider" in Kanuri, an indigenous language spoken in Nigeria. Gender masculine.

Included Species: *Tautau*, gen. nov., is hereby created to accommodate *Tautau ziama*, sp. nov., and a species formerly assigned to *Ricinoides*, *Tautau leonensis* (Legg, 1978), comb. nov.

Distribution: Species of *Tautau* have been recorded in Côte d'Ivoire, Guinea, and Sierra Leone (fig. 7).

Tautau leonensis (Legg, 1978), comb. nov.

Figure 7, table 1

Ricinoides leonensis Legg, 1978a: 93–99, figs. 9–14, 16–25; Legg, 1982: 295; Harvey, 2003: 183; Botero-Trujillo et al., 2021a: 12, 19.

Type Material Examined: Holotype ♂ (BMNH 13588971), **SIERRA LEONE:** *Southern Province*: Bo [07°57′N 11°44′W], vi–x.1964, J. Pollock, beneath log. Paratypes: 1 ♂ (BMNH 13588972), same data as holotype, except: under piece of wood in forest; 2 tritonymphs (BMNH 13588973), 1 protonymph (BMNH 13588974), same locality, viii.1965, J. Pollock.

Diagnosis: *Tautau leonensis* differs from the other species of the genus, *T. ziama*, as follows. The pedipalp tibia of the male is robust along its entire length, entirely covered with dense granulation, and acarinate apically, in *T. leonensis*, whereas it is swollen proximally, predominantly smooth, and bears apical longitudinal carinae (figs. 11E, 31D, E), in *T. ziama*. Furthermore, the fixed process of the male copulatory apparatus does not bear a lanceolate projection and the distalmost tip of the β lobe is simple, in *T. leonensis*, whereas the fixed process bears a large lanceolate projection and the distalmost tip of the β lobe is bicuspid, in *T. ziama* (figs. 20, 33).

Distribution: *Tautau leonensis* is known only from the type locality, Bo, in the Southern Province of Sierra Leone (fig. 7), where it is sympatric with *R. afzelii*.

Remarks: The adult morphology of *T. leonensis* is known only from the male.

***Tautau ziama*,** gen. et sp. nov.

Figures 7, 11E, 14E, 20, 30–33, tables 1, 2

Type Material: Holotype ♂ (MRAC 209.517), **GUINEA:** *Nzérékoré Region*: Forêt

Classée de Ziama [Ziama Forest Reserve, 07°42′N 08°25′W], 5.xi.1999, D. Flomo, rainforest, pitfall.

Diagnosis: *Tautau ziama* differs from the other species of the genus, *T. leonensis*, as follows. The pedipalp tibia of the male is swollen proximally, predominantly smooth, and bears apical longitudinal carinae (figs. 11E, 31D, E), in *T. ziama*, whereas it is robust along its entire length, entirely covered with dense granulation, and acarinate apically, in *T. leonensis*. Furthermore, the fixed process of the male copulatory apparatus bears a large lanceolate projection and the distalmost tip of the β lobe is bicuspid in *T. ziama* (figs. 20, 33) whereas the fixed process does not bear a lanceolate projection and the distalmost tip of the β lobe is simple in *T. leonensis*.

Etymology: The specific epithet is a noun in apposition taken from the type locality, Ziama Forest Reserve, in the extreme southeast of Guinea, near the borders of Côte d'Ivoire and Liberia.

Description of Male: Based on the holotype (MRAC 209.517).

Measurements: Total length, 4.14 mm (table 2).

Coloration: Soma and appendages reddish, pedipalps paler (figs. 30–33). Carapace lateral hyaline lines and semiocelli yellowish. Opisthosomal tergal and pleural membranes yellow, hyaline (figs. 30C, 31C). Cheliceral manus yellow; fingers, finger dentition and manus toothlike process reddish.

Setation: Surfaces densely covered with moderately expanded navicular setae, except ventrally on cucullus, medially on coxosternal region, pedipalp femur lateral and ventral surfaces, pedipalp tibia, and leg tarsi (figs. 30–33). Several setae have fallen out of the carapace and dorsal surface of the opisthosoma.

Tegument surface: Soma and appendages without cuticular pits. Except for pedipalps, tegument densely covered with iridescent granules evenly spaced apart, not clustered together (figs. 30–33). Pedipalp femur finely and densely granular, except ventral surface, which is smooth (fig. 31D); tibia predominantly smooth, with few fine granules basally on ventral surface, raised tubercles absent (fig. 31D, E). Opisthosoma, pleural membranes finely and densely granular (figs. 30C, 31C); tergal membranes more sparsely granular.

Carapace: Carapace as long as wide, broadest between coxae of legs II and III; trapezoidal, lateral margins curved, narrowing anteriorly (fig. 30A); anterior margin linear in dorsal aspect; posterior margin slightly procurved; median longitudinal sulcus, paired posterior marginal transverse sulci, and paired anterolateral longitudinal sulci shallow; paired lateral depressions present, aligned with coxae of legs II; posteromedian moundlike excrescence present; expansion of lateral hyaline lines present, entirely smooth, forming pair of semiocelli with well-defined borders; semiocelli medium sized, aligned with junction of coxae of legs I and II, visible in dorsolateral aspect.

Cucullus: Cucullus broadened laterally, wider than long (table 2); ventrolateral margins rounded (fig. 31B); ventral margin predominantly linear in anterior aspect, shallowly bilobate in ventral aspect; posterior surface without visible row of denticulations (possibly worn); anterior surface shallowly convex, without ventral compressed surface; pair of moderately developed sublateral longitudinal sulci; ventral part unmodified anteromedially.

Chelicerae: Manus dorsal surface with large toothlike process distally. Movable finger longer than fixed finger, tooth row comprising eight very small teeth; sharp prodorsal longitudinal carina parallel to tooth row (opposite fixed finger); mucron broken on both chelicerae. Fixed finger tooth row comprising four small teeth.

Coxosternal region: Tritosternum very small, barely visible, not abutting coxae of legs I (fig. 30B); coxae of legs II–IV abutting one another medially along entire length; coxae of legs II, anterior and posterior margins subparallel, not perpendicular to median axis, inclined anteriorly; suture between coxae of legs II approximately twice length of sutures between coxae of legs III and IV.

Opisthosoma: Opisthosoma oval, longer than wide and narrowing posteriorly (table 2), broadest

at tergite XI (fig. 30C). Posterodorsal and posteroventral margins without spiniform granules (figs. 30C, D, 31C). Tergites X–XIII each comprising median and lateral sclerites; median sclerites of XI and XII wider than long, of XIII longer than wide (table 2), each with paired, shallow submedian depressions near anterior margins, lateral margins converging posteriorly on XI and to lesser extent XII, subparallel on XIII; margins of lateral sclerites adjacent to tergal longitudinal membranes predominantly linear, tergal membranes narrow. Sternites XI–XIII each with pair of shallow submedian depressions similar to tergites (fig. 30D). Pygidium basal segment slightly tilted dorsally (figs. 30C, 31C); opening broad, subcircular, width approximately half lateral width of segment at its base; posterior margin narrow; dorsal surface with V-shaped notch; ventral surface entire.

Pedipalps: Femur globose, length approximately twice depth (table 2) (fig. 31D). Tibia longer than femur; entirely linear; moderately swollen proximally compared with rest of segment, which is noticeably narrower (figs. 11E, 31D, E); apical longitudinal carinae present. Movable finger approximately twice length of fixed finger.

Legs: Leg II longest; legs I–IV femora unmodified, all similar in width (table 2), dorsal surfaces without longitudinal sulci (fig. 32B). Leg I tibia without ventral apophyses; metatarsus subcircular in cross section, without ventral excrescence or proventral proximal depression. Leg II tibia without ventral apophysis (fig. 32C); tibia and metatarsus without pad of long translucent setae ventrally (fig. 32C, D); metatarsus without ventral subproximal depression, submedian concavity, or submedian excrescence; first to third tarsomeres short, subequal, fourth approximately twice length of preceding tarsomeres (fig. 32E); first to fourth tarsomeres movable, fifth tarsomere fixed, fused to fourth. Leg III metatarsus slightly swollen (i.e., compared to tibia), with very deep dorsal concavity forming well-defined chamber extending to attachment point of metatarsal process (figs. 14E, 33); proventral surface without apical brushlike row of setae; prodorsal proximal sulcus present; metatarsus, metatarsal process, and tarsus precisely fitting together to completely enclose copulatory apparatus when tarsus retracted; metatarsal process situated basally near tibia, moderately robust, tapering and curving retrolaterally, apex subtruncate and dorsoventrally compressed, *lamina cyathiformis* of second tarsomere approximately as deep as long, with markedly pointed apex (fig. 33C); subdistal (third) tarsomere without acute dorsodistal process. Leg IV second to fourth tarsomeres swollen (fig. 32F). Legs III and IV terminal tarsomere apex, dorsal margin sublinear, covering ungues. Leg I tarsus and legs II–IV terminal tarsomeres without ventrodistal papillae.

Copulatory apparatus: Fixed process, trunk distal region elongate, distally truncate, and without retrolateral subdistal emargination (figs. 20, 33); margin with large lanceolate projection. *PL* lobe very narrow and predominantly linear, subcircular in cross section except for apex, which is laterally compressed; apex proximal to *rsd* lobe; separated from trunk by broad submedian emargination. Distal lobular region, primary α lobe very large, basally expanded and markedly hook-shaped; margins smooth, without serrations. Primary β lobe very large and compressed, distinctly trifid; tips acute and apically directed, distalmost tip bicuspid. *rsd* lobe vestigial. Secondary *pd* and *rd* lobes absent or indistinct. Movable process slender, slightly flexible, narrowing distally; apex simple, entire.

Female: Unknown.

Distribution: *Tautau ziama* is known only from the type locality, Ziama Forest Reserve, in the Nzérékoré Region of Guinea (fig. 7), where it appears to be sympatric with *B. jocquei* and *R. nzerekorensis*.

Tautau sp.

Figure 7

Material Examined: **CÔTE D'IVOIRE:** *Montagnes and Bas-Sassandra districts*: Forêt de

Taï [Taï National Park, 05°41′N 06°56′W], station of the Ecological Research Center (CRE), 18.ii.2010, J. Jocqué and D. van den Spiegel, forest in direction of river, forest on sandy soil, Winkler extraction, 1 deutonymph (MRAC 230.595).

Remarks: This immature specimen cannot be accurately identified to species.

***Ududo*, gen. nov.**

Figures 1, 2, 4, 11F, 12A, C, F, 14F, 21, 22B, 23B, G, H, 24C, 34–38, tables 1, 2

Type Species: *Ududo tuxeni*, sp. nov., here designated.

Diagnosis: *Ududo* may be separated from other African genera of Ricinulei as follows. The tegument of *Ududo* lacks polygonal (calyxlike to navicular) setae (figs. 34, 35, 36B), which are present in *Bambara* (figs. 25, 26, 27B), *Gizoo*, and *Tautau* (figs. 30, 31), and bears obsolete saucer-shaped granules, which are distinct in *Alantakun*, and absent in the other genera. The granules on the carapace and dorsal surface of the opisthosoma are separated in *Ududo* (figs. 34A, C, 35A, C, 36B), but distinctly clustered in *Alantakun*. The carapace of the male and female of *Ududo* (the female of *U. sjostedtii* is unknown) lacks a posteromedian moundlike excrescence (figs. 34A, 35A), which is present in the males of *Gizoo* and *Tautau* (figs. 30A, 31A) and the females of *Bambara* (fig. 26A) and *Gizoo*. The ventral part of the anterior surface of the cucullus (♂) is shallowly convex and not particularly coarsely granular, in *Ududo* (fig. 36A), whereas the surface is almost flat and coarsely granular, in *Alantakun* (fig. 8F). The ventrolateral margins of the cucullus are rounded in *Ududo* (fig. 36A), but moderately truncate in *Bambara* (except *B. megahanseni*, known only from the female) (figs. 8C, 27A). The ventral margin of the cucullus is bilobate in the male, but not the female of *Ududo* (at least in *U. tuxeni* as the female of *U. sjostedtii* is unknown), whereas it is linear or sublinear in both sexes of the other genera (figs. 8A, B, 31B), except *B. jocquei* in which it is bilobate in the male (fig. 27A) and, to lesser extent, the female. The tritosternum is vestigial, but visible, in *Ududo* (figs. 22B, 34B, 35B), whereas it is extremely small, not exposed, in *Alantakun* (fig. 22A). The pedipalp tibia is moderately swollen proximally in *Ududo* (figs. 11F, 36C, D), robust along its entire length in most *Ricinoides* (except *R. feae* and *R. westermannii*, in which it is not noticeably robust) (fig. 11D) and *T. leonensis*, and markedly swollen proximally in *Alantakun* (fig. 11A), *Bambara* (figs. 11C, 27C, D), *Gizoo*, and *T. ziama* (figs. 11E, 31D, E). The pedipalp tibia lacks apical longitudinal carinae in *Ududo* (figs. 11F, 36C, D), which are present in *Bambara* (figs. 11C, 27C, D) and *T. ziama* (figs. 11E, 31D, E). The distal region of the pedipalp tibia bears raised tubercles that are oval in *Ududo* (figs. 11F, 36C, D), elongate in *Alantakun* (fig. 11B) and *Gizoo*, and absent in *Bambara* (figs. 11C, 27C, D) and *Tautau* (figs. 11E, 31D, E). A dorsal longitudinal sulcus is absent on the leg femora in *Ududo*, but present in *Ricinoides*. The leg I femur (♂) is slightly swollen and moderately robust in *Ududo*, but slender in *Bambara*, *Gizoo*, *Tautau*, and *R. taii*. The leg I tibia (♂) of *Ududo* possesses proventral and, in *U. sjostedtii*, retroventral apophyses (figs. 12A, C, 37C, D), which are absent in the other genera. The leg I metatarsus (♂) is convex ventrally in lateral aspect and dorsoventrally elongate in cross section, in *Ududo* (figs. 12C, 36E), but sublinear in lateral aspect and subcircular in cross section, in the other genera (e.g., fig. 12B). The leg I metatarsus (♂) lacks a proventral proximal depression in *Ududo* (fig. 36E), which is present in *Alantakun* and *Ricinoides* (fig. 12B). The leg II femur (♂) is slender in *Ududo* (fig. 37A, B), but moderately to markedly swollen and robust in *Alantakun* and *Ricinoides*. The leg II tibia (♂) lacks a ventromedian apophysis in *Ududo*, which is present in *Ricinoides* (except *R. westermannii*) (fig. 12D). The leg II metatarsus (♂) of *Ududo* lacks a ventral subproximal depression (fig. 37E), which is present in *Ricinoides* (fig. 12E), and a ventrosubmedian concavity, which is present in *Alantakun*. The terminal (fifth) tarsomere of leg

II is movable, not fused to the preceding tarsomere, in *Ududo*, but fixed, fused to the preceding (fourth) tarsomere, in *Gizoo* and *Tautau* (fig. 32E). The leg III femur (♂) is slightly swollen in *Ududo*, but slender in *Bambara*, *Gizoo*, *Ricinoides* (except *R. afzelii* and *R. iita*), and *Tautau*. The leg III metatarsus (♂) is relatively slender in *Ududo* (figs. 14F, 38) but swollen in *Alantakun* (fig. 14A) and *Tautau* (figs. 14E, 33). The dorsal surface of the leg III metatarsus (♂) is moderately excavated basally in *Ududo* (figs. 14F, 38D), deeply excavated in *Alantakun* (fig. 14A), and not excavated in the other genera (figs. 14B–E, 29D, 33D). The dorsal concavity on the leg III metatarsus (♂) is very deep, forming a well-defined chamber in the distal half of the segment in *Ududo* (figs. 14F, 38D), which extends to the attachment point of the metatarsal process in *Tautau* (figs. 14E, 33D), but is moderately deep, gradually becoming shallower proximally in *Bambara* (figs. 14B, C, 29D), *Gizoo*, and *Ricinoides* (fig. 14D). The prodorsal margin of the second tarsomere of leg III (♂) is sublinear to slightly curved proximally (in prolateral aspect) in *Ududo* (fig. 38B), but moderately angular in *Alantakun* (fig. 13A). The third tarsomere of leg III (♂) lacks an acute dorsodistal process in *Ududo*, which is present in *Ricinoides* (fig. 13B). The second to fourth tarsomeres of leg IV (♂) are swollen in *Ududo* (figs. 12F, 37F), but unmodified in *Ricinoides*. The male copulatory apparatus fixed process is of the *sjostedtii* Type in *Ududo* (fig. 21). The median sclerite of opisthosomal tergite XIII is rectangular to trapezoidal in *Ududo* (figs. 23B, 34C, 35C, 36B), but cup shaped in *Bambara* (except *B. megahanseni*) (figs. 23A, 25C, 26C, 27B). The tergal membranes of the opisthosoma are granular in *Ududo*, but smooth in *Bambara*, *Gizoo*, and *T. leonensis*. The posteroventral and, to a lesser extent, posterodorsal margins of the opisthosoma are armed with posteriorly directed subspiniform granules, in *Ududo* (figs. 23B, 34C, D, 35C, D, 36B), which are absent in *Bambara* (figs. 23A, 25C, D, 26C, D, 27B), *Gizoo*, *Ricinoides*, and *Tautau* (figs. 30C, D, 31C). The opisthosomal dorsal and ventral pleural membranes are finely and densely granular in *Ududo* (figs. 34C, 35C, 36B), whereas the dorsal pleural membrane and, sometimes, the ventral pleural membrane, are moderately to sparsely granular in *Bambara*. The basal segment of the pygidium is parallel to the longitudinal axis of the opisthosoma in *Ududo* (figs. 23G, H, 34C, D, 35C, D, 36B), but slightly tilted dorsally in *Bambara* (figs. 25C, 26C, 27B), *Gizoo* (figs. 23E, F), and *T. ziama* (figs. 30C, 31C). The posterior margin of the basal segment of the pygidium is entirely broad in *Ududo*, more markedly so ventrally (fig. 23G, H), whereas it is only broad ventrally in *Gizoo* (fig. 23E, F), and narrow in *Bambara*, *Ricinoides*, and *Tautau*. The opening of the basal segment of the pygidium is at least half the lateral width of the segment at its base, in *Ududo*, but distinctly narrow, its width two-fifths to one-third the lateral width of the segment, in *Ricinoides*.

Etymology: The generic name means "spider" in Igbo, an indigenous language spoken in Nigeria. Gender masculine.

Included Species: *Ududo*, gen. nov., is hereby created to accommodate *Ududo tuxeni*, sp. nov., and a species formerly assigned to *Ricinoides*, *Ududo sjostedtii* (Hansen and Sørensen, 1904), comb. nov.

Distribution: Species of *Ududo* have been recorded in Cameroon and Nigeria (fig. 4).

Ududo sjostedtii (Hansen and Sørensen, 1904), comb. nov.

Figures 4, 12A, C, 22B, table 1

Cryptostemma sjöstedtii Hansen and Sørensen, 1904: 151–153, unpaginated, pl. VIII, figs. 3a–m; Moritz and Fischer, 1980: 139.

Ricinoides sjostedtii (Hansen and Sørensen, 1904): Legg, 1976b: 2, 51, 54 (part); Harvey, 2003: 183, 184 (part); Botero-Trujillo et al., 2021a: 12 (part).

Ricinoides sjöstedtii: Ewing, 1929: 597; Kästner, 1932: 99, fig. 130.

Ricinoides sjostedti: Pittard, 1970: 11; Pittard and Mitchell, 1972: 6; Tuxen, 1974: 87–89,

98–100, figs. 1b, g, 24–28; Legg, 1978a: 99; Dunlop, 1996: 195, 198, fig. 5.

Ricinoides sjöstedti: Kästner, 1932: 106, figs. 141, 142; 1940: 98, fig. 78; Bolívar y Pieltain, 1942: 201; Zakhvatkin, 1952: 43, fig. 29a; Kennaugh, 1968: 393–396, unpaginated, pls. Ia, b, IIa, IVa.

Ricinoides sjoestedti: Selden, 1992: 597, 598 (part).

Type Material Examined: Lectotype ♂ (NHRS JUST 519), **CAMEROON:** *South-West Region*: N'dian [ca. 04°58′N 08°54′E], vi.1891, Y. Sjöstedt. Paralectotypes: **CAMEROON:** *South-West Region*: 1 tritonymph, in same vial and with same data as lectotype (NHRS JUST 519); 1 tritonymph (ZMB 9838), Johann Albrechts-Höhe [04°39′N 09°25′E], 21.vii–31.viii.1897, L. Conradt; 1 protonymph (ZMUC), Bibundi [04°13′N 08°59′E], viii.1891, Sjöstedt.

Diagnosis: *Ududo sjostedtii* differs from the other species of the genus, *U. tuxeni*, as follows. The leg I tibia of the male possesses a retroventral apophysis in *U. sjostedtii* (fig. 12A, C), which is absent in *U. tuxeni* (fig. 37C, D). The semiocelli are medium sized and clearly visible in *U. sjostedtii*, but slightly smaller and barely visible in dorsal aspect, in *U. tuxeni* (figs. 34A, 35A). The median sclerite of opisthosomal tergite XIII is longer than wide in the male of *U. sjostedtii*, whereas it is wider than long in *U. tuxeni* (table 2; figs. 34C, 35C).

Distribution: *Ududo sjostedtii* is known from several localities in Cameroon (fig. 4). Previous records of *U. sjostedtii* from Nigeria in Finnegan's (1935) account of the collection of over 300 ricinuleids collected during the Percy Sladen Trust Expedition to Nigeria and British Cameroons, are referable to *U. tuxeni*.

Remarks: The precise locality at which the lectotype of *U. sjostedtii* was collected, is unclear. N'dian is a river that flows into the Rio del Rey estuary, in the South-West Region of Cameroon. The course of the river runs close to Mundemba (at 04°58′N 08°54′E), where the lectotype might have been collected.

Due to the absence of adults from Bibundi and Johann Albrechts-Höhe, it is unclear whether immature specimens from these localities are conspecific with the specimens from N'dian. However, the tritonymph from Johann Albrechts-Höhe may be a different species, as it is larger and more coarsely granular than the tritonymph from N'dian.

According to Hansen and Sørensen (1904), a male and female were collected from Johann Albrechts-Höhe, in addition to the tritonymph from that locality. Tuxen (1974: 98) mentioned not having seen those adults, nor are they noted on the original label in the vial. These specimens are presently mislaid, and the female of *U. sjostedtii* remains unknown.

The paralectotype of *U. sjostedtii* from Bibundi has the same collection data as the syntypes of *G. crassipalpe*, i.e., "Cameroon, Bibundi, 1891, Y. Sjöstedt," suggesting that the two species are sympatric at that locality.

***Ududo tuxeni*, gen. et sp. nov.**

Figures 4, 11F, 12F, 14F, 21, 23B, G, H, 24C, 34–38, tables 1, 2

Cryptostemma sjöstedti Hansen and Sørensen, 1904: Finnegan, 1935: 186 (misidentification).

Cryptostemma sjôstedtii: Fage, 1938: 370 (misidentification).

Ricinoides sjostedtii (Hansen and Sørensen, 1904): Legg, 1976b: 2 (part); Harvey, 2003: 183, 184 (part); Botero-Trujillo et al., 2021a: 12 (part) (misidentifications).

Ricinoides sjoestedti: Selden, 1992: 597, 598 (part) (misidentification).

Ricinoides sjoestedtii: Hammen, 1979: 5, 6, 8, 35, fig. 4; Harvey, 1984: 209; Hammen, 1989: 435–436, 439, 441, fig. 232 (misidentifications).

Ricinoides sjostedti: Cloudsley-Thompson, 1958: 129; Savory, 1964: 201; Cooke, 1967: 31; Cloudsley-Thompson, 1968: 161; Mitchell,

1969: 137; Pittard, 1970: 2; Pittard and Mitchell, 1972: 4; Savory, 1977: 219 (misidentifications).

Ricinoides sjöstedti: Millot, 1945b: 1; Mitchell, 1970: 72, 73 (misidentifications).

Type Material: Holotype ♂ (BMNH 13588977 old 1953.3.28.71), **NIGERIA:** *Cross River*: Obubra: Nko [05°53′N 08°11′E], 500 ft [152 m], 28.vi.1933, J.J. Sanderson (Percy Sladen Trust Expedition to Cameroons and Nigeria, 1933). The vial containing the holotype includes a microvial with the detached dextral copulatory apparatus. Paratypes: 1 ♀ (BMNH 13588978 old 1953.3.28.61), 8 tritonymphs, 5 deutonymphs, 4 protonymphs (BMNH 13588939 old 1953.3.28), more than 20 nymphs (BMNH 13588936 old 1953.3.28), 3 larvae (BMNH 13588938 old 1953.3.28), same data as holotype, except: 30.vi.1933; 1 ♀ (BMNH 13588979 old 1953.3.28.63-66), same data, except: 1.vii.1933; 3 ♀ (BMNH 13588980 old 1953.3.28.67-70), 1 ♀, >40 nymphs (BMNH 13588934 old 1953.3.28.-), >50 nymphs (BMNH 13588982 old 1953.3.28), 2 tritonymphs (ZMUC), 3.vii.1933; 1 ♂, 3 ♀ (BMNH 13588981 old 1953.3.28.72-78), >50 nymphs (BMNH 13588935 old 1953.3.28), 7.vii.1933; >30 nymphs (BMNH 13588937 old 1953.3.28), 29.vi.1933.

Diagnosis: *Ududo tuxeni* differs from the other species of the genus, *U. sjostedtii*, known only from the male, as follows. The leg I tibia of the male lacks a retroventral apophysis in *U. tuxeni* (fig. 37C, D), which is present in *U. sjostedtii* (fig. 12A, C). The semiocelli are medium sized, barely visible in dorsal aspect in *U. tuxeni* (figs. 34A, 35A), but slightly larger and more clearly visible in *U. sjostedtii*. The median sclerite of opisthosomal tergite XIII is wider than long in *U. tuxeni* (table 2) (figs. 34C, 35C), whereas it is longer than wide in the male of *U. sjostedtii*.

Etymology: The specific epithet is a patronym honoring the Danish zoologist Sören Ludvig Paul Tuxen (S.L. Tuxen, 1908–1983), whose 1974 publication laid the foundation for all subsequent research on the taxonomy of African ricinuleids.

Description of Male: Based on the holotype (BMNH 13588977 old 1953.3.28.71).

Measurements: Total length, 6.31 mm (table 2).

Coloration: Soma and appendages reddish chestnut (figs. 34, 36–38). Carapace lateral hyaline lines and semiocelli yellow. Opisthosomal tergal and pleural membranes yellow, hyaline (figs. 34C, 36B). Cheliceral manus yellow; fingers, finger dentition and manus toothlike process dark (fig. 34B).

Setation: Surfaces densely covered with short and medium sized, translucent, bristlelike setae, not visibly expanded (figs. 34, 36–38). Polygonal setae absent.

Tegument surface: Tegument irregular, without cuticular pits; covered with coarse granulation resembling tubercles (figs. 34, 36–38); granules noticeably iridescent, especially on prosoma and opisthosoma, some grouped together or touching one another but not forming distinct clusters. Opisthosoma, pleural membranes finely and densely granular (figs. 34C, 36B); tergal membranes more sparsely granular. Pedipalp femur dorsal, prolateral, and retrolateral surfaces finely granular (fig. 36C); tibia smooth proximally, with raised oval tubercles distally (figs. 11F, 36C, D).

Carapace: Carapace wider than long, broadest between coxae of legs II and III; trapezoidal, lateral margins curved, narrowing anteriorly (fig. 34A); anterior margin linear in dorsal aspect; posterior margin slightly procurved; median longitudinal sulcus, paired posterior marginal transverse sulci (evident near lateral margins) and paired anterolateral longitudinal sulci shallow; paired lateral depressions present, aligned with coxae of legs II; posteromedian moundlike excrescence absent; expansion of lateral hyaline lines present, entirely smooth, forming pair of semiocelli with well-defined borders; semiocelli medium sized, aligned with junction of coxae of legs I and II, visible in dorsolateral aspect.

Cucullus: Cucullus broadened laterally, wider than long (table 2); ventrolateral margins rounded (fig. 36A); ventral margin shallowly bilobate in anterior and ventral aspects; posterior surface with median row of small denticulations;

anterior surface shallowly convex, without ventral compressed surface; pair of moderately developed sublateral longitudinal sulci; ventral part unmodified anteromedially.

Chelicerae: Manus dorsal surface with large toothlike process distally. Movable finger longer than fixed finger, tooth row comprising six or seven small teeth; sharp prodorsal longitudinal carina parallel to tooth row (opposite fixed finger); mucron with shallow but distinct prolateral excavation (opposite fixed finger) delimited by two parallel longitudinal carinae. Fixed finger tooth row comprising four small teeth.

Coxosternal region: Tritosternum very small, barely visible, not abutting coxae of legs I (fig. 34B); coxae of legs II–IV abutting one another medially along entire length; coxae of legs II, anterior and posterior margins subparallel, not perpendicular to median axis, inclined anteriorly; coxae of legs II posterior margin slightly V-shaped medially; suture between coxae of legs II approximately twice length of suture between coxae of legs III and IV.

Opisthosoma: Opisthosoma oval, longer than wide (table 2), broadest at tergite XI (fig. 34C). Posteroventral margin and, to lesser extent, posterodorsal margin, armed with series of posteriorly directed subspiniform granules (figs. 23B, 34C, D). Tergites X–XIII each comprising median and lateral sclerites; median sclerites of tergites XI–XIII wider than long, approximately rectangular (table 2), each with paired, shallow submedian depressions near anterior margins, lateral margins converging posteriorly on XI and XII, converging anteriorly on XIII; margins of lateral sclerites adjacent to tergal longitudinal membranes predominantly linear, tergal membranes narrow. Sternites XI–XIII each with pair of shallow submedian depressions similar to tergites (fig. 34D). Pygidium basal segment parallel to longitudinal axis of opisthosoma (figs. 23H, 34C, D); opening relatively broad, subcircular, width approximately half lateral width of segment at its base; posterior margin entirely broad, more markedly so ventrally (figs. 23G, H, 36B); dorsal surface with V-shaped notch; ventral surface entire.

Pedipalps: Femur globose, length slightly more than twice depth (table 2) (fig. 36C). Tibia longer than femur; entirely linear; moderately swollen proximally compared to rest of segment, which is noticeably narrower (figs. 11F, 36C, D); apical longitudinal carinae absent. Movable finger approximately twice length of fixed finger.

Legs: Leg II longest (table 2), femur unmodified, longer than but similar in shape to femora of other legs. All femora similar in appearance, with small differences in width at midline; dorsal surfaces without longitudinal sulci (fig. 37B). Leg I tibia with moderately large proventral apophysis and without retroventral apophysis (fig. 37C, D); metatarsus convex ventrally in lateral aspect, dorsoventrally elongate in cross section, without ventral excrescence or proventral proximal depression (fig. 36E). Leg II tibia without ventromedian apophysis; tibia and metatarsus each without pad of long translucent setae ventrally (fig. 37E); metatarsus without ventral subproximal depression, submedian concavity, or submedian excrescence; first to third tarsomeres short, subequal, fourth approximately twice length of preceding tarsomeres; all tarsomeres movable. Leg III metatarsus not swollen, with very deep dorsal concavity forming well-defined chamber in distal half of segment (figs. 14F, 38); proventral surface without apical brushlike row of setae; prodorsal proximal sulcus present; metatarsus with moderately deep basal excavation on dorsal surface; metatarsus, metatarsal process, and tarsus precisely fitting together to completely enclose copulatory apparatus when tarsus retracted; metatarsal process situated basally near tibia, narrow and tapering, longitudinal axis slightly sinuous, apex acute and dorsoventrally compressed, pointing retrolaterally, *lamina cyathiformis* of second tarsomere approximately as deep as long, with rounded apex (fig. 38C); subdistal (third) tarsomere without acute dorsodistal process. Leg IV second to fourth tarsomeres swollen (figs. 12F, 37F). Legs III and IV terminal tarsomere apex, dorsal margin sublinear, covering ungues. Leg I tarsus and legs II–IV terminal tarsomeres without ventrodistal papillae.

Copulatory apparatus: Fixed process, *PL* lobe narrow and curved, dorsoventrally compressed

(figs. 21, 38). Distal lobular region, primary α lobe moderately large and elongate, somewhat expanded basally; margins nearly smooth, without serrations. Primary β lobe medium sized, entire. *rsd* lobe similar in size to α lobe, larger than β lobe, pronounced and erect, associated with U-shaped subdistal emargination. Secondary *pd* and *rd* lobes obsolete. Movable process slender, slightly flexible, narrowing distally; apex simple, entire.

Supplementary Description of Female: Based on paratypes (soma and appendages: BMNH 13588978 old 1953.3.28.61; spermathecae: BMNH 13588934 old 1953.3.28.-). Resembles male, except as noted.

Measurements: Total length, 5.88 mm (table 2).

Carapace: Posteromedian moundlike excrescence absent (fig. 35A).

Cucullus: Ventrolateral margins rounded; ventral margin predominantly linear in anterior aspect.

Coxosternal region: Coxae of legs II–IV abutting one another medially along entire length (fig. 35B); coxae of legs II posterior margin V-shaped medially.

Opisthosoma: Tergites XI–XIII, median sclerites wider than long (fig. 35C). Pygidium as in male.

Legs: Leg I tibia without ventral apophysis; metatarsus subcircular in cross section, not dorsoventrally elongate. Leg II femur unmodified, longer than but similar in shape to femora of other legs. Leg IV tarsus unmodified.

Spermathecae: Anterior wall of *bursa copulatrix* with pair of small, slightly pigmented, rounded areas (fig. 24C). Anterior surface with seven sacculiform structures sinistrally and four dextrally, variable in size, arranged into two separate clusters. Spermathecae follicular, each comprising soft, elongate tube terminating in tapering duct, situated sublaterally on anterior surface of *bursa copulatrix*, well separated from dorsal margin. Posterior genital lip as illustrated.

Additional Material Examined: **NIGERIA:** *Cross River*: Obubra: Adum [05°53′N 08°11′E], 6.vii.1933, J.J. Sanderson (Percy Sladen Trust Expedition to Cameroons and Nigeria, 1933), 3 deutonymphs, 1 larva (BMNH 13588945 old 1953.3.28.-). **NIGERIA** or **CAMEROON:** J.J. Sanderson (Percy Sladen Trust Expedition to Cameroons and Nigeria, 1932–1933), 1 ♂ (BMNH 13588940 old 1953.3.28.62), 1 ♀ (BMNH 13588941 old 1953.3.28.-), 3 tritonymphs, 4 deutonymphs (BMNH 13588944 old 1953.3.28.-), 1 tritonymph (BMNH 13588942 old 1953.3.28.-), 1 tritonymph (BMNH 13588943 old 1953.3.28.-).

Distribution: *Ududo tuxeni* is known from Nko and Adum, in the Obubra Local Government Area of the state of Cross River, Nigeria (fig. 4).

ACKNOWLEDGMENTS

R.B.-T. was supported by a Theodore Roosevelt Postdoctoral Research Fellowship from the AMNH Richard Gilder Graduate School and U.S. National Science Foundation grant DEB 1655050 to L.P. R.B.-T. thanks John J. Flynn (Dean of the RGGS), Rebecca Johnson (RGGS Director of Administration), James M. Carpenter (former Chair, AMNH Division of Invertebrate Zoology), and David A. Grimaldi (former Acting Chair), for support and assistance during the COVID-19 pandemic, when this work was undertaken. The authors thank the curators and managers of institutional collections who loaned material for study: Janet Beccaloni and Danniella Sherwood (BMNH), Lauren A. Esposito (CAS), Leonardo S. Carvalho (CHNUFPI), Oscar F. Francke (CNAN), Fabio Godoi and Juliana Araujo (CZPB/UFAM), Petra Sierwald and Crystal A. Maier (FMNH), Jhon C. Neita Moreno (IAvH), Eduardo Flórez D. (ICN), Andrés A. Ojanguren Affilastro and Martín J. Ramírez (MACN), Ricardo Ott (MCN), Gonzalo Giribet (MCZ), Peter J. Schwendinger (MHNG), Giovanny Fagua and Dimitri Forero (MPUJ), Christophe Allard and Rudy Jocqué (MRAC), Maria Tavano (MSNG), Julia Stigenberg (NHRS), Zoë Simmons (OUMNH), Peter Jäger (SMF), Hannah Wood and Dana M. DeRoche (USNM), Jason A. Dunlop (ZMB), Nikolaj Scharff and Jan Pedersen (ZMUC); Colby E. Sain (AMNH and City University of New York) for work on a previously published monograph

on African Ricinulei; Steve R. Davis (formerly AMNH) for discussions on morphological characters; Jeremy Huff and Valerio Vignoli for fieldwork in Guinea-Bissau and Senegal in 2005 (supported by NSF grant EAR 0228699 to L.P.); Andrew K. Smith and Morgan Hill for access to imaging equipment at the AMNH Microscopy and Imaging Facility; Martín J. Ramírez and Fabián Tricárico for access to the scanning electron microscope at the MACN; Steve Thurston (AMNH) for assistance with preparing the plates for this contribution; Jairo A. Moreno González (AMNH) for assistance with the ML analysis; Juan Pablo Botero (ICN) for assistance with the maps; Pío A. Colmenares, Stephanie F. Loria, and Louis N. Sorkin for logistical assistance at the AMNH; Leonardo S. Carvalho and Oscar F. Francke for constructive comments on an earlier draft of the manuscript.

REFERENCES

Adis, J., B. Messner, and N.[I.] Platnick. 1999. Morphological structures and vertical distribution in the soil indicate facultative plastron respiration in *Cryptocellus adisi* (Arachnida, Ricinulei) from Central Amazonia. Studies on Neotropical Fauna and Environment 34: 1–9.

Almeida, R.F. de, et al. 2023. Barking up the wrong tree: the dangers of taxonomic misidentification in molecular phylogenetic studies. Plant Ecology and Evolution 156: 146–159.

Armas, L.F. de, and E.O. Agreda. 2016. Una nueva especie de *Pseudocellus* (Ricinulei: Ricinoididae) del suroeste de Guatemala. Revista Ibérica de Aracnología 28: 79–83.

Armas, L.F. de, R. Teruel, and R.J. Miranda. 2021. Ectoparasitic fungi (Ascomycota: Laboulbeniomycetes: Laboulbeniales) associated to scorpions and short-tailed whipscorpions (Arachnida: Scorpiones, Schizomida). Revista Ibérica de Aracnología 39: 144–146.

Ballesteros, J.A., and P.P. Sharma. 2019. A critical appraisal of the placement of Xiphosura (Chelicerata) with account of known sources of phylogenetic error. Systematic Biology 68 (6): 896–917.

Ballesteros, J.A., C.E. Santibáñez-López, Ľ. Kováč, E. Gavish-Regev, and P.P. Sharma. 2019. Ordered phylogenomic subsampling enables diagnosis of systematic errors in the placement of the enigmatic arachnid order Palpigradi. Proceedings of the Royal Society of London B, Biological Sciences 286: 1–9.

Barnes, R.D. 1980. Invertebrate Zoology. 4th ed. Philadelphia: Saunders College.

Barnes, R.D. 1987. Invertebrate Zoology. 5th ed. Philadelphia: Saunders College.

Barreiros, J.A.P., R. Pinto-da-Rocha, and A.B. Bonaldo. 2005. Abundância e fenologia de *Cryptocellus simonis* Hansen & Sørensen, 1904 (Ricinulei, Arachnida) na serapilheira do Bosque Rodrigues Alves, Belém, Pará, Brasil, com a comparação de três técnicas de coleta. Biota Neotropica 5 (1a): 1–9.

Barrows, W.M. 1925. Modification and development of the arachnid palpal claw, with special reference to spiders. Annals of the Entomological Society of America 18: 483–516.

Beccaloni, J. 2009. Arachnids. London: Natural History Museum.

Benavides, L.R., S.R. Daniels, and G. Giribet. 2021. Understanding the real magnitude of the arachnid order Ricinulei through deep Sanger sequencing across its distribution range and phylogenomics, with the formalization of the first species from the Lesser Antilles. Journal of Zoological Systematics and Evolutionary Research 59 (8): 1850–1873.

Bolívar y Pieltain, C. 1942. Estudio de un ricinulideo de la Caverna de Cacahuamilpa, Guerrero, Mex. (Arachnida). Revista de la Sociedad Mexicana de Historia Natural 2: 197–209.

Bonaldo, A.B., and R. Pinto-da-Rocha. 2003. On a new species of *Cryptocellus* from the Brazilian Amazon. Revista Ibérica de Aracnología 7: 103–108.

Börner, C. 1902. Arachnologische Studien (II und III). Zoologischer Anzeiger 25: 433–466.

Botero-Trujillo, R. 2014. A new Colombian species of *Cryptocellus* (Arachnida, Ricinulei), with notes on the taxonomy of the genus. Zootaxa 3814 (1): 121–132.

Botero-Trujillo, R., and E. Flórez. 2017. Two new ricinuleid species from Ecuador and Colombia belonging to the *peckorum* species-group of *Cryptocellus* Westwood (Arachnida, Ricinulei). Zootaxa 4286 (4): 483–498.

Botero-Trujillo, R., and G.A. Pérez. 2008. A new species of *Cryptocellus* (Arachnida, Ricinulei) from northwestern Colombia. Journal of Arachnology 36: 468–471.

Botero-Trujillo, R., and G.A. Pérez. 2009. A new species of *Cryptocellus* (Arachnida, Ricinulei) from the Kofán Territory in southwestern Colombia. Zootaxa 2050: 56–64.

Botero-Trujillo, R., and L. Prendini. 2025. *Cryptocellus armasi*, a new troglomorphic hooded tick-spider from Venezuela (Arachnida: Ricinulei). Zootaxa 5563 (1): 96–108.

Botero-Trujillo, R., and A. Valdez-Mondragón. 2016. A remarkable new species of the *magnus* species-group of *Cryptocellus* (Arachnida, Ricinulei) from Ecuador, with observations on the taxonomy of the New World genera. Zootaxa 4107 (3): 321–337.

Botero-Trujillo, R., C.E. Sain, and L. Prendini. 2021a. Systematics of the "giant" Ricinulei (Ricinoididae: *Ricinoides*) of West Africa, with descriptions of five new species and comparative morphology of the male copulatory apparatus. Bulletin of the American Museum of Natural History 448: 1–68.

Botero-Trujillo, R., L.S. Carvalho, E. Flórez D., and L. Prendini. 2021b. Four new species of "hooded tick-spiders" (Ricinulei, Ricinoididae) from South and Central America, with clarification of the identity of *Cryptocellus leleupi* Cooreman, 1976. American Museum Novitates 3976: 1–35.

Botero-Trujillo, R., J.A. Ochoa, and L. Prendini. 2021c. A new troglomorphic, leaf-litter scorpion from Ecuador (Troglotayosicidae: *Troglotayosicus*). American Museum Novitates 3981: 1–24.

Botero-Trujillo, R., S.R. Davis, P. Michalik, and L. Prendini. 2022. *Hirsutisoma grimaldii* sp. nov., a ca. 99-million-year-old ricinuleid (Primoricinulei, Hirsutisomidae) from Cretaceous Burmese amber with a corticolous, scansorial lifestyle. Palaeoentomology 5 (5): 493–504.

Brusca, R.C., and G.J. Brusca. 1990. Invertebrates. Sunderland: Sinauer Associates.

Brusca, R.C., and G.J. Brusca. 2003. Invertebrates. 2nd ed. Sunderland: Sinauer Associates.

Cloudsley-Thompson, J.L. 1958. Spiders, scorpions, centipedes and mites. New York: Pergamon Press.

Cloudsley-Thompson, J.L. 1968. Spiders, scorpions, centipedes and mites. Revised ed. Oxford: Pergamon Press.

Cooke, J.A.L. 1967. Observations on the biology of Ricinulei (Arachnida) with descriptions of two new species of *Cryptocellus*. Journal of Zoology, London 151: 31–42.

Cooke, J.A.L., and M.U. Shadab. 1973. New and little known ricinuleids of the genus *Cryptocellus* (Arachnida, Ricinulei). American Museum Novitates 2530: 1–25.

Cooke, J.W. 1971. Mating behavior and the functional morphology of the male copulatory apparatus in *Cryptocellus pelaezi* (Arachnida, Ricinulei). M.Sc. thesis, Texas Tech University, Lubbock, TX.

Cooreman, J. 1976. Description d'une stase nymphale d'un Ricinulei de l'Ecuador, *Cryptocellus leleupi* n. sp. *In* N. Leleup (editor), Mission Zoologique Belge aux îles Galapagos et un Ecuador (N. et J. Leleup, 1964–1965), vol. 3: 25–52. Brussels: Koninklijk Museum voor Midden-Afrika.

Dubinin, V.B. 1962. [Chelicerophora]. *In* B.B. Rohdendorf (editor), [Fundamentals of paleontology]: 375–530. Moscow: Academy of Sciences of the U.S.S.R. [in Russian]

Dumitresco, M., and I. Juvara-Balş. 1977a. Position systematique de *Heteroricinoides bordoni* n. g. n. sp. dans la famille Ricinuleididae [sic] (Arachnida). Boletín de la Sociedad Venezolana de Espeleologia 7 (14): 147–180.

Dumitresco, M., and I. Juvara-Balş. 1977b. L'importance de la structure des organes copulateurs femelles dans la systématique des Ricinulei. Travaux de l'Institute de Spéologie "Émile Racovitza" 16: 259–261.

Dunlop, J.[A.] 1994. Ricinuleids. Journal of the British Tarantula Society 10: 55–58.

Dunlop, J.A. 1996. Evidence for a sister group relationship between Ricinulei and Trigonotarbida. Bulletin of the British Arachnological Society 10 (6): 193–204.

Dunlop, J.A., D. Penney, and D. Jekel. 2020. A summary list of fossil spiders and their relatives. *In* World Spider Catalog, version 20.5. Natural History Museum Bern. Online resource (https://wsc.nmbe.ch/resources/fossils/Fossils20.5.pdf), accessed on 22 May 2021.

Ewing, H.E. 1929. A synopsis of the American arachnids of the primitive order Ricinulei. Annals of the Entomological Society of America 22: 583–600.

Fage, L. 1921. Sur une nouvelle espèce du genre *Cryptocellus* (Arachn.: Ricinulei). Bulletin du Muséum National d'Histoire Naturelle, Paris 27: 526–530.

Fage, L. 1938. Quelques arachnides provenant de fourmilières ou de termitières du Costa Rica. Bulletin du Muséum National d'Histoire Naturelle, Paris (2e sér.) 10: 369–376.

Fernández, R., and G. Giribet. 2015. Unnoticed in the tropics: phylogenomic resolution of the poorly known arachnid order Ricinulei (Arachnida). Royal Society Open Science 2: 1–13.

Finnegan, S. 1935. Rarity of the archaic arachnids, Podogona (Ricinulei). Nature 36: 186.

Fritsch [Frič], A. 1904. Palaeozoische Arachniden. Prague: A. Frič.

García, L.F., E. Torrado-León, G. Talarico, and A.V. Peretti. 2015. First characterization of the behavioral repertory in a ricinuleid: *Cryptocellus narino* Platnick & Paz

1979 (Arachnida, Ricinulei, Ricinoididae). Journal of Insect Behavior 28: 447–459.

Gertsch, W.J., and S. Mulaik. 1939. Report on a new ricinuleid from Texas. American Museum Novitates 1037: 1–5.

Gervais, P. 1844. Ordre V. Phalangides. *In* C.A. Walckenaer (editor), Histoire naturelle des insectes. Aptères. 3: 94–131. Paris: Librairie Encyclopédique de Rôret.

Goloboff, P.A., and S.A. Catalano. 2016. TNT version 1.5, including a full implementation of phylogenetic morphometrics. Cladistics 32: 221–238.

Goloboff, P.A., J.S. Farris, and K.C. Nixon. 2008. TNT, a free program for phylogenetic analysis. Cladistics 24: 774–786.

Guérin-Méneville, F.E. 1838. Note sur l'*Acanthodon* et sur le *Cryptostemme*, nouveaux genres d'arachnides. Revue Zoologique 1: 10–14.

Haelewaters, D., and D.H. Pfister. 2019. Morphological species of *Gloeandromyces* (Ascomycota, Laboulbeniales) evaluated using single-locus species delimitation methods. Fungal Systematics and Evolution 3: 19–33.

Hammen, L. van der. 1979. Comparative studies in Chelicerata I. The Cryptognomae (Ricinulei, Architarbi and Anactinotrichida). Zoologische Verhandelingen 174: 1–62.

Hammen, L. van der. 1989. An introduction to comparative arachnology. The Hague: SPB Academic Publishing.

Hansen, H.J. 1921. The Pedipalpi, Ricinulei, and Opiliones (exc. Op. Laniatores) collected by Mr. Leonardo Fea in tropical West Africa and adjacent islands. *In* Studies on Arthropoda 1: 1–55. Copenhagen: Gyldendalske Boghandel.

Hansen, H.J. 1930. On the comparative morphology of the appendages in the Arthropoda. B. Crustacea (supplement), Insecta, Myriopoda, and Arachnida. *In* Studies on Arthropoda 3: 1–376. Copenhagen: Gyldendalske Boghandel.

Hansen, H.J., and W. Sørensen. 1904. On two orders of Arachnida. Cambridge, U.K.: Cambridge University Press.

Harvey, M.S. 1984. The female of *Ricinoides westermannii* (Guérin-Méneville), with notes on those of *R. afzelii* (Thorell) and *R. karschii* (Hansen & Sørensen) (Ricinulei). Bulletin of the British Arachnological Society 6 (5): 205–210.

Harvey, M.S. 2002. The neglected cousins: what do we know about the smaller arachnid orders? Journal of Arachnology 30: 357–372.

Harvey, M.S. 2003. Catalogue of the smaller arachnid orders of the World. Collingwood, Victoria, Australia: CSIRO Publishing.

Hoang, D.T., O. Chernomor, A. von Haeseler, B.Q. Minh, and L.S. Vinh. 2017. UFBoot2: improving the ultrafast bootstrap approximation. Molecular Biology and Evolution 35: 518–522.

International Commission of Zoological Nomenclature (ICZN). 1999. International Code of Zoological Nomenclature. 4th ed. London: International Trust for Zoological Nomenclature. Online resource (https://www.iczn.org/the-code/the-code-online), accessed on 14 July 2024.

Judson, M., and J.D. Hardy. 2001. First record of Ricinulei (Arachnida) from the Lesser Antilles. Caribbean Journal of Science 37(3–4): 290–291.

Kaestner, A. 1968. Arthropod relatives, Chelicerata, Myriapoda. *In* Invertebrate Zoology 2: 472 pp. New York: Wiley.

Karsch, F. 1892a. Ueber *Cryptostemma* Guér. als einzigen recenten Ausläufer der fossilen Arachnoideen-Ordnung der Meridogastra Thor. Berliner Entomologische Zeitschrift 37: 25–32.

Karsch, F. 1892b. Nachschrift zu meinem Aufsatze über *Cryptostemma* Guér. Berliner Entomologische Zeitschrift 37: 64.

Kästner, A. 1932. Ricinulei Thorell. *In* W. Kükenthal, Handbuch der Zoologie 3 (2) (4): 99–116. Berlin and Leipzig: Walter de Gruyter.

Kästner, A. (1940) Arachnida. *In* W. Kükenthal, Handbuch der Zoologie 3 (2) (1): 97–116. Berlin and Leipzig: Walter de Gruyter.

Kennaugh, J.H. 1968. An examination of the cuticle of three species of Ricinulei (Arachnida). Journal of Zoology, London 156: 393–404.

Král, J., et al. 2025. Advances in understanding the karyotype evolution of Tetrapulmonata and two other arachnid taxa, Ricinulei and Solifugae. Genes 16 (207): 1–67.

Lankester, E.R. 1904. The structure and classification of the Arachnida. Quarterly Journal of Microscopical Science (N. S.) 48: 165–269.

Lawrence, R.F. 1969. The trichoid structures on the chelicerae of the short-tailed whip-scorpions (Schizomida; Arachnida). Transactions of the Royal Society of South Africa 38: 123–132.

Legg, G. 1976a. The external morphology of immature stages of *Ricinoides karschi* (Arachnida: Ricinulei). Bulletin of the British Arachnological Society 3 (9): 243–248.

Legg, G. 1976b. The external morphology of a new species of ricinuleid (Arachnida) from Sierra Leone. Zoological Journal of the Linnean Society 59: 1–58.

Legg, G. 1977. Sperm transfer and mating in *Ricinoides hanseni* (Ricinulei: Arachnida). Journal of Zoology, London 182: 51–61.

Legg, G. 1978a. Two new ricinuleids from W. Africa (Arachnida: Ricinulei) with a key to the adults of the genus *Ricinoides*. Bulletin of the British Arachnological Society 4 (2): 89–99.

Legg, G. 1978b. The status of *Ricinoides plebejus* and a note on *R. afzelii* (Ricinulei, Arachnida). Bulletin of the British Arachnological Society 4 (3): 124–125.

Legg, G. 1982. Some Ricinulei (Arachnida) from Ivory Coast, including a new species and a note on the immature stages of *Ricinoides westermanni* (Hansen & Sørensen). Revue Suisse de Zoologie 89 (2): 287–296.

Lewis, P.O. 2001. A likelihood approach to estimating phylogeny from discrete morphological character data. Systematic Biology 50: 913–925.

Lozano-Fernández, J., et al. 2019. Increasing species sampling in chelicerate genomic-scale datasets provides support for monophyly of Acari and Arachnida. Nature Communications 10: 1–8.

Lucas, H. 1838. Phalangiens. *In* F.-E. Guerin (editor), Dictionnaire pittoresque d'histoire naturelle et des phénomènes de la nature 7: 349–354. Paris: Au Bureau de Souscription.

Millot, J. 1945a. La constitution de l'abdomen des Ricinulei (Arachnides). Bulletin de la Société Entomologique de France 59: 72–74.

Millot, J. 1945b. L'anatomie interne des Ricinulei (Arachnides). Annales des Sciences Naturelles, Zoologie 11 (7): 1–29.

Millot, J. 1949a. Classe de Arachnides (Arachnida). I. – Morphologie générale et anatomie interne. *In* P.-P. Grassé (editor), Traité de zoologie, anatomie, systématique, biologie 6: 263–319. Paris: Masson et Cie.

Millot, J. 1949b. Ordre des Ricinuléides. *In* P.-P. Grassé (editor), Traité de zoologie, anatomie, systématique, biologie 6: 744–760. Paris: Masson et Cie.

Mitchell, R.W. 1969. The cover illustration, *Cryptocellus osorioi* (Arachnida; Ricinulei). Southwestern Naturalist 14: 136–138

Mitchell, R.W. 1970. Population size and dispersion and species associations of a Mexican cavernicole ricinuleid (Arachn.). Ciencia, México 27: 63–74.

Moritz, M., and S.C. Fischer. 1980. Die Typen der Arachniden-Sammlung des Zoologischen Museums Berlin. II. Uropygi, Amblypygi, Schizomida, Ricinulei, Solifuga. Mitteilung aus dem Zoologischen Museum in Berlin 56: 137–154.

Murienne, J., L.R. Benavides, L. Prendini, G. Hormiga, and G. Giribet. 2013. Forest refugia in western and central Africa as 'museums' of Mesozoic biodiversity. Biology Letters 9: 2–7.

Naskrecki, P. 2008. A new ricinuleid of the genus *Ricinoides* Ewing (Arachnida, Ricinulei) from Ghana. Zootaxa 1698: 57–64.

Nguyen, L.-T., H.A. Schmidt, A. von Haeseler, and B.Q. Minh. 2015. IQ-TREE: A fast and effective stochastic algorithm for estimating Maximum Likelihood phylogenies. Molecular Biology and Evolution 32: 268–274.

Penney, D., Y. Marusik, C.P. Wheater, and A.M. Langan. 2009. First Gambian Ricinulei (Arachnida: Ricinoididae): northernmost African record for the order. Zootaxa 2021: 66–68.

Petrunkevitch, A. 1913. A monograph of the terrestrial Palaeozoic Arachnida of North America. Transactions of the Connecticut Academy of Arts and Sciences 18: 1–137.

Petrunkevitch, A. 1955. Arachnida. *In* R.C. Moore (editor), Treatise on invertebrate paleontology. Part P. Arthropoda. 2. Chelicerata with sections on Pycnogonida and *Palaeoisopus*: 42–162. Lawrence, KS: Geological Society of America.

Pittard, S.K. 1970. Comparative external morphology of the life stages of *Cryptocellus pelaezi* (Arachnida, Ricinulei). M.Sc. thesis, Texas Tech University, Lubbock, TX.

Pittard, [S.]K., and R.W. Mitchell. 1972. Comparative morphology of the life stages of *Cryptocellus pelaezi* (Arachnida, Ricinulei). Graduate Studies, Texas Tech University 1: 1–78.

Platnick, N.I. 1980. On the phylogeny of Ricinulei. *In* J. Gruber (editor), Verhandlungen 8. Internationaler Arachnologen-Kongress abgehalten an der Universität für Bodenkultur, Wien, 7–12 Juli, 1980: 349–353. Vienna: H. Egermann.

Platnick, N.I. 1988. A new *Cryptocellus* (Arachnida: Ricinulei) from Brazil. Journal of the New York Entomological Society 96: 363–366.

Platnick, N.I. 2002. Ricinulei. *In* J. Adis (editor), Amazonian Arachnida and Myriapoda: 381–386. Sofia: PENSOFT Publishers.

Platnick, N.I., and L.F. García. 2008. Taxonomic notes on Colombian *Cryptocellus* (Arachnida, Ricinulei). Journal of Arachnology 36: 145–149.

Platnick, N.I., and G. Pass. 1982. On a new Guatemalan *Pseudocellus* (Arachnida, Ricinulei). American Museum Novitates 2733: 1–6.

Platnick, N.I., and N. Paz. 1979. On the *Cryptocellus magnus* group (Arachnida, Ricinulei). American Museum Novitates 2677: 1–9.

Platnick, N.I., and M.U. Shadab. 1976. On Colombian *Cryptocellus* (Arachnida, Ricinulei). American Museum Novitates 2605: 1–8.

Platnick, N.I., and M.U. Shadab. 1977. On Amazonian *Cryptocellus* (Arachnida, Ricinulei). American Museum Novitates 2633: 1–17.

Platnick, N.I., and M.U. Shadab. 1981. On Central American *Cryptocellus* (Arachnida, Ricinulei). American Museum Novitates 2711: 1–13.

Pollock, J. 1966. Secret life of the ricinulid. Animals, London 8: 402–405.

Pollock, J. 1967. Notes on the biology of Ricinulei (Arachnida). Journal of the West African Science Association 12: 19–22.

Prendini, L. 2000. Phylogeny and classification of the superfamily Scorpionoidea Latreille 1802 (Chelicerata, Scorpiones): an exemplar approach. Cladistics 16 (1): 1–78.

Prendini, L. 2001. Species or supraspecific taxa as terminals in cladistic analysis? Groundplans versus exemplars revisited. Systematic Biology 50 (2): 290–300.

Prendini, L. 2025. All genera of the world: order Ricinulei (Animalia: Arthropoda: Arachnida). Megataxa 18: 407–412.

Roewer, C.F. 1932. Solifuga, Palpigrada. *In* H.G. Bronn (editor), Klassen und Ordnungen des Tierreichs. V Band: Arthropoda. IV Abteilung: Arachnoidea: 1–160. Leipzig: Akademische Verlagsgesellschaft m. b. H.

Salvatierra, L., and A.L. Tourinho. 2016. The integumentary ultrastructure of *Cryptocellus bordoni* Dumitresco and Jurvara-Bals, 1976 (Arachnida, Ricinulei). Micron 81: 1–19.

Salvatierra, L., A.L. Tourinho, and G. Giribet. 2013. Description of the male, larva and nymphal stages of *Cryptocellus iaci* (Arachnida, Ricinulei), with an overview of tarsal sensilla and other integumental structures. Zootaxa 3709: 149–161.

Santamaria, S. 2001. Los Laboulbeniales, un grupo enigmático de hongos parásitos de insectos. Lazaroa 22, 3–19.

Santamaria, S., H. Enghoff, J. Gruber, and A.S.P.S. Reboleira. 2017. First Laboulbeniales from harvestmen: the new genus *Opilionomyces*. Phytotaxa 305 (4): 285–292.

Santibáñez-López, C.E., et al. 2018. Integration of phylogenomics and molecular modeling reveals lineage-specific diversification of toxins in scorpions. PeerJ 6: 1–23.

Sato, S., et al. 2024. Under the hood: phylogenomics of hooded tick spiders (Arachnida, Ricinulei) uncovers discordance between morphology and molecules. Molecular Phylogenetics and Evolution 193: 1–10.

Savory, T.H. 1964. Arachnida. London: Academic Press.

Savory, T.H. 1977. Arachnida. 2nd ed. London: Academic Press.

Selden, PA. 1992. Revision of the fossil ricinuleids. Transactions of the Royal Society of Edinburgh: Earth Sciences 83: 595–634.

Selden, P.A., and J.A. Dunlop. 1998. Fossil taxa and relationships of chelicerates. *In* G. Edgecombe (editor), Arthropod fossils and phylogeny: 303–331. New York: Columbia University Press.

Selden, P.A., and D. Ren. 2017. A review of Burmese amber arachnids. Journal of Arachnology 45: 324–343.

Sharma, P.P., et al. 2014. Phylogenomic interrogation of Arachnida reveals systemic conflicts in phylogenetic signal. Molecular Biology and Evolution 31 (11): 2963–2984.

Sharma, P.P., et al. 2015. Phylogenomic resolution of scorpions reveals multilevel discordance with morphological phylogenetic signal. Proceedings of the Royal Society of London B, Biological Sciences 282: 1–10.

Sharma, P.P., et al. 2018. A revised dated phylogeny of scorpions: phylogenomic support for ancient divergence of the temperate Gondwanan family Bothriuridae. Molecular Phylogenetics and Evolution 122: 37–45.

Shorthouse, D.P. 2010. SimpleMappr, a web-enabled tool to produce publication-quality point maps. Online resrouce: (http://www.simplemappr.net), accessed 10 May 2025.

Shultz, J.W. 1989. Morphology of locomotor appendages in Arachnida: evolutionary trends and phylogenetic implications. Zoological Journal of the Linnean Society 7: 1–56.

Shultz, J.W. 2007. A phylogenetic analysis of the arachnid orders based on morphological characters. Zoological Journal of the Linnean Society 150: 221–265.

Talarico, G., and P. Michalik. 2010. Spermatozoa of an Old World Ricinulei (*Ricinoides karschii*, Ricinoidae [sic]) with notes about the relationships of Ricinulei within the Arachnida. Tissue and Cell 42: 383–390.

Talarico, G., J.G. Palacios-Vargas, M.F. Silva, and G. Alberti. 2005. First ultrastructural observations on the tarsal pore organ of *Pseudocellus pearsei* and *P. boneti* (Arachnida, Ricinulei). Journal of Arachnology 33: 604–612.

Talarico, G., J.G. Palacios-Vargas, M.F. Silva, and G. Alberti. 2006. Ultrastructure of tarsal sensilla and other integument structures of two *Pseudocellus* species (Ricinulei, Arachnida). Journal of Morphology 267: 441–463.

Talarico, G., L.F. García, and P. Michalik. 2008a. The male genital system of the New World Ricinulei (Arachnida): ultrastructure of spermatozoa and spermiogenesis with special emphasis on its phylogenetic implications. Arthropod Structure and Development 37: 396–409.

Talarico, G., J.G. Palacios-Vargas, and G. Alberti. 2008b. Taste while chewing? Sensory structures in the chelicerae of *Pseudocellus pearsei* (Chamberlin & Ivie, 1938) (Ricinulei, Arachnida). Revista Ibérica de Aracnología 15: 47–53.

Talarico, G., G. Zeck-Kapp, J.G. Palacios-Vargas, and G. Alberti. 2009. Oogenesis and ovary ultrastructure in *Pseudocellus boneti* (Arachnida: Ricinulei). Contributions to Natural History 12: 1373–1386.

Talarico, G., E. Lipke, and G. Alberti. 2011. Gross morphology, histology, and ultrastructure of the alimentary system of Ricinulei (Arachnida) with emphasis on functional and phylogenetic implications. Journal of Morphology 272: 89–117.

Thorell, T. 1892. On an apparently new arachnid belonging to the family Cryptostemmoidae, Westw. Kungliga Svenska Vetenskaps-akademiens Handlingar 17: 1–18.

Tourinho, A.L., and C.S. Azevedo. 2007. A new Amazonian *Cryptocellus* Westwood (Arachnida, Ricinulei). Zootaxa 1540: 55–60.

Tourinho, A.L., N.F. Lo-Man-Hung, and L. Salvatierra. 2014. A new Amazonian species of *Cryptocellus* (Arachnida, Ricinulei), with descriptions of its integumental structures and all free-living life stages. Zootaxa 3814 (1): 81–95.

Tuxen, S.L. 1974. The African genus *Ricinoides* (Arachnida, Ricinulei). Journal of Arachnology 1: 85–106.

Valdez-Mondragón, A., and M.R. Cortez-Roldán. 2021. COI mtDNA barcoding and morphology for the description of a new species of ricinuleid of the genus *Pseudocellus* (Arachnida: Ricinulei: Ricinoididae) from El Triunfo Biosphere Reserve, Chiapas, Mexico. European Journal of Taxonomy 778: 1–25.

Valdez-Mondragón, A., and O.F. Francke. 2011. Four new species of the genus *Pseudocellus* (Arachnida: Ricinulei: Ricinoididae) from Mexico. Journal of Arachnology 39: 365–377.

Valdez-Mondragón, A., and O.F. Francke. 2013. Two new species of ricinuleids of the genus *Pseudocellus* (Arachnida: Ricinulei: Ricinoididae) from southern Mexico. Zootaxa 3635 (5): 545–556.

Valdez-Mondragón, A., and O.F. Francke. 2017. Ricinúlidos de México, un grupo de arácnidos diverso y aún poco conocido en el país. Boletín de la Asociación Mexicana de Sistemática de Artrópodos 1: 11–17.

Valdez-Mondragón, A., O.F. Francke, and R. Botero-Trujillo. 2018. New morphological data for the order Ricinulei with the description of two new species of *Pseudocellus* (Arachnida: Ricinulei: Ricinoididae) from Mexico. Journal of Arachnology 46: 114–132.

Valdez-Mondragón, A., and A.R. Juárez-Sánchez. 2021. A new epigean species of ricinuleid of the genus *Pseudocellus* (Arachnida: Ricinulei: Ricinoididae) from a tropical sub-deciduous forest in Oaxaca, Mexico. Journal of Arachnology 48: 329–338.

Valdez-Mondragón, A., M.R. Cortez-Roldán, and E.F. Campuzano-Granados. 2020. On the Mexican ricinuleids: a new species of the genus *Pseudocellus* (Arachnida: Ricinulei: Ricinoididae) from the cloud forest of Chiapas, Mexico. Revista Mexicana de Biodiversidad 91: 1–12.

Valdez-Mondragón, A., G. Montiel-Parra, and M.R. Cortez-Roldán. 2025. A dimorphic species or underestimated diversity? *Pseudocellus pelaezi* (Coronado Gutiérrez) (Arachnida: Ricinulei: Ricinoididae) from northeastern Mexico assessed with morphological and barcoding data. Journal of Arachnology 53: 30–53.

Weir, A., and P.M. Hammond. 1997. Laboulbeniales on beetles: host utilization patterns and species richness of the parasites. Biodiversity and Conservation 6: 701–719.

Westwood, J.O. 1874. Thesaurus entomologicus oxoniensis. Oxford.: Clarendon Press.

Whalen, N., and P. Selden. 2021. A new, giant ricinuleid (Arachnida, Ricinulei), from the Pennsylvanian of Illinois, and the identification of a new, ontogenetically stable, diagnostic character. Journal of Paleontology 95 (3): 601–612.

Whittick, R.J. 1938. On a second specimen of *Cryptocellus simonis* Hans. & Sør. [Arachnida]. Annals and Magazine of Natural History (11) 2: 479–480.

Wunderlich, J. 2012. Description of the first fossil Ricinulei in amber from Burma (Myanmar), the first report of this arachnid order from the Mesozoic and from Asia, with notes on the related extinct order Trigonotarbida. *In* J. Wunderlich (editor), Fifteen papers on extant and fossil spiders (Araneae). Beiträge zur Araneologie 7: 233–244. Hirschberg, Germany: J. Wunderlich.

Wunderlich, J. 2015. New and rare fossil Arachnida in Cretaceous Burmese amber (Amblypygi, Ricinulei and Uropygi: Thelephonida [sic]). *In* J. Wunderlich

(editor), Spinnen des erdmittelalters. Beiträge zur Araneologie 9: 409–436. Hirschberg, Germany: J. Wunderlich.

Wunderlich, J. 2017. New extinct taxa of the arachnid order Ricinulei, based on new fossils preserved in mid Cretaceous Burmese amber. *In* J. Wunderlich (editor), Ten papers on fossil and extant spiders (Araneae). Beiträge zur Araneologie 10: 48–71. Hirschberg, Germany: J. Wunderlich.

Wunderlich, J. 2022. A new extinct family of the arachnid order Ricinulei in Cretaceous Burmese (Kachin) amber, with notes on the order Trigonotarbida and on sperm transfer in Arachnida. *In* J. Wunderlich (editor), Five papers on extant spiders (Araneida) as well as on fossil spiders and Ricinulei. Beiträge zur Araneologie 15: 185–204. Hirschberg, Germany: J. Wunderlich.

Zakhvatkin, A.A. 1952. [Subdivision of the mites (Acarina) into orders and the position of these in the system of the Chelicerata]. Parazitologicheskii Sbornik Zoologicheskii Institut Akademii Nauk SSSR [Parasitological Collection, Zoological Institute of the USSR Academy of Sciences] 14: 5–46. [in Russian]

APPENDIX 1

Additional Material Examined for Comparative Morphology and Phylogenetic Analysis of African Ricinulei Thorell, 1876

Material of one extinct species of †Poliocheridae Scudder, 1884, and eight extant species in two New World genera of Ricinoididae Ewing, 1929, deposited in the following collections: the American Museum of Natural History (AMNH), including the Ambrose Monell Cryocollection for Molecular and Microbial Research (AMCC), New York; the Coleção de História Natural, Universidade Federal do Piauí (CHNUFPI), Floriano, Brazil; the Colección Nacional de Arácnidos (CNAN), Universidad Nacional Autónoma de México, Mexico City; the Coleção Zoológica Prof. Paulo Bührnheim, Universidade Federal do Amazonas (CZPB/UFAM), Manaus, Brazil; the Instituto de Investigación de Recursos Biológicos "Alexander von Humboldt" (IAvH), Villa de Leyva, Colombia; the Arachnological Collection, Instituto de Ciencias Naturales (ICN), Universidad Nacional de Colombia, Bogotá; the Museo Argentino de Ciencias Naturales "Bernardino Rivadavia" (MACN), Buenos Aires; the Museu de Ciências Naturais (MCN), Fundação Zoobotânica do Rio Grande do Sul, Porto Alegre, Brazil; the Museo Javeriano de Historia Natural "Lorenzo Uribe, S.J.," Pontificia Universidad Javeriana (MPUJ), Bogotá; the Oxford University Museum of Natural History (OUMNH); the Senckenberg Forschungsinstitut und Naturmuseum, Frankfurt (SMF), Germany; and the Natural History Museum of Denmark, University of Copenhagen (ZMUC).

Family †Poliocheridae Scudder, 1884

?†*Poliochera cretacea* Wunderlich, 2012: **MYANMAR:** 1 ♀ adult [or tritonymph] (AMNH), embedded in piece of Cretaceous Burmese amber [ca. 99 Ma]. 1 ♀ [?], 1 tritonymph, 1 tritonymph [?], 1 deutonymph, 1 protonymph [or larva] (AMNH), embedded in piece (26 × 14 × 6 mm) of Cretaceous Burmese amber [ca. 99 Ma].

Family Ricinoididae Ewing, 1929

Cryptocellus becki Platnick and Shadab, 1977: **BRAZIL:** *Amazonas*: Manaus, Reserva Florestal Adolpho Ducke, Dichter Urwald in Bachniederung [dense jungle in creek lowlands], 1966, L. Beck, holotype ♂ (SMF 12961); Manaus, Reserva Florestal Adolpho Ducke, 6–9.viii.1992, A.D. Brescovit, 1 ♂ (MCN Ric 003), viii.1971, Becker, 1 ♀ (MACN Ar 39262), 14.iii.1987, A.A. Lise, 1 ♂ (MCN Ric 004), 18–25.ii.1992, A.D. Brescovit, 1 ♂ (MCN Ric 002), 02°55′40.5″S 59°58′14.1″W, 99 m, 6.xi.2016, L.S. Carvalho, 1 ♂ (CHNUFPI 2509); Manaus, BR 174, Fazenda Experimental da UFAM, 02°38′58.9″S 60°02′56.9″W, 8–11.ii.2019, G.F.A. Rodrigues, I.F. Araújo, M.L. Espirito Santo, and J.P. Nobrega, 1 ♂ (CZPB/UFAM), 8–11.ii.2019, G.S. Santos, A.M. Menezes, S.B. Freitas, and T.F. Gomes, 1 ♂ (CZPB/UFAM), 8–11.ii.2019, P.R. Silva et al., 1 ♀ (CZPB/UFAM), 8–11.ii.2019, P.J.S. Barbosa, T.S. Caetano, S.L. da Silva, and I.A.C. Lima, 1 protonymph (CZPB/UFAM); Estação Experimental de Silvicultura Tropical, 45 km from Manaus on BR-174, 02°35′54″S 60°02′15″W, 131 m, 19.xi.2013, B.T. Faleiro, 1 ♀ (CHNUFPI 2513); Tarumã Mirim River, 03°02′S 60°17′W, 29.xii.1982, J.M. Gomes Rodrigues, secondary dryland forest, soil extract, 1 ♂ (AMNH IZC 325035).

Cryptocellus islacolon Botero-Trujillo et al., 2021: **PANAMA:** *Bocas del Toro*: Isla Colón [09°24′N 82°16′W], 24.i–7.iii.2010, M. Sears and R. Wallace, under rotten wood, holotype ♂ (OUMNH 2010-028-001), paratypes: 15 ♂ (OUMNH 2010-028-003–17), 14 ♀ (OUMNH 2010-028-018–30, 2010-028-002).

Cryptocellus jamari Botero-Trujillo et al., 2021: **BRAZIL:** *Rondônia*: Jamari, Floresta Nacional do Jamari, 09°11′32.7″S 63°06′32.3″W, 143 m, 23.x.2016, L.S. Carvalho, holotype ♂ (CHNUFPI 2221), paratypes: 1 ♀ (CHNUFPI 3622), 4 tritonymphs, 1 deutonymph (CHNUFPI 3623), 2 tritonymphs (CHNUFPI 2222, 2223).

Cryptocellus peckorum Platnick and Shadab, 1977: **COLOMBIA:** *Amazonas*: Leticia, 24–28.ii.1974, S. and J. Peck, forest litter, 1 ♂ (AMNH IZC 324929); Leticia, 24.xi–15.xii.2007, L.E. Franco,

Winkler trap, 1 ♀ (IAvH I 2834), 1 ♀ (IAvH I 2835); Leticia, 7 km W of Tarapacá, 100 m, 26.x.1996, E. Flórez, 1 tritonymph (ICN Ari 001); Leticia, 7 km to Tarapacá, 120 m, 30.x.2002, UNAL students, 1 ♀ (ICN Ari 007); Leticia, 22 km to Tarapacá, Reserva Tucano, 95 m, 5.xi.2003, F. Fernández, 1 tritonymph (ICN Ari 006); Monilla Amena, Várzea, 70 m, 6.ix.2005, G. Rodríguez, pitfall, 1 ♀ (MPUJ ENT 1752).

Pseudocellus monjarazi Valdez-Mondragón and Francke, 2013: **MEXICO:** *Chiapas*: La Trinitaria, Cueva de San Francisco, 16°05′58.956″N 92°02′48.839″W, 1546 m, 18.vi.2011, A. Valdez Mondragón, O.F. Francke, C. Santibáñez, J. Cruz, R. Monjaraz, G. Contreras, and K. Zárate, holotype ♂ (CNAN T0708), 1 ♂, 1 ♀ paratypes (CNAN T0709), 26.vii.2013, O.F. Francke, A. Valdez Mondragón, K. Zárate, J. Mendoza, R. Monjaraz, and C. Santibáñez, 1 ♀ (CNAN Rc00040); La Trinitaria, Gruta de Zapaluta, 17.viii.1969, S. and J. Peck, 1 ♀, 1 tritonymph, 2 deutonymphs, 1 protonymph (AMNH IZC 325108); Grutas de Zapaluta, 4 mi. SE of Zapaluta, 20.viii.1967, J. Reddell, J. Fish, and T.R. Evans, 2 ♂, 3 ♀, 1 deutonymph (AMNH IZC 325043); Grutas de Zapaluta, 6.5 km NE Zapaluta, 20.viii.1967, J. Reddell, J. Fish, and T.R. Evans, 2 ♀ (AMNH IZC 325109, 325110).

Pseudocellus paradoxus (Cooke, 1972): **CUBA:** *Santiago de Cuba* [formerly *Oriente*]: Santiago de Cuba, Puerto Boniato, 500 m, 6.xi.1971, L.F. de Armas, 2 ♀ paratypes (AMNH IZC 324897), 18.v.1972, L.F. de Armas, under stone, 2 ♀ (AMNH IZC 324955), vi.1975, L.F. de Armas, 2 ♂ (AMNH IZC 324898).

Pseudocellus pelaezi (Coronado Gutiérrez, 1970): **MEXICO:** *Nuevo León*: Chorros de Agua, 19. vii.1973, J.M. Rowland, 1 ♂ (AMNH IZC 324995), 23.vii.1973, J.M. Rowland and J.R. Reddell, 1 ♂ (AMNH IZC 324996); Chorros de Agua, E of Rayones, 13 mi. W of Montemorelos, 19.vi.1969, S. and J. Peck, under rock, 1 ♀, 1 tritonymph (AMNH IZC 324997). *San Luis Potosí*: Valles, Cueva de Taninul, 7.vi.1964, J. Reddell and D. McKenzie, 1 ♂, 2 ♀, 2 tritonymphs (AMNH IZC 324891), 1 ♂, 1 ♀ (AMNH IZC 324964), 5.vi.1967, R. Mitchell, 1 ♀ (AMNH IZC 324961); El Sótano del Toro, 11 km SE of Ciudad Valles, 1 ♀ (AMNH IZC 325054). *Tamaulipas*: Cueva de La Florida, 2 ♂, 1 ♀ (AMNH IZC 325009), 1 ♂, 1 ♀ (AMNH IZC 325003), 1 ♂, 1 ♀ (AMNH IZC 325005), 3.vi.1968, R.W. Mitchell, 2 ♂, 3 ♀, 2 tritonymphs, 2 captive-born larvae (ZMUC), 5.i.1970, 1 ♀ (AMNH IZC 325007), 26.iii.1970, 1 ♀ (AMNH IZC 324990); Cueva de La Florida, near entrance, 16.ii.1973, 1 ♀ (AMNH IZC 325010); Cueva de La Florida, 10 mi. SW of Mante, 1967, R. Remington, 1 tritonymph (AMNH IZC 324992), 2.ii.1968, W. Russell, 21 ♀, 5 tritonymphs (AMNH IZC 324912); Cueva de La Florida, 50 mi. SW of Mante, 2.ii.1968, W. Russell, 10 ♂ (AMNH IZC 324910); Cueva de La Florida, near El Pachón village, 12 km S and 10 km W of Mante, i.1973, W. Overal and E. Linn, 1 ♂, 3 ♀ (AMNH IZC 324991); Sierra de El Abra, Cueva de Florida, 16.ii.1970, J.A.L. Cooke, 3 ♂, 7 ♀, 3 tritonymphs (AMNH IZC 325004), 1 ♂ (AMNH IZC 325008); Mante, 16 km SSW, 20.vii.1973, J. Reddell and J.M. Rowland, 1 ♀, 1 deutonymph (AMNH IZC 324993); Gómez Farías, 13.iii.1972, J.A.L. Cooke, 1 ♀ (AMNH IZC 324982); Gómez Farías, road cut, 15.ii.1970, 1 ♂ (AMNH IZC 324986); Gómez Farías, 300 m, 6. vi.1983, S. and J. Peck, ravine litter, 1 ♂ (AMNH IZC 324985), 2 ♀, 1 tritonymph, 2 larvae (AMNH IZC 324994); Gómez Farías, 3 mi. S, nacimiento del Río Frío, 12.iii.1969, J. Reddell, 1 ♀ (AMNH IZC 324911); Sierra de El Abra, Arroyo del Río Frío, 16.ii.1970, J.A.L. Cooke, under stone and in litter, 1 ♀, 1 tritonymph, 1 deutonymph (AMNH IZC 324989); Arroyo del nacimiento del Río Frío, 16. ii.1970, 6 ♂, 1 ♀, 1 tritonymph (AMNH IZC 324988), 15.iii.1972, J.A.L. Cooke, 1 ♂, 1 ♀, 2 tritonymphs (AMNH IZC 324980); San Rafael de los Castros, 0.5 km NNW, viii.1969, W.H. Russell, under rocks in forest litter, 1 ♂ (AMNH IZC 324987). *Yucatán*: Cueva de Maya, "xerxa" de Maya, ix.1972, W.R. Russell, B. Russell, and J. Cooke, 2 ♂ (AMNH IZC 324972) [dubious record].

Pseudocellus seacus Platnick and Pass, 1982: **GUATEMALA:** *Alta Verapaz*: Finca Seacté, near Cobán, iii.1975–viii.1976, G. Kramer and G. Pass, holotype ♂, paratype ♀ (AMNH IZC 324867).

APPENDIX 2

List of Morphological Characters Used for Phylogenetic Analysis of African Ricinulei Thorell, 1876

Characters refer to male and female unless specified otherwise. Ten uninformative characters and 23 autapomorphic, nonhomoplastic character states indicated by †.

Tegument

1. Tegument, polygonal (calyxlike to navicular) setae: **0,** absent; **1,** present.
2. Tegument, saucer-shaped granules: **0,** absent; **1,** present. These small, round, low granules, slightly raised above the tegument, with a flat to moderately concave dorsal surface, are the saucer-shaped tubercles of Kennaugh (1968) and Tuxen (1974).

†3. Tegument, saucer-shaped granules: **0,** obsolete; **†1,** distinct. Saucer-shaped granules only occur in *Alantakun*, gen. nov., and *Ududo*, gen. nov. These granules are ubiquitous and readily visible on the soma, cucullus, pedipalps (except the tibia), and legs, in *Alantakun*, whereas they are obsolete and barely visible, often only identified by their slight iridescence, in *Ududo*.

†4. Prosoma and opisthosoma, dorsal surfaces, granules: **0,** separate, if present; **†1,** forming distinct clusters. In species with the first state, some granules may be adjacent, but this is not repeated across the tegument nor does it present an organized, well-defined pattern, unlike the second state, in which all or most of the granules are distinctly clustered.

Carapace

5. Carapace dorsolateral pale areas or "pseudocellar spots": **0,** absent; **1,** present. The pale areas form part of the setose dorsal surface of the carapace. They are visible in dorsal aspect near the carapace lateral margins, as a pair of diffuse, yellowish areas without well-defined borders that are at least partially covered with setae.
6. Carapace ventrolateral margin, posterolateral pleurite: **0,** absent or indistinct, corresponding area not sclerotized; **1,** distinct, sclerotized. The pleurite is a small, sclerotized area, appended to each posterolateral corner of the carapace, immediately ventral to the lateral hyaline line and dorsal to the leg coxae. Due to its position, the pleurite is visible only in lateral aspect. In some species of *Ricinoides* Ewing, 1929, *Gizoo*, gen. nov., *Tautau*, gen. nov., and *Ududo*, the corresponding area is granular; however, it is not sclerotized (i.e., similar in color to the lateral hyaline line) and there is no distinct sclerite.
7. Carapace ventrolateral margin, lateral hyaline line: **0,** unmodified, linear and narrow along entire length; **1,** expanded dorsal to border between coxae I and II, forming semiocellus (i.e., approximately semicircular in shape). The lateral hyaline line is an asetose longitudinal yellowish stripe, similar in appearance to the opisthosomal tergal and pleural membranes, extending laterally along each side of the prosoma. It is situated immediately ventral to the carapace lateral margin and dorsal to the leg coxae. Although visible in lateral aspect, it is obscured by the carapace in dorsal aspect.
8. Carapace lateral hyaline lines, expansions or semiocelli: **†0,** vestigial; **1,** moderate; **2,** large; **†3,** very large. Depending on the degree of development, moderate to large semiocelli are visible dorsolaterally (if moderate) or both dorsolaterally and dorsally (if large) whereas vestigial semiocelli are visible laterally as a slight expansion of the hyaline line.
9. Carapace posteromedian moundlike excrescence (♀): **0,** absent; **1,** present.
10. Carapace posteromedian moundlike excrescence (♂): **0,** absent; **1,** present.

Cucullus

11. Cucullus anterior surface, ventral part, median area (♂): **0,** unmodified, without anteromedian pronouncement; **1,** with anteromedian elevation; **2,** with anteromedian group

of raised granules; **†3,** with pronounced anteromedian knoblike tubercle.

12. Cucullus anterior surface, sublateral longitudinal sulci: **0,** absent or obsolete; **1,** distinct.
13. Cucullus anterior surface, ventral part, shape (♂): **0,** undifferentiated, shallowly convex as rest of cucullus; **†1,** with triangular, approximately flat surface; **†2,** with semitriangular, markedly concave surface.

†14. Cucullus anterior surface, ventral part, surface (♂): **0,** smooth, finely and/or sparsely granular; **†1,** coarsely granular. In species with coarse granulation, the granulation is distinctly coarser in the male.

15. Cucullus ventrolateral margins, shape in anterior aspect: **0,** rounded; **1,** moderately truncate. Truncate ventrolateral margins are usually more evident in the male.
16. Cucullus ventral margin, shape in anterior aspect: **0,** linear; **1,** bilobate. The bilobate ventral margin is often more evident in the male.
17. Cucullus ventral margin, posterior surface, median row of small denticulations: **0,** absent; **1,** present. When denticulations are present, the ventral margin itself is irregular and denticulate, not granular (e.g., elsewhere on the cucullus). The denticulations are often very small and may be difficult to identify if worn or covered by dirt.

Coxosternal Region

18. Coxosternal region, tritosternum: **†0,** extremely small, not exposed (only visible when pedipalp coxae are pulled); **1,** vestigial, barely visible; **2,** small but evident, tuberculate (if very small in male, more evident in female, e.g., *Cryptocellus becki* Platnick and Shadab, 1977); **3,** large, very distinct, planar.
19. Coxosternal region, position of leg I coxae relative to tritosternum: **0,** abutting tritosternum (if slightly separated in male, then abutting in female); **1,** separated from tritosternum by pedipalp coxae.

Chelicerae

20. Cheliceral manus, dorsal toothlike process: **0,** absent; **1,** present. This process has been referred to as the "*Ricinoides* tooth" (e.g., Legg, 1982; Botero-Trujillo et al., 2021a), a term no longer appropriate following the redefinition of *Ricinoides* presented herein.
21. Cheliceral movable finger, prodorsal longitudinal carina: **0,** absent; **1,** moderate, subtly raised; **2,** pronounced, forming sharp ridge. The prodorsal longitudinal carina is difficult to identify in males of the *foedus* group of *Cryptocellus* Westwood, 1874, in which the movable finger is modified compared to that of the female.
22. Cheliceral movable finger, mucron, prolateral excavation: **0,** absent; **1,** present, delimited by two parallel carinae.
23. Cheliceral movable finger, dentition: **0,** tooth row comprising several small teeth and one noticeable, moderately to markedly larger proximal tooth, often with very small denticles proximal to it; **1,** tooth row comprising several small teeth, sometimes gradually increasing in size distally, without large proximal tooth.

Pedipalps

24. Pedipalp tibia, proximal swelling: **0,** unmodified or slightly swollen proximally compared to rest of segment; **1,** moderately swollen proximally compared to rest of segment, which is slightly narrower; **2,** markedly swollen proximally compared to rest of segment, which is very narrow; **3,** robust along entire length. In the first state, the tibia often narrows slightly distally in dorsal aspect, whereas the dorsal and ventral margins are subparallel in lateral aspect (often with slight to moderate narrowing ventrosubmedially). In the second and third states, the proximal swelling of the tibia is apparent in both dorsal and lateral aspects whereas, in the fourth state, the tibial margins are parallel in dorsal and lateral aspects.
25. Pedipalp tibia, apical longitudinal carinae: **0,** absent; **1,** present.
26. Pedipalp tibia, distal region, dorsal and lateral surfaces, raised tubercles: **0,** absent; **1,** present, oval; **2,** present, elongate.

27. Pedipalp tibia distal region, dorsal and ventral surfaces, subtriangular granules: **0,** absent (or if one or two retroventral granules present in male, none present in female); **1,** present on ventral surface only; **†2,** present on dorsal and ventral surfaces.

Legs

28. Leg femora, dorsal longitudinal sulcus: **0,** absent; **1,** present. If present, this sulcus is usually distinct, but may be shallow and difficult to identify when leg II is greatly enlarged in the male.
29. Leg tarsi, ventrodistal papillae: **0,** absent; **1,** present. Ventrodistal papillae may vary from a single papilla to clusters of two to four papillae.
30. Leg I femur, shape (♂): **0,** unmodified, slender; **1,** slightly swollen, moderately robust. The states of this character are best observed by comparing the femur of leg I to the femora of other legs, especially the narrowest, as well as to the femur of leg I in the female.
31. Leg I tibia, proventral apophysis (♂): **0,** absent; **1,** present.

†32. Leg I tibia, retroventral apophysis (♂): **0,** absent; **†1,** present.

33. Leg I metatarsus (♂): **0,** sublinear in lateral aspect, subcircular in cross section; **1,** markedly convex ventrally in lateral aspect, dorsoventrally elongate in cross section. The metatarsus is very slightly elongate dorsoventrally in the male and female of some species, which were scored for the first state.
34. Leg I metatarsus, proventral proximal depression (♂): **0,** absent; **1,** present.
35. Leg II femur, shape (♂): **0,** unmodified, slender; **1,** slightly swollen, moderately robust; **2,** markedly swollen, noticeably robust. The first and second states are best observed by comparing the femur of leg II to the femora of other legs, especially the narrowest, and to the femur of leg II in the female. In the third state, the femur is markedly robust and swollen, far more than those of other legs of the male and/or the femur of leg II in the female.
36. Leg II tibia, ventromedian apophysis (♂): **0,** absent; **1,** present.
37. Leg II tibia and metatarsus, ventral pad of bristlelike setae (♂): **0,** absent; **1,** present.
38. Leg II metatarsus, ventral subproximal depression (♂): **0,** absent; **1,** present.
39. Leg II metatarsus, ventrosubmedian concavity (♂): **0,** absent; **1,** present.
40. Leg II, fourth tarsomere, length relative to other tarsomeres: **0,** short, similar to or slightly shorter than third tarsomere, never longer than second tarsomere; **1,** moderate, at least slightly longer than third tarsomere but not twice its length, and not shorter than third tarsomere; **2,** very long, at least twice length of previous tarsomeres.
41. Leg II, fifth (terminal) tarsomere: **0,** movable, not fused to preceding tarsomere; **1,** fixed, fused to preceding tarsomere.
42. Leg III femur, shape (♂): **0,** unmodified, slender; **1,** slightly swollen, moderately robust; **2,** markedly swollen, noticeably robust. The first and second states are best observed by comparing the femur of leg III to the femora of other legs, especially the narrowest, and to the femur of leg III in the female. In the third state, the femur is markedly robust and swollen, far more than in other legs of the male and/or the femur of leg III of the female.
43. Leg III metatarsus, shape relative to tibia, lateral aspect (♂): **0,** unmodified, not swollen; **1,** slightly swollen; **†2,** markedly swollen.
44. Leg III metatarsus, dorsal surface, basal region (♂): **0,** unmodified; **1,** excavated.

†45. Leg III metatarsus, dorsal surface, basal excavation (♂): **0,** shallowly excavated; **†1,** deeply excavated.

46. Leg III metatarsus, dorsal concavity (♂): **0,** moderate distally, gradually becoming shallower proximally; **1,** very deep, forming well-defined chamber in distal half of segment; **2,** very deep, forming well-defined chamber extending to attachment point of metatarsal process. The dorsal concavity accommodates part of the copulatory apparatus when the tarsus is retracted.

47. Leg III metatarsus, prodorsal proximal sulcus (♂): **0,** absent; **1,** present. The metatarsal process is contiguous with the prodorsal proximal sulcus, on which it rests.
48. Leg III metatarsus, prodorsal margin distal region, planar excrescence on ipsilateral surface (♂): **0,** absent; **1,** present.
49. Leg III metatarsus, proventral apical brush-like row of long yellow setae (♂): **0,** absent; **1,** present.
50. Leg III metatarsus and tarsus, dorsal surfaces, reciprocal fit when tarsus retracted (♂): **0,** imprecise, copulatory apparatus largely exposed; **1,** precise, copulatory apparatus completely enclosed.
†51. Leg III, second tarsomere, prodorsal margin, prolateral aspect (♂): **0,** unmodified, sublinear or slightly curved; **†1,** moderately or markedly angular proximally.
52. Leg III, third tarsomere, acute dorsodistal process (♂): **0,** absent; **1,** present.
53. Legs III and IV, terminal tarsomere apex: **0,** dorsal and lateral margins projected, sublinear (ungues predominantly covered in dorsal and lateral aspects); **1,** lateral margins projected, dorsal margin deeply emarginate (ungues exposed in dorsal aspect).
54. Leg IV femur, shape (♂): **0,** unmodified, slender; **1,** slightly swollen, moderately robust; **†2,** markedly swollen, noticeably robust. The first and second states are best observed by comparing the femur of leg IV to the femora of other legs, especially the narrowest, and to the femur of leg IV in the female. In the third state, the femur is markedly robust and swollen, far more than in other legs of the male and/or the femur of leg IV of the female.
55. Leg IV tarsus, second to fourth tarsomeres, shape (♂): **0,** unmodified, not swollen; **1,** swollen. The states of this character are best observed by comparing the tarsus of the male with that of the female, especially when the swelling is not pronounced (e.g., in *Pseudocellus seacus* Platnick and Pass, 1982).

Male Copulatory Apparatus

56. Copulatory apparatus, fixed process, apex (♂): **0,** simple, apex entire or shallowly emarginate; **†1,** markedly bilobate, each lobe situated on opposite surfaces of fixed process (relative to dorsal longitudinal sulcus); **2,** three-pronged, approximately trident-shaped, with two prolateral tips (relative to dorsal longitudinal sulcus) forming flap, visible in dorsal aspect; **3,** with distinct raised lobular region situated on prolateral surface (relative to dorsal longitudinal sulcus), comprising two primary lobes and, usually, with ventral secondary lobes in more proximal position.
†57. Copulatory apparatus, fixed process, apex (♂): **0,** pigmented, sclerotized, resembling rest of apparatus; **†1,** whitish, membranous, "fleshy" in appearance unlike rest of apparatus. The term "fleshy" was first used by Tuxen (1974: 100).
58. Copulatory apparatus, fixed process, prolateral laminar (*PL*) lobe (♂): **0,** absent; **1,** present.
59. Copulatory apparatus, fixed process, prolateral laminar (*PL*) lobe, apex, proximity to distal region of trunk (♂): **0,** proximate, separated by narrow submedian emargination; **1,** distant, separated by broad submedian emargination.
60. Copulatory apparatus, fixed process, prolateral laminar (*PL*) lobe, apex (♂): **0,** dorsoventrally compressed; **1,** laterally compressed.
61. Copulatory apparatus, fixed process, distal lobular region, alpha (α) lobe (♂): **0,** entire, simple; **1,** partially (apically) or completely bifid.
62. Copulatory apparatus, fixed process, distal lobular region, beta (β) lobe (♂): **0,** entire, simple; **1,** bicuspid; **2,** trifid.
†63. Copulatory apparatus, fixed process, distal lobular region, beta (β) lobe, subdistal accessory denticular process (♂): **0,** absent; **†1,** present.
64. Copulatory apparatus, fixed process, distal lobular region, beta (β) lobe, retrolateral accessory granule (♂): **0,** absent; **1,** present.

65. Copulatory apparatus, fixed process, distal lobular region, prolateral distal (*pd*) lobe (♂): **0,** absent or indistinct; **1,** simple, undivided; **†2,** divided into two prolateral distal lobes (pd_1 and pd_2).
66. Copulatory apparatus, fixed process, distal lobular region, retrolateral distal (*rd*) lobe (♂): **0,** absent or indistinct; **1,** present, simple; **†2,** present, forming cluster of small spiniform projections.
67. Copulatory apparatus, fixed process, apices of retrolateral subdistal (*rsd*) lobe and prolateral laminar (*PL*) lobe, alignment (♂): **0,** apices of *rsd* lobe and *PL* lobe aligned; **1,** apex of *rsd* lobe distal to apex of *PL* lobe.
68. Copulatory apparatus, fixed process, base of distal lobular region, ventral surface (♂): **0,** unmodified, curved to slightly obtuse; **1,** markedly truncate.
†69. Copulatory apparatus, fixed process, base of distal lobular region, lanceolate projection (♂): **0,** absent; **†1,** present.
70. Copulatory apparatus, movable process, origin relative to fixed process and peduncular base (♂): **0,** originating dorsally from fixed process, origin visible in prolateral aspect; **1,** originating dorsally from fixed process, origin obscured by bulb of peduncular base in prolateral aspect; **2,** originating from dorsal surface of thickened portion of fixed process, origin visible in prolateral aspect.

Opisthosoma

†71. Tergite X, lateral sclerites: **0,** well developed; **†1,** absent or obsolete.
72. Tergite XIII, median sclerite, shape: **0,** rectangular to trapezoid; **1,** cup shaped.
73. Tergal membranes, surface: **0,** smooth; **1,** granular.
74. Opisthosomal segment XIII, posterior granulation: **0,** posterodorsal and posteroventral margins without series of large granules; **1,** posteroventral margin and, to lesser extent, posterodorsal margin, armed with large, posteriorly directed subspiniform granules.
75. Opisthosoma dorsal and ventral pleural membranes, surface: **0,** entirely smooth; **1,** at least dorsal pleural membrane moderately to sparsely granular; **2,** finely and densely granular.
76. Pygidium basal segment, orientation relative to longitudinal axis of opisthosoma: **0,** markedly curved dorsally; **1,** slightly tilted dorsally; **2,** parallel to longitudinal axis of opisthosoma.
77. Pygidium basal segment, posterior margin: **0,** uniformly narrow; **†1,** broad ventrally; **2,** entirely broad, more markedly so ventrally.
78. Pygidium basal segment, posterior opening, width: **0,** broad, at least half lateral width of basal segment; **1,** narrow, between two-fifths and one-third lateral width of basal segment.

Female Genital Structures

79. Spermathecae, type (♀): **0,** vesicular type, i.e., two pairs of weakly sclerotized receptacles of variable shape; **1,** capsular type, i.e., one pair of moderately to heavily sclerotized compartments; **2,** follicular type, i.e., one pair of elongate tubes not visibly sclerotized.
80. *Bursa copulatrix*, anterior wall, supernumerary sacculiform formations (♀): **0,** absent; **1,** present.

APPENDIX 3

Distribution of Morphological Characters Used for Phylogenetic Analysis of African Ricinulei Thorell, 1876

Character states scored 0–3, inapplicable (-), or unknown (?). Square brackets indicate polymorphic characters. First nine taxa are outgroups. Root indicated by †.

	1–5	6–10	11–15	16–20	21–25	26–30	31–35	36–40
†?*Poliochera cretacea*	00-00	?0-0?	?0??0	00310	???00	0001?	?????	????0
Cryptocellus becki	00-00	11200	00200	00210	10111	00011	00-00	00001
Cryptocellus islacolon	00-00	11300	00000	00210	10121	00010	00000	00001
Cryptocellus jamari	00-00	11111	00000	00210	10111	00010	00000	00001
Cryptocellus peckorum	00-00	11200	00000	00210	10111	00010	00001	00001
Pseudocellus monjarazi	00-01	10-00	00001	01300	00010	00011	00000	00000
Pseudocellus paradoxus	00-00	10-00	00000	01300	00000	01010	00002	00010
Pseudocellus pelaezi	00-01	10-00	10000	01300	00[01]00	00010	00102	00000
Pseudocellus seacus	00-01	10-00	00000	01310	00010	00010	00002	00010
Alantakun karschii	01110	01100	01110	01011	21120	2000[01]	0001[12]	00012
Bambara hanseni	10-00	01110	01001	01111	21121	0[01]000	00000	00002
Bambara jocquei	10-00	01110	01001	11111	21121	00000	00000	00002
Bambara megahanseni	10-00	0111?	?1??0	??111	21121	0100?	?????	????2
Gizoo crassipalpe	10-00	01111	01000	01111	21120	20000	00000	00002
Ricinoides afzelii	00-00	01100	31000	01111	21130	10101	00012	10102
Ricinoides atewa	00-00	01100	21000	01111	21130	10101	00012	10102
Ricinoides eburneus	00-00	011?0	01000	01111	21130	10101	00012	11102
Ricinoides feae	00-00	01100	01000	01111	21100	10101	00012	10102
Ricinoides iita	00-00	010?0	11000	0?111	21130	10101	00012	10102
Ricinoides kakum	00-00	01100	21000	01111	21130	10101	00012	10102
Ricinoides nzerekorensis	00-00	01100	01000	01111	21130	10101	00012	11102
Ricinoides taii	00-00	01100	01000	01111	21130	10100	00011	10102
Ricinoides westermannii	00-00	011?0	01000	01111	21100	10101	00012	00102
Tautau leonensis	10-00	011?1	01000	01111	21130	02000	00000	00002
Tautau ziama	10-00	011?1	01000	0?111	2?121	00000	00000	00002
Ududo sjostedtii	01000	011?0	01000	11111	21110	10001	11100	00002
Ududo tuxeni	01000	01100	01000	11111	21110	10001	10100	00002

APPENDIX 3 *continued*

	41–45	46–50	51–55	56–60	61–65	66–70	71–75	76–80
†?*Poliochera cretacea*	0????	?????	??1??	?????	?????	?????	00000	200??
Cryptocellus becki	0220–	10000	00120	000––	–––––	––––2	00000	00010
Cryptocellus islacolon	0000–	00000	00100	100––	–––––	––––2	00000	00010
Cryptocellus jamari	0000–	00000	00100	000––	–––––	––––2	00001	00010
Cryptocellus peckorum	0000–	10000	00100	000––	–––––	––––2	00000	00010
Pseudocellus monjarazi	0200–	00000	00110	200––	–––––	––––1	00000	10000
Pseudocellus paradoxus	0000–	00000	00100	000––	–––––	––––1	00000	10000
Pseudocellus pelaezi	0110–	10000	00100	000––	–––––	––––1	00000	10000
Pseudocellus seacus	0000–	00000	00101	200––	–––––	––––1	00000	10000
Alantakun karschii	01111	11101	1001[01]	31100	00002	10000	00[01]12	22021
Bambara hanseni	0000–	01101	00001	30100	10011	10000	01001	10021
Bambara jocquei	0000–	01101	00001	30100	10011	10000	01001	10021
Bambara megahanseni	0????	?????	??0??	?????	?????	?????	00001	10021
Gizoo crassipalpe	1000–	01101	00001	30100	00100	00000	00002	110??
Ricinoides afzelii	0100–	01111	01010	30100	00001	10000	00102	20121
Ricinoides atewa	0000–	01101	01000	30100	01001	10000	00102	20121
Ricinoides eburneus	0000–	01101	01000	30100	01001	10000	00102	201??
Ricinoides feae	0000–	01101	01000	30100	01001	20000	00102	20121
Ricinoides iita	0100–	01111	01010	30100	01001	10000	00102	201??
Ricinoides kakum	0000–	01101	01000	30100	01001	10000	10102	20121
Ricinoides nzerekorensis	0000–	01101	01000	30100	01001	10000	00102	20121
Ricinoides taii	0000–	01101	01000	30100	01001	10000	00102	20121
Ricinoides westermannii	0000–	01101	0100?	30100	01001	10000	00102	201??
Tautau leonensis	1010–	21101	00001	30111	02000	01100	00002	200??
Tautau ziama	1010–	21101	00001	30111	02000	01110	00102	100??
Ududo sjostedtii	01010	11101	00011	30100	00001	10000	00112	220??
Ududo tuxeni	01010	11101	00011	30100	00001	10000	00112	22021

Scientific Publications of the American Museum of Natural History

American Museum Novitates
Bulletin of the American Museum of Natural History
Anthropological Papers of the American Museum of Natural History

Submission procedures can be found at http://research.amnh.org/scipubs

All issues of *Novitates* and *Bulletin* are available on the web (https://digitallibrary.amnh.org/handle/2246/5). Order printed copies on the web from:
https://shop.amnh.org/books/scientific-publications.html

or via standard mail from:
American Museum of Natural History—Scientific Publications
Central Park West at 79th Street
New York, NY 10024

♾ This paper meets the requirements of ANSI/NISO Z39.48-1992 (permanence of paper).

On the cover: Alantakun karschii (Hansen and Sørensen, 1904), comb. nov., ♂, Añisok Co., Equatorial Guinea. Photograph courtesy of I. Malaxetxebarria.